PHYSICAL REVIEW D **95,** 063515 (2017)

# Cosmological evolution of a complex scalar field with repulsive or attractive self-interaction

Abril Suárez[1,2,*] and Pierre-Henri Chavanis[1,†]

[1]*Laboratoire de Physique Théorique, Université Paul Sabatier, 118 route de Narbonne 31062 Toulouse, France*

[2]*Departamento de Aeronáutica, Universidad Politécnica Metropolitana de Hidalgo, Ex-Hacienda San Javier, Tolcayuca, Hgo. C.P. 43860, Mexico*

(Received 17 September 2016; published 15 March 2017)

We study the cosmological evolution of a complex scalar field with a self-interaction potential $V(|\varphi|^2)$, possibly describing self-gravitating Bose-Einstein condensates, using a fully general relativistic treatment. We generalize the hydrodynamic representation of the Klein-Gordon-Einstein equations in the weak field approximation developed in our previous paper [A. Suárez and P.-H. Chavanis, Phys. Rev. D **92**, 023510 (2015)]. We establish the general equations governing the evolution of a spatially homogeneous complex scalar field in an expanding background. We show how they can be simplified in the fast oscillation regime (equivalent to the Thomas-Fermi, or semiclassical, approximation) and derive the equation of state of the scalar field in parametric form for an arbitrary potential $V(|\varphi|^2)$. We explicitly consider the case of a quartic potential with repulsive or attractive self-interaction. For repulsive self-interaction, the scalar field undergoes a stiff matter era followed by a pressureless dark matter era in the weakly self-interacting regime and a stiff matter era followed by a radiationlike era and a pressureless dark matter era in the strongly self-interacting regime. For attractive self-interaction, the scalar field undergoes an inflation era followed by a stiff matter era and a pressureless dark matter era in the weakly self-interacting regime and an inflation era followed by a cosmic stringlike era and a pressureless dark matter era in the strongly self-interacting regime (the inflation era is suggested, not demonstrated). We also find a peculiar branch on which the scalar field emerges suddenly at a nonzero scale factor with a finite energy density. At early times, it behaves as a gas of cosmic strings. At later times, it behaves as dark energy with an almost constant energy density giving rise to a de Sitter evolution. This is due to spintessence. We derive the effective cosmological constant produced by the scalar field. Throughout the paper, we analytically characterize the transition scales of the scalar field and establish the domain of validity of the fast oscillation regime. We analytically confirm and complement the important results of Li, Rindler-Daller, and Shapiro [Phys. Rev. D **89**, 083536 (2014)]. We determine the phase diagram of a scalar field with repulsive or attractive self-interaction. We show that the transition between the weakly self-interacting regime and the strongly self-interacting regime depends on how the scattering length of the bosons compares with their effective Schwarzschild radius. We also constrain the parameters of the scalar field from astrophysical and cosmological observations. Numerical applications are made for ultralight bosons without self-interaction (fuzzy dark matter), for bosons with repulsive self-interaction, and for bosons with attractive self-interaction (QCD axions and ultralight axions).

DOI: 10.1103/PhysRevD.95.063515

## I. INTRODUCTION

There is compelling observational evidence for the existence of dark matter (DM) and dark energy (DE) in the Universe. The suggestion that DM may constitute a large part of the Universe was raised by Zwicky [1] in 1933. Using the virial theorem to infer the average mass of galaxies within the Coma cluster, he obtained a much higher value than the mass of luminous material. He realized therefore that some mass was "missing" to account for the observations. The existence of DM has been confirmed by more precise observations of rotation curves [2], gravitational lensing [3], and hot gas in clusters [4]. On the other hand, DE is responsible for the ongoing acceleration of the Universe revealed by the high redshift of type Ia supernovae treated as standardized candles [5–7]. Recent observations of baryonic acoustic oscillations provide another independent support to the DE hypothesis [8]. In both cases (DM and DE) more indirect measurements come from the cosmic microwave background (CMB) and large scale structure observations [9–11].

The variations in the temperature of the thermal CMB radiation at 3K throughout the sky imply $\Omega_{k,0} \sim 0$ and $\Omega_{\mathrm{r},0} \sim 10^{-4}$, while the power spectrum of the spatial distributions of large scale structures gives $\Omega_{\mathrm{m},0} \sim 0.3$, where $\Omega_{k,0}$ is the effective curvature of spacetime, $\Omega_{\mathrm{r},0}$ is the present energy density in the relativistic CMB radiation (photons)

*asuarez@upmh.edu.mx
†chavanis@irsamc.ups-tlse.fr

 

accompanied by the low mass neutrinos that almost homogeneously fill the space, and $\Omega_{m,0}$ is the current mean energy density of nonrelativistic matter which mainly consists of baryons and nonbaryonic DM. These observations give a value of $\Omega_{\Lambda,0} \sim 0.7$ for the present DE density [11].

One of the most fundamental problems in modern cosmology concerns the nature of DM and DE. In the last decades, various DM and DE models have been studied. The simplest model of DM consists in particles moving slowly compared to the speed of light (they are cold) and interacting very weakly with ordinary matter and electromagnetic radiation. These particles, known as weakly interacting massive particles (WIMPS), behave as dust with an equation of state (EOS) parameter $w = P/\epsilon \simeq 0$ [12–14]. They may correspond to supersymmetric (SUSY) particles [15]. On the other hand, the simplest manner to explain the accelerated expansion of the Universe is to introduce a cosmological constant $\Lambda$ in the Einstein equations [16]. In that case, the value of the energy density $\epsilon_\Lambda = \Lambda c^2/8\pi G$ stored in the cosmological constant represents the DE.

The standard model of cosmological structure formation in the Universe is known as the cold dark matter model with a cosmological constant ($\Lambda$CDM) [17–20]. Cosmological observations at large scales support the $\Lambda$CDM model with a high precision.

However, this model has some problems at small (galactic) scales for the case of DM [21–24]. In particular, it predicts that DM halos should be cuspy [25] while observations reveal that they have a flat core [26]. On the other hand, the $\Lambda$CDM model predicts an overabundance of small-scale structures (subhalos/satellites), much more than what is observed around the Milky Way [27]. These problems are referred to as the "cusp problem" and "missing satellite problem." The expression "small-scale crisis of CDM" has been coined.

Furthermore, the value of the cosmological constant $\Lambda$ assigned to DE has to face important fine-tuning problems [28–30]. From the point of view of particle physics, the cosmological constant can be interpreted naturally in terms of the vacuum energy density whose scale is of the order of the Planck density $\rho_P = 5.16 \times 10^{99}\ \mathrm{g\,m^{-3}}$. However, observationally, the cosmological constant is of the order of the present value of the Hubble parameter squared, $\Lambda \sim H_0^2 = (2.18 \times 10^{-18}\ \mathrm{s^{-1}})^2$, which corresponds to a dark energy density $\rho_\Lambda = \Lambda/8\pi G \sim 10^{-24}\ \mathrm{g\,m^{-3}}$. The Planck density and the cosmological density differ from each other by 123 orders of magnitude. This leads to the so-called cosmological constant problem [28–30].

Since the $\Lambda$CDM model poses problems, some efforts have been done in trying to understand the nature of DM and DE from the framework of quantum field theory. In particle physics and string theory, scalar fields (SF) arise in a natural way as bosonic spin-0 particles described by the Klein-Gordon (KG) equation [31,32]. Examples include the Higgs particle, the inflaton, the dilaton field of superstring theory, tachyons etc. SFs also arise in the Kaluza-Klein and Brans-Dicke theories [33]. In cosmology, SFs were introduced to explain the phase of inflation in the primordial Universe [34]. SF models have then been used in cosmology in various contexts and they continue to play an important role as potential DM and DE candidates.

For example, the source of DE can be attributed to a SF. A variety of SF models have been inferred for this purpose (see for example [17,35,36]). Quintessence [37,38], which is the simplest case, is described by an ordinary SF minimally coupled to gravity. It generally has a density and EOS parameter $w(t)$ that vary with time, hence making it dynamic. By contrast, a cosmological constant is static, with a fixed energy density and $w = -1$. Phantom fields [39–42] are associated with a negative kinetic term. This strange property leads to an EOS parameter $w \leq -1$ implying that the energy density increases as the Universe expands, possibly leading to a big rip. It has also been suggested that, in a class of string theories, tachyonic SF [43] can condense and have cosmological applications. Tachyons have an interesting EOS whose parameter smoothly interpolates between $-1$ and 0, thus behaving as DE and pressureless DM. SF models describing DE usually feature masses of the order of the current Hubble scale ($m \sim H_0\hbar/c^2 \sim 10^{-33}\ \mathrm{eV}/c^2$) [44,45].

Concerning DM, it has been proposed that DM halos can be made of a SF described by the Klein-Gordon-Einstein (KGE) equations (see, e.g., [46–49] for reviews and [50] for high resolution numerical simulations showing the viability of this scenario). In general, SFDM models suppose that DM is a real or complex SF minimally coupled to gravity. This SF can be self-interacting but it does not interact with the other particles and fields, except gravitationally. SFs that interact only with gravity could be gravitationally produced by inflation [51]. The SF may represent the wave function of the bosons having formed a Bose-Einstein condensate (BEC). The KGE equations describe a relativistic SF/BEC. General relativity is necessary to model compact SF objects such as boson stars [52–54] and neutron stars with a superfluid core [55,56]. It is also necessary in cosmology to model the phase of inflation and the evolution of the early Universe [34]. However, in the context of DM halos, Newtonian gravity is sufficient. The evolution of a nonrelativistic SF/BEC is described by the Gross-Pitaevskii-Poisson (GPP) equations. There are several models of SFDM, e.g. noninteracting (fuzzy) DM [57], self-interacting DM [58], or axionic DM [59–63].[1]

[1]Axions can be produced in the early Universe through two mechanisms. At the quantum chromodynamics (QCD) phase transition where a BEC of axions forms and these very cold particles behave as CDM; and through the decay of strings formed at the Peccei-Quinn phase transition [64,65]. Unless inflation occurs after the Peccei-Quinn phase transition, strings are thought to be the dominant mechanism for axion production [66]. Recent analysis confirms that strings are likely to be the dominant source of axions, even though strings will not produce an interesting level of density fluctuations as their predicted mass per unit length is far too small to be cosmologically interesting [67].

Most of these models are based on the assumption that DM is made of extremely light scalar particles with masses between $10^{-23}\ \mathrm{eV}/c^2 \leq m \leq 10^{-2}\ \mathrm{eV}/c^2$. Within this mass scale, SFDM displays a wave (quantum) behavior at galactic scales that could solve many of the problems of the ΛCDM model. Indeed, the wave properties of bosonic DM may stabilize the system against gravitational collapse, providing halo cores and sharply suppressing small-scale linear power. This may solve the cusp problem and the missing satellite problem. Therefore, the main virtues of the SF/BEC model are that it can reproduce the cosmological evolution of the Universe for the background and behave as CDM at large scales where its wave nature is invisible, while at the same time it solves the problems of the CDM model at small scales where its wave nature manifests itself.

In quantum field theory, ultralight SFs seem unnatural but renormalization effects tend to drive these scalar masses up to the scale of a new physics. Given the present observational status of cosmology, and despite all the efforts that have been made, it is fair to say that the nature of DM and DE remains a mystery. As a result, the SF scenario is an interesting suggestion that deserves to be studied in more detail.

Instead of working directly in terms of field variables, a fluid approach can be adopted. In the nonrelativistic case, this hydrodynamic approach was introduced by Madelung [68] who showed that the Schrödinger equation is equivalent to the Euler equations for an irrotational fluid with an additional quantum potential arising from the finite value of $\hbar$ and accounting for Heisenberg's uncertainty principle. This approach has been generalized to the GPP equations in the context of DM halos by [69–71] among others. In the relativistic case, de Broglie [72–74] in his so-called pilot wave theory, showed that the KG equations are equivalent to hydrodynamic equations including a covariant quantum potential. This approach has been generalized to the Klein-Gordon-Poisson (KGP) and KGE equations in the context of DM halos by [75–79].[2] In this hydrodynamic representation, DM halos result from the balance between the gravitational attraction and the quantum pressure arising from the Heisenberg uncertainty principle or from the self-interaction of the bosons. At small scales, pressure effects are important and can prevent the formation of singularities and solve the cusp problem and the missing satellite problem. At large scales, pressure effects are generally negligible (except in the early Universe) and one recovers the ΛCDM model.

The formation of large-scale structures is an important topic of cosmology. This problem was first considered by Jeans [80] (before the discovery of the expansion of the Universe) who studied the instability of an infinite homogeneous self-gravitating classical collisional gas (see [81] for a review). This study has been generalized in the context of SF theory. The Jeans instability of an infinite homogeneous self-gravitating system in a static background was studied by [82] for a relativistic SF described by the generalized KGP equations, using the field representation. The same problem was studied in [70,83] for a nonrelativistic SF described by the GPP equations in the context of Newtonian cosmology, and in [77,78] for a relativistic SF described by the KGE equations, using the hydrodynamic representation.

The growth of perturbations of a relativistic real SF in an expanding Universe was considered in [84,85] using the field representation. The same problem was addressed in [77,83] for a complex SF using the hydrodynamic representation. Analytical results were obtained in the (nonrelativistic) matter era where the background Universe has an Einstein-de Sitter (EdS) evolution [77,83]. The matter era is valid at sufficiently late times, after the radiation-matter equality. At earlier times, the SF affects the background evolution of the Universe so we can no more assume that the scale factor follows the EdS solution.

The classical evolution of a real SF described by the KGE equations with a potential of the form $V(\varphi) = a\varphi^n$ in an isotropic and homogeneous cosmology was first investigated by Turner [86] (see also the subsequent works of [51,87,88]). He showed that the SF experiences damped oscillations but that, in average, it is equivalent to a perfect fluid with an EOS $P = [(n-2)/(n+2)]\epsilon$ (this result is valid if we neglect particle creation due to the time variation of $\varphi$). For $n = 2$ the SF behaves as pressureless matter and for $n = 4$ it behaves as radiation. Turner also mentioned the possibility of a stiff EOS. The cosmological evolution of a spatially homogeneous real self-interacting SF with a repulsive $\varphi^4$ potential described by the KGE equations competing with baryonic matter, radiation and dark energy was considered by [84]. In this work, it is found that a real self-interacting SF displays fast oscillations and that, on the mean, it undergoes a radiationlike era followed by a matterlike era. In the noninteracting case, the SF undergoes only a matterlike era [89]. In any case, at sufficiently late times, the SF reproduces the cosmological predictions of the standard ΛCDM model.

The cosmological evolution a complex self-interacting SF representing BECDM has been considered by [83,90] who solved the (relativistic) Friedmann equations with the EOS of the BEC derived from the (nonrelativistic) GP equation after identifying $\rho_m c^2$, where $\rho_m$ is the rest-mass density, with the energy density $\epsilon$. However, as clarified in [91], this approach is not valid in the early Universe as it combines relativistic and nonrelativistic equations. These studies may still have interest in cosmology in a different context, as discussed in [92,93].

[2]The pilot wave theory of de Broglie [72–74] is the relativistic version of Madelung's hydrodynamics [68]. The works of de Broglie and Madelung were developed independently. See the Introduction of [79] for a short history of the early development of quantum mechanics.

The exact relativistic cosmological evolution of a complex self-interacting SF/BEC described by the KGE equations with a repulsive $|\varphi|^4$ potential has been considered by Li *et al.* [94] (see also the previous works of [95–98]). In this work, the evolution of the homogeneous background is studied. It is shown that the SF undergoes three successive phases: a stiff matter era, followed by a radiationlike era (that only exists for self-interacting SFs), and finally a matterlike era similar to the one appearing in the CDM model. Another cosmological model displaying a primordial stiff matter era has been developed in [91]. Interestingly, it leads to a completely analytical cosmological solution generalizing the EdS model and the (anti)-ΛCDM model.

In general, the SF oscillates in time and it is not clear how these oscillations can be measured in practice because there is no direct access to field variables such as $\varphi$. As a result, the hydrodynamic representation of the SF may be more physical than the KG equation itself because it is easier to measure hydrodynamic variables such as the energy density $\epsilon$, the rest-mass density $\rho_m$, and the pressure $P$. In our previous paper [77], we showed that the three phases of a relativistic SF with a repulsive $|\varphi|^4$ potential (stiff matter, radiation and pressureless matter) could be obtained from the hydrodynamic approach in complete agreement with the field theoretic approach of Li *et al.* [94].

In the present paper, we complete and generalize our study in different directions: we formulate the problem for an arbitrary SF potential $V(|\varphi|^2)$, not just for a $|\varphi|^4$ potential; we solve the equations in the fast oscillation regime and obtain several analytical results in different asymptotic limits that complement the work of Li *et al.* [94]; we consider repulsive and attractive self-interaction and show that the later can lead to very peculiar results. The case of attractive self-interaction is of considerable interest since axions, that have been proposed as a serious DM candidate, usually have an attractive self-interaction. The case of attractive self-interaction has been studied previously in [70,77,83,99,100]. It is shown in [77,83] that an attractive self-interaction can accelerate the growth of structures is cosmology. On the other hand, it is shown in [70,99,100] that stable DM halos with an attractive self-interaction can exist only below a maximum mass that severely constrains the parameters of the SF.

The paper is organized as follows. In Sec. II, we introduce the KG and Friedmann equations describing the cosmological evolution of a spatially homogeneous complex[3] SF with an arbitrary self-interaction potential $V(|\varphi|^2)$ in an expanding background and provide their hydrodynamic representation. We show that these hydrodynamic equations can be simplified in the fast oscillation regime equivalent to the Thomas-Fermi (TF), or semiclassical, approximation where the quantum potential can be neglected. We derive the EOS of the SF in parametric form for an arbitrary potential $V(|\varphi|^2)$. In Sec. III, we consider the cosmological evolution of a spatially homogeneous SF with a repulsive quartic self-interaction. In agreement with previous works [77,94], we show that the SF undergoes a stiff matter era ($w = 1$) in the slow oscillation regime, followed by a radiationlike era ($w = 1/3$) and a pressureless dark matter era ($w \simeq 0$) in the fast oscillation regime. We analytically determine the transition scales between these different periods and show that the radiationlike era can only exist for sufficiently large values of the self-interaction parameter. More precisely, the transition between the weakly self-interacting and strongly self-interacting regimes depends on how the scattering length of the bosons $a_s$ compares with their effective Schwarzschild radius $r_S = 2\,Gm/c^2$. We determine the phase diagram of a SF with repulsive self-interaction. We also analytically recover the bounds on the ratio $a_s/m^3$ obtained by Li *et al.* [94] by requiring that the SF must be nonrelativistic at the epoch of matter-radiation equality and by using constraints from the big bang nucleosynthesis (BBN). In Sec. IV, we consider the evolution of a spatially homogeneous SF with an attractive quartic self-interaction. In the fast oscillation regime, the SF emerges at a nonzero scale factor with a finite energy density. At early time, it behaves as a gas of cosmic strings ($w = -1/3$). At later time, two evolutions are possible. On the normal branch, the SF behaves as pressureless DM ($w \simeq 0$). On the peculiar branch, it behaves as DE ($w = -1$) with an almost constant energy density giving rise to a de Sitter evolution. We derive the effective cosmological constant produced by the SF. We establish the domain of validity of the fast oscillation regime. We argue that, in the very early Universe, a complex SF with an attractive self-interaction undergoes an inflation era. If the self-interaction constant is sufficiently small, the inflation era is followed by a stiff matter era. We determine the phase diagram of a SF with attractive self-interaction. We also set constraints on the parameters of the SF using cosmological observations. Numerical applications are made for standard (QCD) axions and ultralight axions. This is indicative because QCD axions are real SFs while certain results of ours are only valid for complex SFs. In Sec. V, we study the evolution of the SF in the total potential $V_{\rm tot}(|\varphi|^2)$ incorporating the rest-mass energy. A SF with repulsive self-interaction descends the potential. A SF with attractive self-interaction descends the potential on the normal branch and ascends the potential on the peculiar branch. This is possible because of the effect of a centrifugal force that is specific to a complex SF. This is called spintessence [97]. The concluding Sec. VI summarizes the main results of our

[3]Complex SFs are potentially more relevant than real SFs because they can form stable DM halos while DM halos made of real SFs are either dynamically unstable or oscillating. If DM halos were stable "oscillatons" [101], their oscillations would probably have been detected. On the other hand, bosons described by a complex SF with a global $U(1)$ symmetry associated with a conserved charge (Noether theorem) can form BECs even in the early Universe while this is more difficult for a boson described by a real SF (like the QCD axion).

study and regroups the numerical applications of astrophysical relevance. The Appendices contain additional material that is needed to interpret our results.

## II. SPATIALLY HOMOGENEOUS COMPLEX SF

In our previous paper [77], we have derived a hydrodynamic representation of the KGE equations in an expanding background in the weak field approximation. We considered a complex SF with a quartic self-interaction potential. This study was extended to the case of an arbitrary SF potential of the form $V(|\varphi|^2)$ in [78,79]. In this section, we consider the case of a spatially homogeneous complex SF. For the clarity and the simplicity of the presentation, we assume that the Universe is only composed of a SF, although it would be straightforward to include in the formalism other components such as normal radiation, baryonic matter, and dark energy (e.g., a cosmological constant).

### A. The KG equation for a spatially homogeneous complex SF

The cosmological evolution of a spatially homogeneous complex SF $\varphi(t)$ with a self-interaction potential $V(|\varphi|^2)$ in a Friedmann-Lemaître-Robertson-Walker (FLRW) universe is described by the KG equation

$$\frac{1}{c^2}\frac{d^2\varphi}{dt^2}+\frac{3H}{c^2}\frac{d\varphi}{dt}+\frac{m^2c^2}{\hbar^2}\varphi+2\frac{dV}{d|\varphi|^2}\varphi=0, \tag{1}$$

where $H=\dot{a}/a$ is the Hubble parameter and $a(t)$ is the scale factor. The second term in Eq. (1) is the Hubble drag. The rest-mass term (third term) can be written as $\varphi/\lambda_C^2$ where $\lambda_C=\hbar/mc$ is the Compton wavelength of the bosons.

The energy density $\epsilon(t)$ and the pressure $P(t)$ of the SF are given by

$$\epsilon=\frac{1}{2c^2}\left|\frac{d\varphi}{dt}\right|^2+\frac{m^2c^2}{2\hbar^2}|\varphi|^2+V(|\varphi|^2), \tag{2}$$

$$P=\frac{1}{2c^2}\left|\frac{d\varphi}{dt}\right|^2-\frac{m^2c^2}{2\hbar^2}|\varphi|^2-V(|\varphi|^2). \tag{3}$$

The EOS parameter is defined by $w=P/\epsilon$.

### B. The Friedmann equations

From Eqs. (1)–(3), we can obtain the energy equation

$$\frac{d\epsilon}{dt}+3H(\epsilon+P)=0. \tag{4}$$

This equation can also be directly obtained from the Einstein field equations and constitutes the first Friedmann equation [102]. From this equation we deduce that, as the Universe expands, the energy density decreases when $w>-1$, increases when $w<-1$, and remains constant when $w=-1$. In the second case, the Universe is "phantom" [39]. The second Friedmann equation, obtained from the Einstein field equations, writes

$$H^2=\frac{8\pi G}{3c^2}\epsilon. \tag{5}$$

We have assumed that the Universe is flat in agreement with the observations of the CMB. From Eqs. (4) and (5), we easily obtain the acceleration equation

$$\frac{\ddot{a}}{a}=-\frac{4\pi G}{3c^2}(\epsilon+3P) \tag{6}$$

which constitutes the third Friedmann equation. From this equation, we deduce that the expansion of the Universe is decelerating when $w>-1/3$ and accelerating when $w<-1/3$. The intermediate case, in which the scale factor increases linearly with time, corresponds to $w=-1/3$.

### C. Hydrodynamic representation of a spatially homogeneous complex SF

Instead of working with the SF $\varphi(t)$, we will use hydrodynamic variables like those considered in our previous works [77–79]. We define the pseudo rest-mass density by

$$\rho=\frac{m^2}{\hbar^2}|\varphi|^2. \tag{7}$$

We stress that it is only in the nonrelativistic limit $c\to+\infty$ that $\rho$ has the interpretation of a rest-mass density. In the relativistic regime, $\rho$ does not have a clear physical interpretation but it can always be defined as a convenient notation [77–79]. We write the SF in the de Broglie form

$$\varphi(t)=\frac{\hbar}{m}\sqrt{\rho(t)}e^{iS_{\rm tot}(t)/\hbar}, \tag{8}$$

where $\rho$ is the pseudo rest-mass density and $S_{\rm tot}=(1/2)i\hbar\ln(\varphi^*/\varphi)$ is the real action. The total energy of the SF (including its rest mass $mc^2$ energy) is

$$E_{\rm tot}(t)=-\frac{dS_{\rm tot}}{dt}. \tag{9}$$

Substituting Eq. (8) into the KG equation (1) and separating real and imaginary parts, we get

$$\frac{1}{\rho}\frac{d\rho}{dt}+\frac{3}{a}\frac{da}{dt}+\frac{1}{E_{\rm tot}}\frac{dE_{\rm tot}}{dt}=0, \tag{10}$$

$$E_{\rm tot}^2=\hbar^2\frac{\frac{d^2\sqrt{\rho}}{dt^2}}{\sqrt{\rho}}+3H\hbar^2\frac{\frac{d\sqrt{\rho}}{dt}}{\sqrt{\rho}}+m^2c^4+2m^2c^2V'(\rho). \tag{11}$$

On the other hand, from Eqs. (2) and (8), we find that the Friedmann equation (5) takes the form

$$\frac{3H^2}{8\pi G}=\frac{\hbar^2}{8m^2c^4}\frac{1}{\rho}\left(\frac{d\rho}{dt}\right)^2+\frac{\rho E_{\rm tot}^2}{2m^2c^4}+\frac{1}{2}\rho+\frac{1}{c^2}V(\rho). \quad (12)$$

Equations (10)–(12) can also be obtained from the general hydrodynamic equations derived in [77–79] by considering the particular case of a spatially homogeneous SF ($\rho(\vec{x},t)=\rho(t)$, $\vec{v}(\vec{x},t)=\vec{0}$, $\Phi(\vec{x},t)=0$, and $S(\vec{x},t)=S(t)$). In that case, Eq. (10) is deduced from the continuity equation, Eq. (11) from the quantum Bernoulli or Hamilton-Jacobi equation, and Eq. (12) from the Einstein equations. In this connection, we note that the first two terms (the terms proportional to $\hbar^2$) in the right-hand side of Eq. (11) correspond to the relativistic de Broglie quantum potential

$$Q_{\rm dB}=\frac{\hbar^2}{2m}\frac{\Box\sqrt{\rho}}{\sqrt{\rho}} \quad (13)$$

for a spatially homogeneous SF. We stress that the hydrodynamic equations (10)–(12) are equivalent to the KGE equations (1), (2), and (5). Finally, we note that the hydrodynamic equations (10)–(12) with the terms in $\hbar$ neglected provide a TF, or semiclassical, description of relativistic SFs.

The continuity equation (10) can be rewritten as a conservation law

$$\frac{d}{dt}(E_{\rm tot}\rho a^3)=0. \quad (14)$$

Therefore, the total energy of the SF is exactly given by

$$\frac{E_{\rm tot}}{mc^2}=\frac{Qm}{\rho a^3}, \quad (15)$$

where $Q$ is a constant which represents the conserved charge of the complex SF [77,94,98,103].[4]

In the hydrodynamic representation, the energy density and the pressure of a homogeneous SF can be expressed as

$$\epsilon=\frac{\hbar^2}{8m^2c^2}\frac{1}{\rho}\left(\frac{d\rho}{dt}\right)^2+\frac{\rho E_{\rm tot}^2}{2m^2c^2}+\frac{1}{2}\rho c^2+V(\rho), \quad (16)$$

$$P=\frac{\hbar^2}{8m^2c^2}\frac{1}{\rho}\left(\frac{d\rho}{dt}\right)^2+\frac{\rho E_{\rm tot}^2}{2m^2c^2}-\frac{1}{2}\rho c^2-V(\rho). \quad (17)$$

### D. Cosmological evolution of a spatially homogeneous complex SF in the fast oscillation regime

The exact equations (10)–(12) are complicated. In the case of a quartic potential with a positive scattering length, Li *et al.* [94] have identified two regimes in which these equations can be simplified. When the oscillations of the SF are slower than the Hubble expansion ($\omega\ll H$), the SF is equivalent to a stiff fluid with an EOS $P=\epsilon$. This approximation is valid in the early Universe. At later times, when the oscillations of the SF are faster than the Hubble expansion ($\omega\gg H$), it is possible to average over the fast oscillations in order to obtain a simpler dynamics. The resulting equations can be obtained either from the field theoretic approach [94] or from the hydrodynamic approach [77]. We note that the equations obtained in the fast oscillation regime specifically depend on the form of the SF potential. In this section, we generalize these results to the case of an arbitrary SF potential $V(|\varphi|^2)$. We use the hydrodynamic approach. The field theoretic approach is exposed in Appendix A.

The simplified equations valid in the fast oscillation regime can be obtained from Eqs. (11) and (12) by neglecting the terms involving a time derivative. Interestingly, this is equivalent to neglecting the terms in $\hbar$. Therefore, the fast oscillation regime is equivalent to the TF, or semiclassical, approximation where the quantum potential (arising from Heisenberg's uncertainty principle) is neglected. In that case, we obtain

$$E_{\rm tot}^2=m^2c^4+2m^2c^2V'(\rho), \quad (18)$$

$$\frac{3H^2}{8\pi G}=\frac{\rho E_{\rm tot}^2}{2m^2c^4}+\frac{1}{2}\rho+\frac{1}{c^2}V(\rho). \quad (19)$$

Keeping only the solution of Eq. (18) that leads to a positive total energy (the solution with a negative total energy corresponds to antibosons), we get

$$E_{\rm tot}=mc^2\sqrt{1+\frac{2}{c^2}V'(\rho)}. \quad (20)$$

Combining Eqs. (15) and (20), we obtain

$$\rho\sqrt{1+\frac{2}{c^2}V'(\rho)}=\frac{Qm}{a^3}. \quad (21)$$

This equation determines the pseudo rest-mass density $\rho$ as a function of the scale factor $a$. Substituting Eq. (18) into Eq. (19), we find

[4]The conserved charge (normalized by the elementary charge $e$) of a complex SF is given by $Q=\frac{1}{ec}\int J_e^0\sqrt{-g}d^3x$, where $(J_e)_\mu=\frac{ie}{2\hbar}(\varphi^*\partial_\mu\varphi-\varphi\partial_\mu\varphi^*)$ is the quadricurrent of charge of the SF (see, e.g., [79] for details). The charge density is $\rho_e=(J_e)_0/c$. Using Eqs. (8) and (9), we find that $\rho_e=e\rho E_{\rm tot}/m^2c^2$. The conserved charge of a spatially homogeneous SF in an expanding Universe is $Q=\rho_e a^3/e=\rho E_{\rm tot}a^3/m^2c^2$, corresponding to Eq. (15).

$$\frac{3H^2}{8\pi G}=\rho+\frac{1}{c^2}[V(\rho)+\rho V'(\rho)]. \tag{22}$$

Equations (21) and (22) determine the evolution of the scale factor $a(t)$ of the Universe induced by a spatially homogeneous SF in the regime where its oscillations are faster than the Hubble expansion. The energy $E_{\rm tot}$ of the SF is then given by Eq. (20).

It is not convenient to solve the differential equation (22) for the scale factor $a$ because we would need to inverse Eq. (21) in order to express $\rho$ as a function of $a$ in the right-hand side of Eq. (22). Instead, it is more convenient to view $a$ as a function of $\rho$, given by Eq. (21), and transform Eq. (22) into a differential equation for $\rho$. Taking the logarithmic derivative of Eq. (21), we get

$$\frac{\dot a}{a}=-\frac{1}{3}\frac{\dot\rho}{\rho}\left[1+\frac{\rho V''(\rho)}{c^2+2V'(\rho)}\right]. \tag{23}$$

Substituting this expression into Eq. (22), we obtain the differential equation

$$\frac{c^2}{24\pi G}\left(\frac{\dot\rho}{\rho}\right)^2=\frac{\rho c^2+V(\rho)+\rho V'(\rho)}{[1+\frac{\rho V''(\rho)}{c^2+2V'(\rho)}]^2}. \tag{24}$$

For a given SF potential $V(\rho)$, this equation can be solved easily as it is just a first order differential equation for $\rho$. The temporal evolution of the scale factor $a$ is then obtained by plugging the solution of Eq. (24) into Eq. (21).

In the fast oscillation regime, the energy density and the pressure are given by

$$\epsilon=\frac{\rho E_{\rm tot}^2}{2m^2c^2}+\frac{1}{2}\rho c^2+V(\rho), \tag{25}$$

$$P=\frac{\rho E_{\rm tot}^2}{2m^2c^2}-\frac{1}{2}\rho c^2-V(\rho). \tag{26}$$

Using Eq. (18), we get

$$\epsilon=\rho c^2+V(\rho)+\rho V'(\rho), \tag{27}$$

$$P=\rho V'(\rho)-V(\rho). \tag{28}$$

The pseudo velocity of sound is

$$c_s^2=P'(\rho)=\rho V''(\rho). \tag{29}$$

We note that the pressure $P(t)$ of a spatially homogeneous SF in the fast oscillation regime coincides with the pseudo pressure $p(\vec x,t)=p(t)$ that arises in the Euler equation obtained in the hydrodynamic representation of a complex SF [77–79], i.e. $P(t)=p(t)$ (compare Eq. (28) with Eq. (38) of [78]). This extends to an arbitrary SF potential $V(|\varphi|^2)$ the result obtained in [77] for a quartic potential (we note that this equivalence is not true for a spatially inhomogeneous SF and for a homogeneous SF outside of the fast oscillation regime).

On the other hand, Eqs. (27) and (28) define the EOS $P(\epsilon)$ of the SF in parametric form for an arbitrary potential. The EOS parameter can be written as

$$w=\frac{P}{\epsilon}=\frac{\rho V'(\rho)-V(\rho)}{\rho c^2+V(\rho)+\rho V'(\rho)}. \tag{30}$$

The Universe is accelerating ($w<-1/3$) when $4\rho V'(\rho)-2V(\rho)<-\rho c^2$. Introducing the total potential $V_{\rm tot}(\rho)=V(\rho)+\rho c^2/2$ (see Sec. V), this condition can be rewritten as $2\rho V'_{\rm tot}(\rho)<V_{\rm tot}(\rho)$. The Universe is phantom ($w<-1$) when $2V'(\rho)/c^2<-1$ or, equivalently, when $V'_{\rm tot}(\rho)<0$. However, this condition is never realized in the fast oscillation regime because of the constraint imposed by Eq. (20).

For a given EOS $P(\epsilon)$, we can obtain the potential $V(\rho)$ as follows (inverse problem [104]). Equations (27) and (28) can be rewritten as $\epsilon=V_{\rm tot}(\rho)+\rho V'_{\rm tot}(\rho)$ and $P=\rho V'_{\rm tot}(\rho)-V_{\rm tot}(\rho)$ leading to $\epsilon-P=2V_{\rm tot}(\rho)$ and $\epsilon+P=2\rho V'_{\rm tot}(\rho)$. From these equations, we obtain

$$\int\frac{1-P'(\epsilon)}{\epsilon+P(\epsilon)}d\epsilon=\ln\rho,\qquad V_{\rm tot}(\rho)=\frac{1}{2}[\epsilon-P(\epsilon)]. \tag{31}$$

The first equation determines the relationship between $\rho$ and $\epsilon$. The second relation then determines the total potential $V_{\rm tot}(\rho)$.

*Remark:* From Eqs. (27) and (28), we can obtain the EOS $P(\epsilon)$. Solving the energy equation (4) with this EOS, we can obtain $\epsilon(a)$. The relation $\epsilon(a)$ can also be obtained from Eqs. (21) and (27). We can easily check that the relations are the same. Indeed, from Eqs. (4), (27), and (28) we obtain the differential equation

$$[c^2+2V'(\rho)+\rho V''(\rho)]\frac{d\rho}{da}+\frac{3}{a}[\rho c^2+2\rho V'(\rho)]=0. \tag{32}$$

This differential equation is equivalent to Eq. (21). This can be seen easily by taking the logarithmic derivative of Eq. (21) which leads to Eq. (32). This shows the consistency of our approximations.

### E. The nonrelativistic limit

In order to take the nonrelativistic limit $c\to+\infty$ of the previous equations, we need to subtract the contribution of the rest mass energy $mc^2$ of the SF. To that purpose, we make the Klein transformation

$$\varphi(t)=\frac{\hbar}{m}e^{-imc^2t/\hbar}\psi(t), \tag{33}$$

where $\psi$ is the wave function such that $\rho = |\psi|^2$. Substituting Eq. (33) into Eq. (1) and taking the limit $c \to +\infty$, we obtain the GP equation

$$i\hbar\frac{d\psi}{dt} + \frac{3}{2}i\hbar H\psi = m\frac{dV}{d|\psi|^2}\psi \tag{34}$$

for a nonrelativistic spatially homogeneous SF. On the other hand, in the nonrelativistic limit, Eqs. (2) and (3) become

$$\epsilon \sim \rho c^2, \qquad P/c^2 \to 0. \tag{35}$$

As explained previously, it is convenient to work in terms of hydrodynamic variables. We write the wave function under the Madelung form

$$\psi(t) = \sqrt{\rho(t)}e^{iS(t)/\hbar} \tag{36}$$

and introduce the energy

$$E(t) = -\frac{dS}{dt}. \tag{37}$$

Substituting Eq. (36) into the GP equation (34) and separating real and imaginary parts, we get

$$\frac{1}{\rho}\frac{d\rho}{dt} + \frac{3}{a}\frac{da}{dt} = 0, \tag{38}$$

$$E = mV'(\rho). \tag{39}$$

On the other hand, using Eq. (35), we find that the Friedmann equation (5) takes the form

$$\frac{3H^2}{8\pi G} = \rho. \tag{40}$$

We also note that the energy equation (4) reduces to Eq. (38). It can be integrated into $\rho \propto 1/a^3$ which, together with Eq. (40), leads to the EdS solution $a \propto t^{2/3}$ and $\rho = 1/6\pi G t^2$. Equations (38)–(40) can also be obtained from the general hydrodynamic equations derived in [77–79] by considering the particular case of a spatially homogeneous SF in the nonrelativistic limit $c \to +\infty$.

Finally, comparing Eqs. (8), (33) and (36) we find that $S_{\rm tot} = S - mc^2 t$ and $E_{\rm tot} = E + mc^2$. Substituting this decomposition into Eqs. (10)-(12) and taking the limit $c \to +\infty$ we recover Eqs. (38)–(40). We also find that Eq. (15) reduces to

$$\rho = \frac{Qm}{a^3}. \tag{41}$$

*Remarks:* the hydrodynamic equations (10)–(12) and (38)–(40) do not involve viscous terms because they are equivalent to the KG and GP equations. As a result, they describe a superfluid. We note that Eq. (11) for $S_{\rm tot}(t)$ or $E_{\rm tot}(t)$ is necessary in the relativistic case in order to have a closed system of equations [since $E_{\rm tot}$ appears explicitly in Eqs. (10) and (12)] while Eq. (39) for $S(t)$ or $E(t)$ is not strictly necessary in the nonrelativistic case [since $E$ does not appear in Eq. (38) and (40)].

### F. The quartic potential

In the case where the SF describes a BEC at zero temperature, the self-interaction potential can be written as

$$V(|\varphi|^2) = \frac{2\pi a_s m}{\hbar^2}|\varphi|^4, \tag{42}$$

where $m$ is the mass of the bosons and $a_s$ is their scattering length (see Appendix B for other expressions of the self-interaction constant). A repulsive self-interaction corresponds to $a_s > 0$ and an attractive self-interaction corresponds to $a_s < 0$. In the first case, $a_s$ may be interpreted as the "effective radius" of the bosons if we make an analogy with a classical hard spheres gas.

In terms of the pseudo rest-mass density $\rho$ and wave function $\psi$, the quartic potential (42) can be rewritten as

$$V(\rho) = \frac{2\pi a_s\hbar^2}{m^3}\rho^2, \qquad V(|\psi|^2) = \frac{2\pi a_s\hbar^2}{m^3}|\psi|^4. \tag{43}$$

From Eqs. (28) and (29), we obtain

$$P(\rho) = \frac{2\pi a_s\hbar^2}{m^3}\rho^2, \qquad c_s^2 = \frac{4\pi a_s\hbar^2}{m^3}\rho. \tag{44}$$

The pressure law $P(\rho)$ corresponds to a polytropic EOS of index $\gamma = 2$ (quadratic).

## III. THE CASE OF A QUARTIC POTENTIAL WITH A POSITIVE SCATTERING LENGTH

From now on, we restrict ourselves to a SF with a quartic potential given by Eq. (42). We focus on the evolution of a homogeneous SF in the regime where its oscillations are faster than the Hubble expansion. We first consider the case of a SF with a positive scattering length $a_s \geq 0$ corresponding to a repulsive self-interaction (the noninteracting case corresponds to $a_s = 0$). This is the most studied case in the literature. A very nice study has been done by Li *et al.* [94]. Here, we complement their study and provide more explicit analytical results.

### A. The basic equations

The equations of the problem are

$$\rho\sqrt{1 + \frac{8\pi a_s\hbar^2}{m^3c^2}\rho} = \frac{Qm}{a^3}, \tag{45}$$

$$\frac{3H^2}{8\pi G}=\rho\left(1+\frac{6\pi a_s\hbar^2}{m^3c^2}\rho\right), \tag{46}$$

$$\epsilon=\rho c^2\left(1+\frac{6\pi a_s\hbar^2}{m^3c^2}\rho\right), \tag{47}$$

$$P=\frac{2\pi a_s\hbar^2}{m^3}\rho^2, \tag{48}$$

$$w=\frac{\frac{2\pi a_s\hbar^2}{m^3c^2}\rho}{1+\frac{6\pi a_s\hbar^2}{m^3c^2}\rho}, \tag{49}$$

$$E_{\rm tot}=mc^2\sqrt{1+\frac{8\pi a_s\hbar^2}{m^3c^2}\rho}. \tag{50}$$

Equation (47) gives the relation between the energy density $\epsilon$ and the pseudo rest-mass density $\rho$. This is a second degree equation for $\rho$. The only physically acceptable solution (the one that is positive) is

$$\rho=\frac{m^3c^2}{12\pi a_s\hbar^2}\left(\sqrt{1+\frac{24\pi a_s\hbar^2}{m^3c^4}\epsilon}-1\right). \tag{51}$$

Combining Eqs. (48) and (51), we obtain the EOS [84,88,94]:

$$P=\frac{m^3c^4}{72\pi a_s\hbar^2}\left(\sqrt{1+\frac{24\pi a_s\hbar^2}{m^3c^4}\epsilon}-1\right)^2. \tag{52}$$

It coincides with the EOS obtained by Colpi *et al.* [54] in the context of boson stars (see also [56]). For a noninteracting SF ($a_s=0$), Eq. (52) reduces to $P=0$ meaning that a noninteracting SF behaves as pressureless matter.

### B. The evolution of the parameters with the scale factor *a*

The evolution of the pseudo rest-mass density $\rho$ with the scale factor $a$ is plotted in Fig. 1 (in the figures, unless otherwise specified, we use the dimensionless parameters defined in Appendix C). It starts from $+\infty$ at $a=0$ and decreases to 0 as $a\to+\infty$. For $a\to 0$:

$$\rho\sim\left(\frac{Q^2m^5c^2}{8\pi a_s\hbar^2}\right)^{1/3}\frac{1}{a^2}. \tag{53}$$

For $a\to+\infty$:

$$\rho\sim\frac{Qm}{a^3}. \tag{54}$$

The evolution of the energy density $\epsilon$ with the scale factor $a$ is plotted in Fig. 2. It starts from $+\infty$ at $a=0$ and decreases to 0 as $a\to+\infty$. For $a\to 0$:

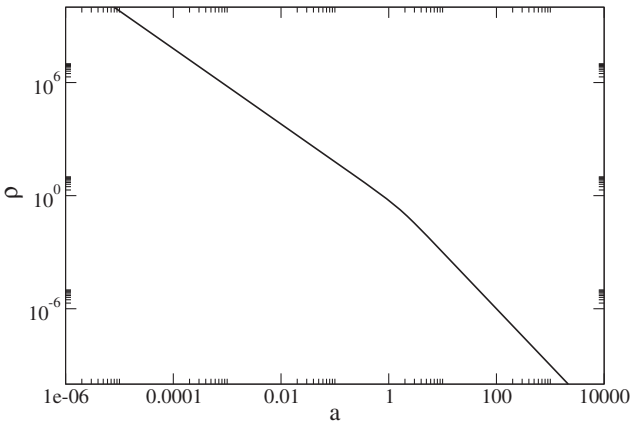


FIG. 1. Pseudo rest-mass density $\rho$ as a function of the scale factor $a$.

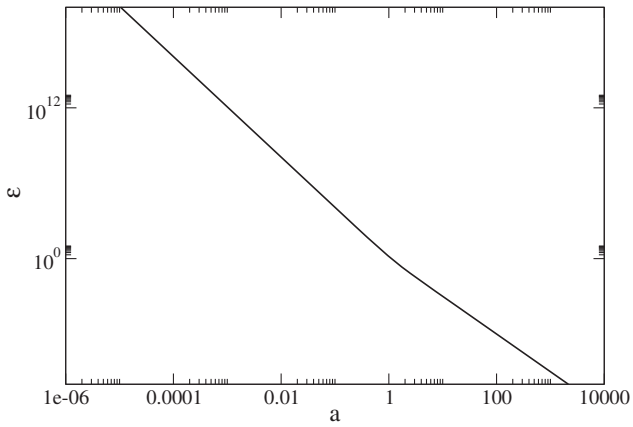


FIG. 2. Energy density $\epsilon$ as a function of the scale factor $a$.

$$\epsilon\sim\frac{6\pi a_s\hbar^2}{m^3}\rho^2\sim\frac{3}{2}(Q^4\pi m a_s\hbar^2c^4)^{1/3}\frac{1}{a^4}. \tag{55}$$

For $a\to+\infty$:

$$\epsilon\sim\rho c^2\sim\frac{Qmc^2}{a^3}. \tag{56}$$

The pressure is always positive. It starts from $+\infty$ at $a=0$ and decreases to 0 as $a\to+\infty$. For $a\to 0$:

$$P\sim\frac{1}{3}\epsilon\sim\frac{1}{2}(Q^4\pi m a_s\hbar^2c^4)^{1/3}\frac{1}{a^4}. \tag{57}$$

For $a\to+\infty$:

$$P\sim\frac{2\pi a_s\hbar^2}{m^3c^4}\epsilon^2\sim\frac{2\pi a_s\hbar^2Q^2}{ma^6}\simeq 0. \tag{58}$$

The relationship between the pressure and the energy density is plotted in Fig. 3.

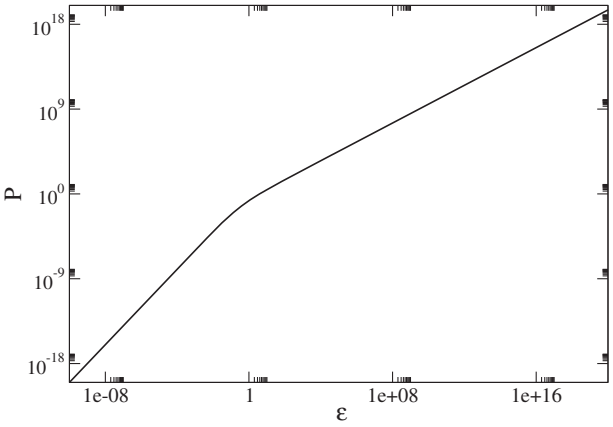


FIG. 3. Pressure $P$ as a function of the energy density $\epsilon$.

The evolution of the EOS parameter $w = P/\epsilon$ with the scale factor $a$ is plotted in Fig. 4. It starts from

$$w_i = \frac{1}{3} \tag{59}$$

when $a = 0$ and decreases to 0 as $a \to +\infty$. For $a \to 0$:

$$w \simeq \frac{1}{3} - \frac{1}{6}\left(\frac{m^2c^2}{\pi a_s \hbar^2 Q}\right)^{2/3} a^2. \tag{60}$$

For $a \to +\infty$:

$$w \sim \frac{2\pi a_s \hbar^2 Q}{m^2 c^2 a^3}. \tag{61}$$

The total energy $E_{\rm tot}$ starts from $+\infty$ at $a = 0$ and decreases up to $mc^2$ as $a \to +\infty$. For $a \to 0$:

$$\frac{E_{\rm tot}}{mc^2} \sim \left(\frac{8\pi a_s \hbar^2 Q}{m^2 c^2}\right)^{1/3} \frac{1}{a}. \tag{62}$$

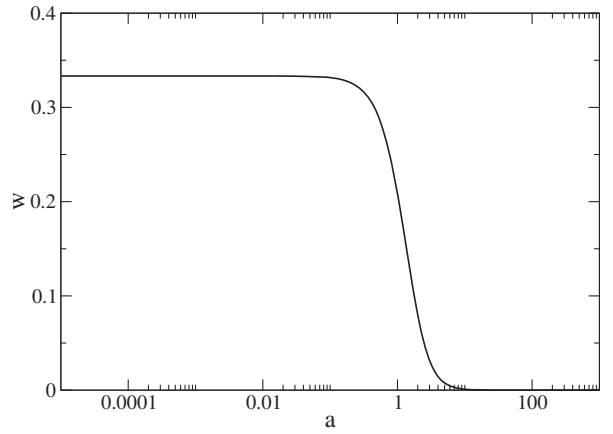


FIG. 4. EOS parameter $w$ as a function of the scale factor $a$.

For $a \to +\infty$:

$$\frac{E_{\rm tot}}{mc^2} \simeq 1 + \frac{4\pi a_s \hbar^2 Q}{m^2 c^2 a^3}. \tag{63}$$

### C. The temporal evolution of the parameters

In this section, we determine the temporal evolution of the parameters assuming that the Universe contains only the SF. For a quartic potential with $a_s \geq 0$, the differential equation (24) becomes

$$\left(\frac{d\rho}{dt}\right)^2 = 24\pi G\rho^3 \frac{(1+\frac{6\pi a_s\hbar^2}{m^3c^2}\rho)(1+\frac{8\pi a_s\hbar^2}{m^3c^2}\rho)^2}{(1+\frac{12\pi a_s\hbar^2}{m^3c^2}\rho)^2}. \tag{64}$$

The solution of this differential equation which satisfies the condition that $\rho \to +\infty$ as $t \to 0$ is

$$\int_{\frac{2\pi a_s\hbar^2}{m^3c^2}\rho}^{+\infty} \frac{(1+6x)dx}{x^{3/2}(1+3x)^{1/2}(1+4x)} = \left(\frac{12Gm^3c^2}{a_s\hbar^2}\right)^{1/2} t. \tag{65}$$

The integral can be computed analytically:

$$\int \frac{(1+6x)dx}{x^{3/2}(1+3x)^{1/2}(1+4x)} = 4\tan^{-1}\left(\sqrt{\frac{x}{1+3x}}\right) - 2\sqrt{\frac{1+3x}{x}}. \tag{66}$$

From these equations, we can obtain the temporal evolution of the pseudo rest-mass density $\rho(t)$. Then, using Eqs. (45)–(50), we can obtain the temporal evolution of all the parameters. The temporal evolution of the scale factor $a$ is plotted in Fig. 5. It starts from $a = 0$ at $t = 0$ and increases to $+\infty$ as $t \to +\infty$. We do not show the other curves because they can be easily deduced from Figs. 1, 2 and 4 since $a$ is a monotonic function of time. However, we provide below the asymptotic behaviors of all the parameters.

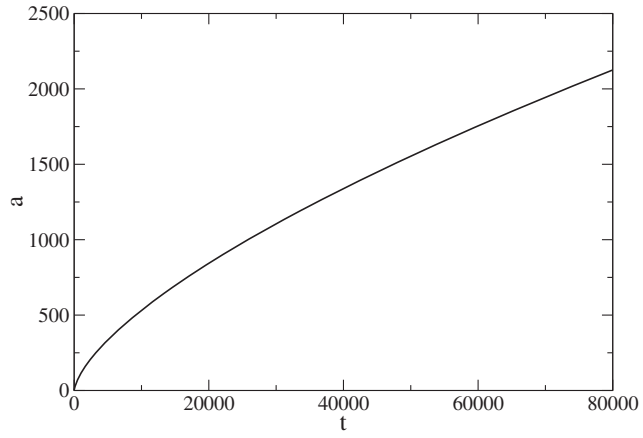


FIG. 5. Temporal evolution of the scale factor $a$.

For $t \to 0$:

$$a \sim 2\left(\frac{\pi^4 G^3 Q^4 m a_s \hbar^2}{c^2}\right)^{1/12} t^{1/2}, \tag{67}$$

$$\rho \sim \frac{m^{3/2} c}{8\pi\hbar a_s^{1/2} G^{1/2} t}, \tag{68}$$

$$\epsilon \sim \frac{3c^2}{32\pi G t^2}, \tag{69}$$

$$P \sim \frac{c^2}{32\pi G t^2}, \tag{70}$$

$$w \simeq \frac{1}{3} - \frac{2m^{3/2} G^{1/2} c}{3\hbar a_s^{1/2}} t, \tag{71}$$

$$\frac{E_{\rm tot}}{mc^2} \sim \left(\frac{a_s \hbar^2}{m^3 G c^2}\right)^{1/4} \frac{1}{t^{1/2}}. \tag{72}$$

For $t \to +\infty$:

$$a \sim (6\pi G Q m t^2)^{1/3}, \tag{73}$$

$$\rho \sim \frac{1}{6\pi G t^2}, \tag{74}$$

$$\epsilon \sim \frac{c^2}{6\pi G t^2}, \tag{75}$$

$$P \sim \frac{a_s \hbar^2}{18\pi G^2 m^3 t^4}, \tag{76}$$

$$w \sim \frac{a_s \hbar^2}{3 G m^3 c^2 t^2}, \tag{77}$$

$$\frac{E_{\rm tot}}{mc^2} \simeq 1 + \frac{2 a_s \hbar^2}{3 m^3 G c^2 t^2}. \tag{78}$$

### D. The different eras

In the fast oscillation regime, a SF with a repulsive self-interaction ($a_s \geq 0$) undergoes two distinct eras. For $a \to 0$, the EOS (52) reduces to Eq. (57) so the SF behaves as radiation. The scale factor increases like $a \propto t^{1/2}$. For $a \to +\infty$, the EOS (52) reduces to Eq. (58) so the SF behaves essentially as pressureless matter (dust) like in the EdS model.[5] The scale factor increases like $a \propto t^{2/3}$. Therefore, the SF undergoes a radiationlike era ($w = 1/3$) followed by a matterlike era ($w = 0$). Since $w > -1/3$, the Universe is always decelerating. As emphasized by Li *et al.* [94], the radiationlike era is due to the self-interaction of the SF ($a_s \neq 0$). There is no such phase for a noninteracting SF ($a_s = 0$). This remark will be made more precise in Sec. III E. On the other hand, if we identify the SF as the source of DM, it is possible to determine its charge $Q$ by considering its asymptotic behavior in the matterlike era. It is given by Eq. (E12) of Appendix E.

In conclusion, a SF with a repulsive self-interaction behaves at early times as radiation and at late times as dust. We can estimate the transition between the radiationlike era and the matterlike era of the SF as follows. First of all, using Eqs. (45) and (49), we find that the scale factor corresponding to a value $w$ of the EOS parameter is

$$a = \left(\frac{2\pi a_s \hbar^2 Q}{m^2 c^2}\right)^{1/3} \frac{(1-3w)^{1/2}}{w^{1/3}(1+w)^{1/6}}. \tag{79}$$

Interestingly, this equation provides an analytical expression of the function $a(w)$, the inverse of the function $w(a)$ plotted in Fig. 4. If we consider that the transition between the radiationlike era and the matterlike era of the SF corresponds to $w_t = 1/6$,[6] we obtain

$$a_t = \frac{\sqrt{3}}{7^{1/6}} \left(\frac{2\pi a_s \hbar^2 Q}{m^2 c^2}\right)^{1/3}. \tag{80}$$

This corresponds to $\epsilon_t = 2\rho_t c^2 = m^3 c^4/3\pi a_s \hbar^2$. In order to make numerical applications here and in the following sections, it is convenient to introduce the reference scale factor $a_*$ defined in Appendix C. Using the expression (E12) of the charge of the SF, we get

$$a_* \equiv \left(\frac{2\pi |a_s| \hbar^2 Q}{m^2 c^2}\right)^{1/3} = \left(\frac{2\pi |a_s| \hbar^2 \Omega_{\rm dm,0} \epsilon_0}{m^3 c^4}\right)^{1/3} = 6.76 \times 10^{-7} \left(\frac{|a_s|}{\rm fm}\right)^{1/3} \frac{{\rm eV}/c^2}{m}. \tag{81}$$

Therefore, $a_t = (\sqrt{3}/7^{1/6}) a_*$. According to Eq. (81), we note that $a_t$ depends only on the ratio $a_s/m^3$ (see Sec. III I). For a SF with a ratio $a_s/m^3$ given by Eq. (D7), we get $a_t = 1.26 \times 10^{-5}$. For a SF with a ratio $a_s/m^3$ given by Eq. (D23), we get $a_t = 1.35 \times 10^{-5}$. This analytical result is in good agreement with the numerical result of Li *et al.* [94] (see their Fig. 1).

[5] The pressure of the SF is nonzero but since $P \propto \epsilon^2 \ll \epsilon$ for $\epsilon \to 0$, everything happens in the cosmological Friedmann equations (4) and (5) describing the large scales as if the Universe were pressureless. In particular, Eq. (4) implies $\epsilon \propto a^{-3}$ for $a \to +\infty$ as when $P = 0$. However, the nonzero pressure of the SF is important at small scales, i.e. at the scale of dark matter halos, because it can prevent singularities and avoid the cusp problem and the missing satellite problem as discussed in the Introduction (see also Appendix D).

[6] This value is obtained by analogy with the standard model (see Appendix E). Since $P_{\rm m} = 0$ and $P_{\rm r} = \epsilon_{\rm r}/3$, the EOS parameter of the standard model (neglecting here dark energy) is $w = P_{\rm r}/(\epsilon_{\rm r} + \epsilon_{\rm m}) = \epsilon_{\rm r}/[3(\epsilon_{\rm r} + \epsilon_{\rm m})]$. At the radiation-matter equality ($\epsilon_{\rm r} = \epsilon_{\rm m}$), we get $w = 1/6$. This transition value is also the arithmetic mean of $w = 1/3$ (radiation) and $w = 0$ (dust).

### E. Validity of the fast oscillation regime

The previous results are valid in the fast oscillation regime $\omega \gg H$. In this section, we determine the domain of validity of this regime.

For a spatially homogeneous SF, the pulsation is given by $\omega = d\theta/dt = (1/\hbar)dS_{\rm tot}/dt = -E_{\rm tot}/\hbar$ (see Appendix A) and the Hubble parameter is given by $H^2 = 8\pi G\epsilon/3c^2$ (see Sec. II B). Therefore, the fast oscillation regime corresponds to

$$\frac{E_{\rm tot}^2}{\hbar^2} \gg \frac{8\pi G}{3c^2}\epsilon. \tag{82}$$

Introducing the dimensionless variables of Appendix C, this condition can be rewritten as

$$\tilde{E}_{\rm tot}^2 \gg \tilde{\epsilon}/\sigma, \tag{83}$$

where

$$\sigma = \frac{3a_s c^2}{4Gm} \tag{84}$$

is a new dimensionless parameter that can be interpreted as the ratio $\sigma = 3a_s/2r_S$ between the effective Schwarzschild radius $r_S = 2Gm/c^2$ of the bosons (see Sec. III H) and their scattering length $a_s$. Introducing proper normalizations, we get

$$\sigma = 5.67\times 10^{47}\,\frac{a_s}{\rm fm}\frac{{\rm eV}/c^2}{m}. \tag{85}$$

The dimensionless variables $\tilde{E}_{\rm tot}^2$ and $\tilde{\epsilon}$ are plotted as a function of $\tilde{a}$ in Fig. 6. Their ratio $\tilde{E}_{\rm tot}^2/\tilde{\epsilon}$ is plotted as a function of $\tilde{a}$ in Fig. 7. The intersection of this curve with the line $\tilde{E}_{\rm tot}^2/\tilde{\epsilon} = 1/\sigma$ determines the domain of validity of the fast oscillation regime.

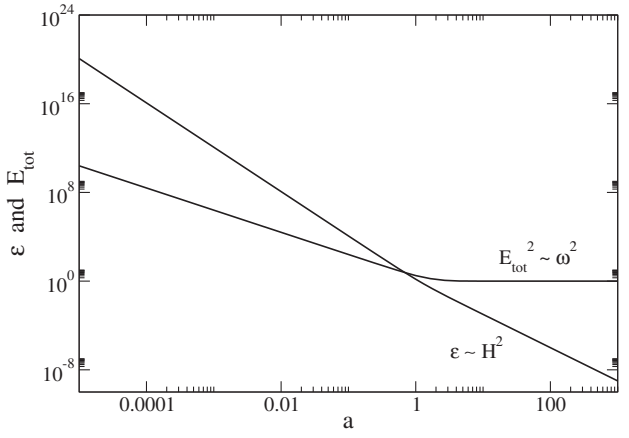


FIG. 6. Graphical construction determining the validity of the fast oscillation regime. The transition scale $a_v$ corresponds to the intersection of the curves $\sigma\tilde{E}_{\rm tot}^2$ and $\tilde{\epsilon}$.

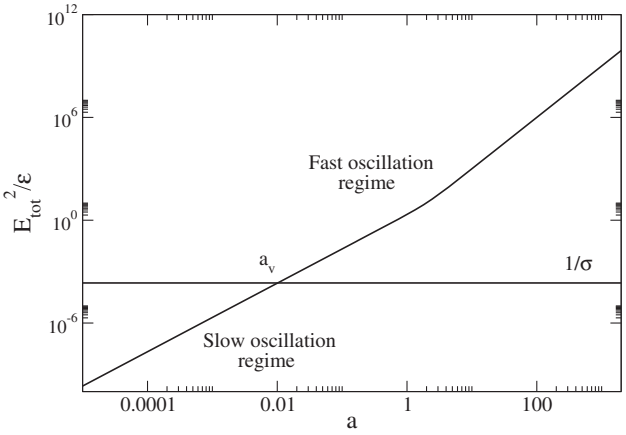


FIG. 7. Ratio $(\omega/H)^2$ as a function of the scale factor $a$.

Combining Eqs. (45), (47), and (50), we find that the fast oscillation regime is valid for $a \gg a_v$ with

$$a_v = \left(\frac{2\pi a_s\hbar^2 Q}{m^2c^2}\right)^{1/3} f\left(\frac{3a_s c^2}{4Gm}\right), \tag{86}$$

where the function $f(\sigma)$ is defined by

$$f(\sigma) = \frac{1}{r^{1/3}(1+4r)^{1/6}} \tag{87}$$

with

$$r = \frac{4\sigma - 1 + \sqrt{(4\sigma-1)^2 + 12\sigma}}{6}. \tag{88}$$

For $\sigma \to 0$:

$$f(\sigma) \sim \frac{1}{\sigma^{1/3}}. \tag{89}$$

For $\sigma \to +\infty$:

$$f(\sigma) \sim \frac{\sqrt{3}}{2^{4/3}}\frac{1}{\sigma^{1/2}}. \tag{90}$$

These asymptotic results can be written more explicitly by restoring the original variables. When $a_s = 0$:

$$a_v(0) = \left(\frac{8\pi GQ\hbar^2}{3mc^4}\right)^{1/3}. \tag{91}$$

This corresponds to $\epsilon_v(0) = \rho_v(0)c^2 = 3m^2c^6/8\pi G\hbar^2$. Using the expression of the charge given by Eq. (E12), and introducing proper normalizations, we obtain

$$a_v(0) \simeq 8.17\times 10^{-23}\left(\frac{{\rm eV}/c^2}{m}\right)^{2/3}. \tag{92}$$

This value corresponds to the beginning of the fast oscillation regime in the noninteracting case ($\omega = mc^2/\hbar \gg H$). When $a_s \gg r_S$:

$$a_v \sim \left(\frac{\pi^2 G^3 \hbar^4 Q^2}{a_s m c^{10}}\right)^{1/6}. \tag{93}$$

Using the expression of the charge given by Eq. (E12), and introducing proper normalizations, we obtain

$$a_v \simeq 6.17 \times 10^{-31} \left(\frac{\mathrm{fm}}{a_s}\right)^{1/6} \left(\frac{\mathrm{eV}/c^2}{m}\right)^{1/2}. \tag{94}$$

This value corresponds to the beginning of the fast oscillation regime in the strongly self-interacting case.

For $a \gg a_v$, we are in the fast oscillation regime in which the SF behaves successively as radiation and matter. For $a \ll a_v$, we are in the slow oscillation regime in which the SF behaves as stiff matter. Therefore, $a_v$ marks the end of the stiff matter era (see Appendix F). A complex SF generically undergoes three successive eras: a stiff matter era for $a < a_v$, a radiationlike era for $a_v < a < a_t$, and a matterlike era for $a > a_t$. The transition scales $a_v$ and $a_t$ are given analytically by Eqs. (86) and (80) respectively. Actually, the radiationlike era only exists if $a_t > a_v$. This corresponds to $f(\sigma) < \sqrt{3}/7^{1/6}$ leading to the condition

$$\sigma = \frac{3a_s c^2}{4Gm} > \frac{2}{7}, \qquad \text{i.e.,} \qquad a_s > \frac{8}{21}\frac{Gm}{c^2} = \frac{4}{21} r_S. \tag{95}$$

When $a_s < (4/21) r_S$, the SF undergoes only two successive eras: a stiff matter era for $a < a_v$ and a matterlike era for $a > a_v$. There is no radiationlike era even though the SF is self-interacting. This generalizes the result of Li *et al.* [94] according to which a noninteracting SF ($a_s = 0$) does not present a radiationlike era. This result remains true as long as $a_s < (4/21) r_S$. In this regime, the transition scale $a_v$ depends very weakly on the scattering length $a_s$ of the bosons (see below). In the noninteracting case ($a_s = 0$), $a_v$ is given by Eq. (91). We note that the transition between the stiff matter era and the matterlike era happens later with decreasing mass. This is in agreement with the observation of Li *et al.* [94] but Eq. (91) provides an explicit analytical formula refining this statement. This formula, together with Eq. (E12), displays a $m^{-2/3}$ scaling for $a_v(0)$.

### F. Phase diagram

We can represent the previous results on a phase diagram (see Fig. 8) where we plot the transition scales $a_v$ and $a_t$ as a function of the scattering length $a_s$. To that purpose, it is convenient to normalize the scale factor $a$ by the reference value $a_v(0)$ given by Eq. (91) that is independent of $a_s$. The scattering length $a_s$ can be normalized by the effective Schwarzschild radius $r_S$ using the parameter $\sigma = 3a_s/2r_S$ defined by Eq. (84). With these normalizations, the transition scale $a_v$ between the slow and fast oscillation regimes is given by

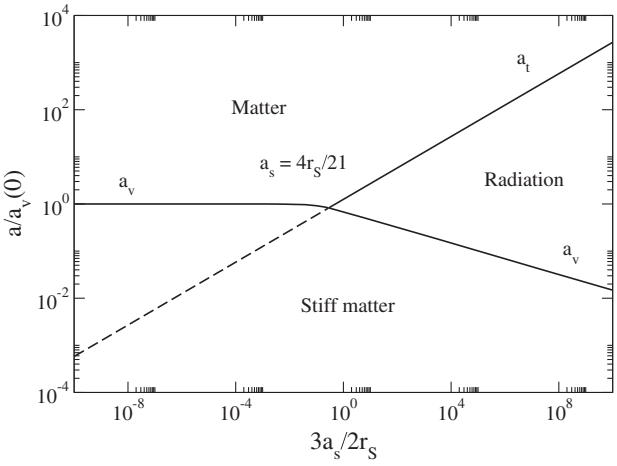


FIG. 8. Phase diagram showing the different eras of the SF during the evolution of the Universe as a function of the scattering length of the bosons in the case of a repulsive self-interaction.

$$\frac{a_v}{a_v(0)} = f(\sigma)\sigma^{1/3}. \tag{96}$$

For $\sigma = 0$:

$$\frac{a_v}{a_v(0)} = 1. \tag{97}$$

For $\sigma = 2/7$:

$$\frac{a_v}{a_v(0)} = \frac{\sqrt{3}}{7^{1/6}}\left(\frac{2}{7}\right)^{1/3} \simeq 0.825. \tag{98}$$

For $\sigma \to +\infty$:

$$\frac{a_v}{a_v(0)} \sim \frac{1}{4^{1/6}}\left(\frac{3}{4}\right)^{1/2}\frac{1}{\sigma^{1/6}}. \tag{99}$$

The transition scale $a_v$ starts from the value $a_v(0)$ given by Eq. (91) for $a_s = 0$, decreases slowly up to $a_v = (\sqrt{3}/7^{1/6})(2/7)^{1/3} a_v(0)$ when $a_s = (4/21) r_S$, and decreases like $a_s^{-1/6}$ according to Eq. (93) for $a_s \gg r_S$. Therefore, the domain of validity of the fast oscillation regime is larger when the self-interaction is stronger (the stiff matter era ends earlier). On the other hand, the transition scale $a_t$ between the radiationlike era and the matterlike era is given by

$$\frac{a_t}{a_v(0)} = \frac{\sqrt{3}}{7^{1/6}}\sigma^{1/3}. \tag{100}$$

It starts from 0 at $a_s = 0$ and increases like $a_s^{1/3}$ according to Eq. (80). The transition scales $a_v$ and $a_t$ cross each other

at $a_s=(4/21)r_S$. At that point $a_v = a_t = (\sqrt{3}/7^{1/6})(2/7)^{1/3}a_v(0)$.

We can now describe the phase diagram (see Fig. 8). When $a_s \leq (4/21)r_S$, the SF is in the stiff matter era for $0 \leq a \leq a_v$ and in the matterlike era for $a \geq a_v$.[7] When $a_s \geq (4/21)r_S$, the SF is in the stiff matter era for $0 \leq a \leq a_v$, in the radiationlike era for $a_v \leq a \leq a_t$, and in the matterlike era for $a \geq a_t$. Therefore, when $a_s \leq (4/21)r_S$, $a_v$ determines the transition scale between the stiff matter era and the matterlike era. When $a_s \geq (4/21)r_S$, $a_v$ determines the transition scale between the stiff matter era and the radiationlike era. We note that the radiationlike era starts earlier and lasts longer as the self-interaction strength $a_s$ increases (the stiff matter era ends earlier and the matterlike era starts later). This is in agreement with Fig. 1 of Li *et al.* [94].

Let us make a numerical application. We first consider a noninteracting SF. Using the value of $m$ given by Eq. (D3), we obtain $a_v(0) = 1.86 \times 10^{-8}$. This is the transition scale between the stiff matter era and the matterlike era. For a self-interacting SF, using the values of $(m, a_s)$ given by Eq. (D8), we obtain $\sigma = 2.27 \times 10^{45}$ and $a_v = 1.45 \times 10^{-28}$. In that case, the stiff matter era (if it really physically exists) ends very early. On the other hand, using the values of $(m, a_s)$ given by Eq. (D22), we obtain $\sigma = 2.10 \times 10^{10}$ and $a_v = 5.14 \times 10^{-11}$. In the two cases $\sigma \gg 2/7$ so the SF is deep in the strongly self-interacting regime and there is a radiationlike era. Therefore, $a_v$ determines the transition between the stiff matter era and the radiationlike era (see Sec. III D for the determination of the transition scale between the radiationlike era and the matterlike era). Our analytical result $a_v = 5.14 \times 10^{-11}$ is in good agreement with the numerical result obtained by Li *et al.* [94] (see their Fig. 1).

*Particular cases:* When $m = a_s = 0$, Eqs. (2) and (3) imply $P = \epsilon$, so there is only a stiff matter era. When $m \neq 0$ and $a_s = 0$ (noninteracting case), there is only a stiff matter era and a pressureless matterlike era. The transition takes place at $a_v(0)$ given by Eq. (91). It scales as $m^{-2/3}$ and tends to $+\infty$ when $m \to 0$. When $m = 0$ and $a_s > 0$ (massless case), there is only a stiff matter era and a radiationlike era. The transition takes place at

$$a_v = \left(\frac{8\pi^3 G^3 \hbar^3 Q^2}{\lambda c^9}\right)^{1/6} \tag{101}$$

obtained from Eq. (93) by replacing $a_s$ by $\lambda$, using Eq. (B1). It scales as $\lambda^{-1/6}$ (assuming $Q$ independent of $\lambda$) and tends to $+\infty$ when $\lambda \to 0$.

[7]For $a_s = 0$, the stiff matter era may be connected to the matterlike era by a short period of inflation with a constant energy density (plateau) as argued in [98].

### G. Inflation era?

It is well known that a massive real SF with a quartic potential (or a sufficiently flat potential) undergoes a stiff matter era followed by an inflation era which is an attractor of the KGE equations [105,106]. Finally, it oscillates and behaves on average as radiation and pressureless matter. We may wonder whether a complex SF also experiences an inflation era. This would be the case if $S_{\rm tot} \simeq 0$ in the early Universe because, in that case, it would behave as a real SF. However, because of the charge conservation constraint (15), the condition $S_{\rm tot} \simeq 0$ implies $E_{\rm tot} \simeq Q \simeq 0$. Therefore, the charge of the SF should be extremely small [95,96] which may be considered artificial.

### H. Weakly and strongly self-interacting regimes

We note that the phase diagram of Fig. 8 depends on a dimensionless control parameter $\sigma$ which is, up to a factor $3/2$, the ratio between the scattering length $a_s$ of the bosons and their effective Schwarzschild radius

$$r_S = \frac{2Gm}{c^2} = 2.65 \times 10^{-48} \frac{m}{\mathrm{eV}/c^2}\,\mathrm{fm}. \tag{102}$$

The strongly self-interacting regime corresponds to $a_s \gg r_S$ and the weakly self-interacting regime corresponds to $a_s \ll r_S$. In general $r_S$ is very small. For example, for bosons with $m = 2.92 \times 10^{-22}$ eV$/c^2$ (see Appendix D), we have $r_S = 7.74 \times 10^{-70}$ fm. Therefore, even when $a_s \sim 10^{-68}$ fm we are in the strongly self-interacting regime, not in the weakly self-interacting regime, although this value of $a_s$ may seem very "small" at first sight.

We note that the effective Schwarzschild radius of the bosons is much smaller than their Compton wavelength

$$\lambda_C = \frac{\hbar}{mc} = 0.197 \frac{\mathrm{GeV}/c^2}{m}\,\mathrm{fm} \tag{103}$$

because their mass $m$ is much smaller than the Planck mass $M_P = (\hbar c/G)^{1/2} = 1.22 \times 10^{19}$ GeV$/c^2$. For example, for bosons with $m = 2.92 \times 10^{-22}$ eV$/c^2$, we have $\lambda_C = 6.75 \times 10^{29}$ fm.

The condition of validity of the strongly self-interacting regime can also be expressed in terms of the variables introduced in Appendix B. Using the dimensionless self-interaction constant (B1), we find that the strongly self-interacting regime $a_s \gg r_S$ corresponds to

$$\frac{\lambda}{8\pi} \gg \frac{r_S}{\lambda_C} = 2\left(\frac{m}{M_P}\right)^2. \tag{104}$$

For bosons with $m = 2.92 \times 10^{-22}$ eV$/c^2$, we get $\lambda/8\pi \gg 1.15 \times 10^{-99}$. Therefore, even when $\lambda/8\pi \sim 10^{-98}$ we are in the strongly self-interacting regime, not in the

noninteracting regime $\lambda = 0$ (!). A similar remark was made in Appendix A. 3 of [99] using different arguments. Therefore, it is important to take the self-interaction of the bosons into account even if the self-interaction constant seems to be very small. Many works (see, e.g., [49,50]) neglect the self-interaction of the bosons. Their results may substantially change if it is taken into account.

Finally, using the dimensional self-interaction constant (B2), we find that the strongly self-interacting regime $a_s \gg r_S$ corresponds to

$$\lambda_s \gg \frac{8\pi G\hbar^2}{c^2} = 1.295 \times 10^{-69}\ \mathrm{eV\,cm^3}. \tag{105}$$

We note that this bound is independent of the mass of the bosons.

According to the previous results, the dimensionless parameter $\sigma$ that measures the strength of the self-interaction for our problem can be written as

$$\sigma = \frac{3a_s}{2r_S} = \frac{3}{4}\frac{\lambda}{8\pi}\left(\frac{M_P}{m}\right)^2 = \frac{3\lambda_s c^2}{16\pi G\hbar^2}. \tag{106}$$

The weakly self-interaction regime corresponds to $\sigma \ll 1$ and the strongly self-interaction regime corresponds to $\sigma \gg 1$. The dimensionless self-interaction constant $\lambda$ has a different meaning. We can be in the strongly self-interaction regime $\sigma \gg 1$ for our problem even when $\lambda \ll 1$ (weak self-interaction in quantum field theory) due to the large factor $(M_P/m)^2$ when $m \ll M_P$.

### I. The ratio $a_s/m^3$

Using the expression (E12) of the charge $Q$ of the SF, we see that the equations of the problem (45)–(50) depend on the mass $m$ of the SF and on its scattering length $a_s$ only through the ratio $a_s/m^3$.[8] In this section, we show how cosmological (large scale) observations can constrain the ratio $a_s/m^3$. We then compare these constraints with the value of $a_s/m^3$ obtained from astrophysical (small scale) observations (see Appendix D).

[8]This is because, as noted in Sec. II D, the simplified equations (45)–(50) are obtained in a TF, or semiclassical, approximation where the quantum potential is neglected ($\hbar = 0$). By contrast, the scale $a_v$ marking the transition between the slow and fast oscillation regimes is due to quantum mechanics ($\hbar \neq 0$) so it depends on the two individual parameters $a_s$ and $m$, or equivalently $a_s/m^3$ and $a_s/m$ as is apparent on Eq. (86) with Eq. (E12). To see the effect of $\hbar$ in the equations, it is better to use the parameter $\lambda_s/(mc^2)^2$ instead of $4\pi a_s\hbar^2/m^3c^4$ [see Eq. (B5)] because the appearance of $\hbar$ in the latter does not correspond to the quantum potential and can be absorbed in the self-interaction constant. Equations (45)–(50) can then be written in terms of $\lambda_s/(mc^2)^2$ only, in which $\hbar$ does not appear (TF approximation). By contrast, $a_v$ given by Eq. (96), depends on $m/\hbar$ [through Eqs. (91) and (E12)] and on $\lambda_s/\hbar^2$ [through Eq. (106)], in which $\hbar$ appears explicitly.

Following Li *et al.* [94], we impose that, at the epoch of matter-radiation equality, corresponding to the scale factor $a_{\rm eq} = 2.95 \times 10^{-4}$ (see Appendix E), the SF should be nonrelativistic, i.e., it should behave as pressureless matter (CDM-like phase). This is a constraint imposed by CMB. This condition can be expressed by the inequality

$$w(a_{\rm eq}) \leq \chi, \tag{107}$$

where $\chi$ is a small constant that Li *et al.* [94] take equal (somehow arbitrarily) to $\chi = 10^{-3}$. In the matterlike era where $w \ll 1$, the function $w(a)$ can be approximated by Eq. (61) so that

$$w(a_{\rm eq}) \simeq \frac{2\pi a_s\hbar^2 Q}{m^2c^2a_{\rm eq}^3}. \tag{108}$$

Using the expression (E12) of the charge $Q$ of the SF and the expression (E9) of the scale factor at the epoch of matter-radiation equality, we obtain

$$w(a_{\rm eq}) \simeq \frac{2\pi a_s\hbar^2\epsilon_0\Omega_{\rm dm,0}\Omega_{\rm m,0}^3}{m^3c^4\Omega_{\rm r,0}^3}. \tag{109}$$

Introducing proper normalizations, we get

$$w(a_{\rm eq}) = 1.20 \times 10^{-8}\frac{a_s}{\rm fm}\left(\frac{\mathrm{eV}/c^2}{m}\right)^3. \tag{110}$$

The condition of Eq. (107) implies

$$\frac{a_s}{m^3} \leq \frac{\chi c^4\Omega_{\rm r,0}^3}{2\pi\hbar^2\Omega_{\rm dm,0}\Omega_{\rm m,0}^3\epsilon_0}, \tag{111}$$

i.e.,

$$\frac{a_s}{\rm fm}\left(\frac{\mathrm{eV}/c^2}{m}\right)^3 \leq 8.31 \times 10^4. \tag{112}$$

Using the results of Appendix B, we analytically recover the result $\lambda_s/(mc^2)^2 \leq 4.07 \times 10^{-17}\ \mathrm{cm^3/eV}$ of Li *et al.* [94] [see their Eq. (38)].

Using astrophysical considerations related to the minimum size of DM halos (Fornax) observed in the Universe and interpreted as the ground state of a self-gravitating BEC (see Appendix D), we find that the ratio $a_s/m^3$ has the value $(a_s/\mathrm{fm})((\mathrm{eV}/c^2)/m)^3 = 3.28 \times 10^3$ leading to $w(a_{\rm eq}) = 3.94 \times 10^{-5}$. These values are much smaller than the bounds implied by Eqs. (107) and (112) for $\chi = 10^{-3}$. These inequalities are fulfilled by two orders of magnitude. The same remark applies to the values $(a_s/\mathrm{fm})((\mathrm{eV}/c^2)/m)^3 = 4.10 \times 10^3$ and $w(a_{\rm eq}) = 4.92 \times 10^{-5}$ corresponding to the fiducial model of Li *et al.* [94].

Actually, we can relate the EOS parameter $w(a_{\rm eq})$ at the epoch of matter-radiation equality (cosmology/large scales) to the minimum size $R$ of the DM halos observed in the Universe (astrophysics/small scales). Indeed, combining Eqs. (109) and (D5), we get

$$w(a_{\rm eq}) = \frac{2\epsilon_0 G R^2 \Omega_{\rm dm,0}\Omega_{\rm m,0}^3}{\pi c^4 \Omega_{r,0}^3}. \quad (113)$$

Introducing proper normalizations, Eq. (113) can be rewritten as

$$w(a_{\rm eq}) = 3.94\times 10^{-5}\left(\frac{R}{\rm kpc}\right)^2. \quad (114)$$

The condition $w(a_{\rm eq}) \leq 10^{-3}$ corresponds to a minimum halo size less than $R = 5.04$ kpc, a condition which is observationaly realized. Inversely, taking $R = 1$ kpc (Fornax), we get $w(a_{\rm eq}) = 3.94\times 10^{-5}$. Taking $R = 1.12$ kpc, corresponding to the fiducial model of Li *et al.* [94], we get $w(a_{\rm eq}) = 4.92\times 10^{-5}$.

We can also compare the scale $a_t$ corresponding to the transition between the radiationlike era and the matterlike era of the SF (see Sec. III E) with the scale $a_{\rm eq}$ corresponding to the matter-radiation equality. Combining Eqs. (80) and (108), we obtain

$$\frac{a_t}{a_{\rm eq}} = \frac{\sqrt{3}}{7^{1/6}} w(a_{\rm eq})^{1/3}. \quad (115)$$

We first note that the condition $w(a_{\rm eq}) \ll 1$ is equivalent to $a_t \ll a_{\rm eq}$, i.e., the transition between the radiationlike era and the matterlike era of the SF must take place long before the standard radiation-matter equality. Taking $w(a_{\rm eq}) \leq 10^{-3}$, we obtain the constraint $a_t/a_{\rm eq} \leq 0.125$. Taking $w(a_{\rm eq}) = 3.94\times 10^{-5}$, corresponding to the model of Appendix D (Fornax), we obtain $a_t/a_{\rm eq} = 4.26\times 10^{-2}$. Taking $w(a_{\rm eq}) = 4.92\times 10^{-5}$, corresponding to the fiducial model of Li *et al.* [94], we obtain $a_t/a_{\rm eq} = 4.59\times 10^{-2}$. Since $a_t$ is much below $a_{\rm eq}$, we confirm that, at the radiation-matter equality epoch, the SF behaves as pressureless matter, i.e., it is nonrelativistic.

Finally, we can obtain the value of the ratio $\mu = \epsilon_{\rm SF}/\epsilon_{\rm r}$ between the radiation of the SF and the standard radiation in the radiationlike era of the SF (see Appendix E). Combining Eqs. (E15) and (109), we obtain

$$\mu = \left(\frac{27}{16}\right)^{1/3}\frac{\Omega_{\rm dm,0}}{\Omega_{\rm m,0}} w(a_{\rm eq})^{1/3}. \quad (116)$$

We first note that the condition $w(a_{\rm eq}) \ll 1$ is equivalent to $\mu \ll 1$ i.e. the radiation of the SF must be much smaller than the standard radiation. Taking $w(a_{\rm eq}) \leq 10^{-3}$, we obtain the constraint $\mu \leq 0.100$. Therefore, the energy of SF radiation must be about one order of magnitude smaller than the energy of standard radiation. Taking $w(a_{\rm eq}) = 3.94\times 10^{-5}$, corresponding to the model of Appendix D (Fornax), we obtain $\mu = 3.42\times 10^{-2}$. Taking $w(a_{\rm eq}) = 4.92\times 10^{-5}$, corresponding to the fiducial model of Li *et al.* [94], we obtain $\mu = 3.68\times 10^{-2}$. This is in good agreement with the value inferred from their Fig. 3. We also find that the effective temperature of the SF [see Eq. (E22)] is $T_{\rm eff} \simeq 0.43T$.

We can be more precise by introducing the fraction of standard radiation $\Omega_{\rm r} = \epsilon_{\rm r}/\epsilon$ and the fraction of SF $\Omega_{\rm SF} = \epsilon_{\rm SF}/\epsilon$. During the radiationlike era of the SF, i.e. for $a_v \leq a \leq a_t$, since $\epsilon_{\rm r}$ and $\epsilon_{\rm SF}$ both decay as $a^{-4}$, the fraction of SF has a constant value

$$\Omega_{\rm SF}({\rm plateau}) = \frac{\epsilon_{\rm SF}}{\epsilon_{\rm SF}+\epsilon_{\rm r}} = \frac{\mu}{\mu+1}. \quad (117)$$

For the fiducial model of Li *et al.* [94], we obtain $\Omega_{\rm SF}({\rm plateau}) = 3.55\times 10^{-2}$ in good agreement with the value inferred from their Fig. 3. More generally, using their constraint coming from BBN [94],

$$0.028 \leq \Omega_{\rm SF}({\rm plateau}) \leq 0.132, \quad (118)$$

we obtain $2.88\times 10^{-2} \leq \mu \leq 0.152$, giving [see Eq. (E17)]

$$1.95\times 10^3 \leq \frac{a_s}{\rm fm}\left(\frac{{\rm eV}/c^2}{m}\right)^3 \leq 2.87\times 10^5. \quad (119)$$

Using the results of Appendix B, we analytically recover the result $9.54\times 10^{-19}\ {\rm eV}^{-1}\,{\rm cm}^3 \leq \lambda_s/(mc^2)^2 \leq 1.40\times 10^{-16}\ {\rm eV}^{-1}\,{\rm cm}^3$ of Li *et al.* [94] [see their Eq. (43)]. The cosmological constraints corresponding to the bounds of Eq. (118) are illustrated in Fig. 9.

The approach of Li *et al.* [94] is more general than ours because they make precisely the matching between the slow oscillation regime and the fast oscillation regime. This allows them to obtain precise bounds on $m$ and $a_s$ from BBN. We can, however, obtain a bound on $m$ by the following (rough) argument. We require that the stiff matter era is over at the beginning of the neutron-proton ratio freeze-out $a_{\rm n/p} \sim 10^{-10}$, i.e., when BBN begins. This leads to the constraint $a_v \leq a_{\rm n/p}$. Using Eq. (94), we obtain the condition

$$\frac{m}{{\rm eV}/c^2} \geq \frac{6.17\times 10^{-31}}{a_{\rm n/p}}\left(\frac{\rm fm}{a_s}\right)^{1/6}\left(\frac{m}{{\rm eV}/c^2}\right)^{1/2}. \quad (120)$$

Combining this equation with Eq. (119), we obtain the constraint

$$m \geq 1.75\times 10^{-21}\ {\rm eV}/c^2 \quad ({\rm approx}) \quad (121)$$

which is very close to the exact constraint $m \geq 2.4\times 10^{-21}\ {\rm eV}/c^2$ obtained by Li *et al.* [94].

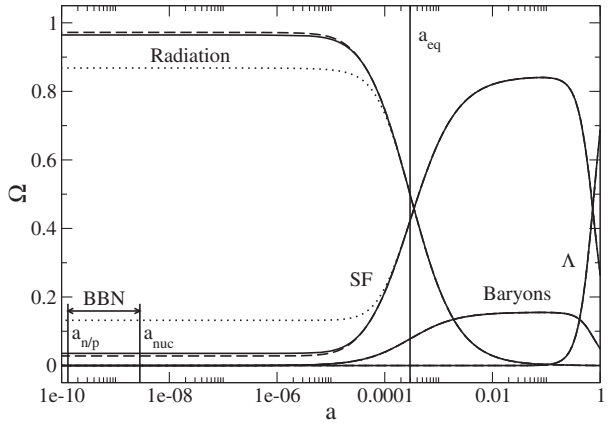


FIG. 9. Evolution of the fraction of the energy density of each component (standard radiation, SF, baryons, DE) during the fast oscillation regime of the SF (see Appendix E 3). We have taken the values of $(m, a_s)$ corresponding to the fiducial model of Li *et al.* [94] (full lines). The dashed and dotted lines correspond to the models leading to the bounds of Eq. (118). In this figure, $a$ is the true scale factor (not $\tilde{a}$). Figure 3 of Li *et al.* [94] is more general since it takes into account the stiff matter era that prevails for $a \lesssim 10^{-10}$.

In conclusion, we confirm the important results of Li *et al.* [94]. An interest of our approach is that we obtain all the relevant quantities analytically, so we can understand better where they come from. This also allows us to play more easily with the parameters. The case of a SF at nonzero temperature ($T_{\rm SF} \neq 0$) will be considered in a future work [107].

*Remark:* As shown by Li *et al.* [94], cosmological constraints from CMB and BBN exclude the possibility that the bosons are noninteracting. Indeed, according to the inequality of Eq. (119) resulting from the constraint (118) coming from BBN, the SF must be self-interacting. If we ignore the constraint (118), take $a_s = 0$, and impose the constraint $a_v(0) \leq a_{\rm n/p}$, we find from Eq. (92) that $m \geq 7.38 \times 10^{-19}$ eV/c$^2$. This cosmological constraint is in contradiction with the astrophysical constraint of Eq. (D3). This confirms that the SF must be self-interacting.

## IV. THE CASE OF A QUARTIC POTENTIAL WITH A NEGATIVE SCATTERING LENGTH

We now consider the case of a SF with a negative scattering length $a_s < 0$ corresponding to an attractive self-interaction. This is the case, for example, of the axion field that has been proposed as a dark matter candidate.

### A. The basic equations

The equations of the problem are

$$\rho\sqrt{1-\frac{8\pi|a_s|\hbar^2}{m^3c^2}\rho}=\frac{Qm}{a^3}, \tag{122}$$

$$\frac{3H^2}{8\pi G}=\rho\left(1-\frac{6\pi|a_s|\hbar^2}{m^3c^2}\rho\right), \tag{123}$$

$$\epsilon=\rho c^2\left(1-\frac{6\pi|a_s|\hbar^2}{m^3c^2}\rho\right), \tag{124}$$

$$P=-\frac{2\pi|a_s|\hbar^2}{m^3}\rho^2, \tag{125}$$

$$w=\frac{-\frac{2\pi|a_s|\hbar^2}{m^3c^2}\rho}{1-\frac{6\pi|a_s|\hbar^2}{m^3c^2}\rho}, \tag{126}$$

$$E_{\rm tot}=mc^2\sqrt{1-\frac{8\pi|a_s|\hbar^2}{m^3c^2}\rho}. \tag{127}$$

Solving Eq. (124) for $\rho$, we find two acceptable solutions

$$\rho=\frac{m^3c^2}{12\pi|a_s|\hbar^2}\left(1\pm\sqrt{1-\frac{24\pi|a_s|\hbar^2}{m^3c^4}\epsilon}\right). \tag{128}$$

Substituting Eq. (128) into Eq. (125), we obtain the EOS

$$P=-\frac{m^3c^4}{72\pi|a_s|\hbar^2}\left(1\pm\sqrt{1-\frac{24\pi|a_s|\hbar^2}{m^3c^4}\epsilon}\right)^2. \tag{129}$$

### B. The evolution of the parameters with the scale factor *a*

The evolution of the pseudo rest-mass density $\rho$ with the scale factor $a$ is plotted in Fig. 10. The curve $\rho(a)$ has two branches. These two branches start from the same point corresponding to the minimum scale factor

$$a_i=\left(\frac{12\sqrt{3}\pi|a_s|\hbar^2Q}{m^2c^2}\right)^{1/3} \tag{130}$$

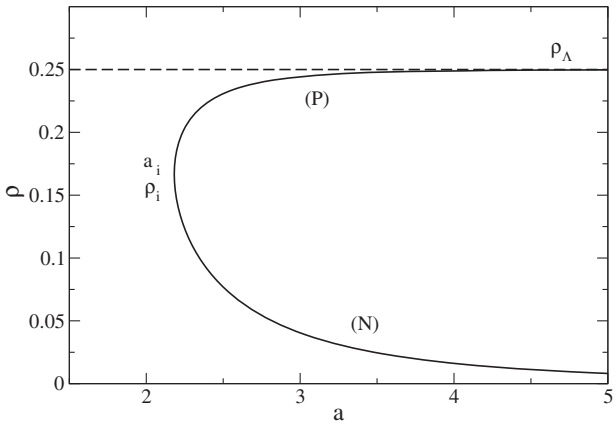


FIG. 10. Pseudo rest-mass density $\rho$ as a function of the scale factor $a$.

and to the density

$$\rho_i = \frac{m^3c^2}{12\pi|a_s|\hbar^2}. \tag{131}$$

For $a \to a_i$:

$$\rho \simeq \rho_i\left[1 \pm \sqrt{2\left(\frac{a}{a_i}-1\right)}\right]. \tag{132}$$

On the "normal" branch (sign $-$), the pseudo rest-mass density decreases as the scale factor increases and asymptotically tends to 0. For $a \to +\infty$:

$$\rho \sim \frac{Qm}{a^3}. \tag{133}$$

On the "peculiar" branch (sign $+$), the rest-mass density increases as the scale factor increases[9] and asymptotically tends to a maximum density

$$\rho_\Lambda = \frac{m^3c^2}{8\pi|a_s|\hbar^2}. \tag{134}$$

For $a \to +\infty$:

$$\rho \simeq \rho_\Lambda\left[1 - \left(\frac{8\pi Q|a_s|\hbar^2}{m^2c^2a^3}\right)^2\right]. \tag{135}$$

The evolution of the energy density $\epsilon$ with the scale factor $a$ is plotted in Fig. 11. It starts at $a = a_i$ from

$$\epsilon_i = \frac{1}{2}\rho_i c^2 = \frac{m^3c^4}{24\pi|a_s|\hbar^2}. \tag{136}$$

For $a \to a_i$:

$$\epsilon \simeq \epsilon_i\left[1 - \left(\frac{\rho}{\rho_i}-1\right)^2\right] \simeq \epsilon_i\left[1 - 2\left(\frac{a}{a_i}-1\right) \pm \frac{4\sqrt{2}}{3}\left(\frac{a}{a_i}-1\right)^{3/2}\right]. \tag{137}$$

On the normal branch, the energy density decreases as the scale factor increases and asymptotically tends to 0. For $a \to +\infty$:

$$\epsilon \sim \rho c^2 \sim \frac{Qmc^2}{a^3}. \tag{138}$$

On the peculiar branch, the energy density decreases as the scale factor increases and asymptotically tends to a minimum density given by

$$\epsilon_\Lambda = \frac{1}{4}\rho_\Lambda c^2 = \frac{m^3c^4}{32\pi|a_s|\hbar^2}. \tag{139}$$

[9]Although the pseudo rest-mass density increases with the scale factor, the Universe is not phantom, contrary to our claim in Ref. [77]. Indeed, as shown below, the energy density $\epsilon$ always decreases with the scale factor $a$, even on the peculiar branch.

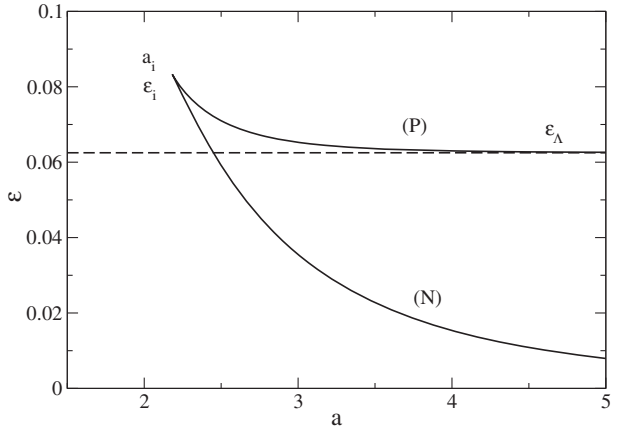


FIG. 11. Energy density $\epsilon$ as a function of the scale factor $a$.

For $a \to +\infty$:

$$\epsilon \simeq \frac{3}{4}\rho_\Lambda c^2 - \frac{1}{2}\rho c^2 \simeq \epsilon_\Lambda\left[1 + 2\left(\frac{8\pi Q|a_s|\hbar^2}{m^2c^2a^3}\right)^2\right]. \tag{140}$$

The evolution of the pressure $P$ with the scale factor $a$ is plotted in Fig. 12. The pressure is always negative. It starts at $a = a_i$ from

$$P_i = -\frac{1}{6}\rho_i c^2 = -\frac{m^3c^4}{72\pi|a_s|\hbar^2} = -\frac{\epsilon_i}{3}. \tag{141}$$

For $a \to a_i$:

$$P \simeq P_i\left(1 \pm 2\sqrt{1-\frac{\epsilon}{\epsilon_i}}\right) \simeq P_i\left[1 \pm 2\sqrt{2\left(\frac{a}{a_i}-1\right)}\right]. \tag{142}$$

On the normal branch, the pressure increases as the scale factor increases and asymptotically tends to 0. For $a \to +\infty$:

$$P \sim -\frac{2\pi|a_s|\hbar^2}{m^3c^4}\epsilon^2 \sim -\frac{2\pi|a_s|\hbar^2Q^2}{ma^6} \simeq 0. \tag{143}$$

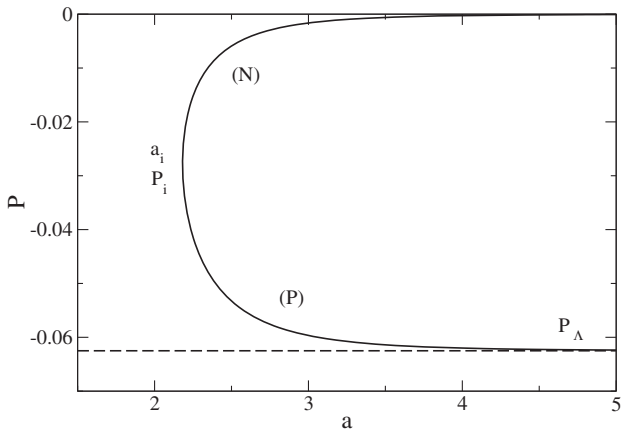


FIG. 12. Pressure $P$ as a function of the scale factor $a$.

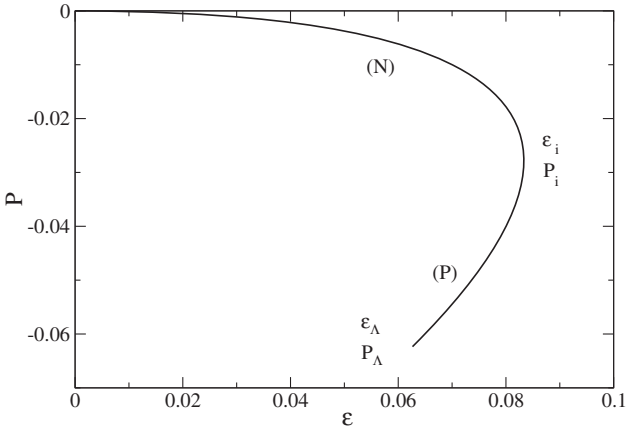


FIG. 13. Pressure $P$ as a function of the energy density $\epsilon$.

On the peculiar branch, the pressure decreases as the scale factor increases and asymptotically tends to the minimum value

$$P_\Lambda = -\epsilon_\Lambda. \tag{144}$$

For $a \to +\infty$:

$$P \simeq \epsilon - 2\epsilon_\Lambda \simeq -\epsilon_\Lambda\left[1 - 2\left(\frac{8\pi Q|a_s|\hbar^2}{m^2c^2a^3}\right)^2\right]. \tag{145}$$

The relationship between the pressure and the energy density is plotted in Fig. 13. The normal branch corresponds to $0 \leq \rho \leq \rho_i$, $0 \leq \epsilon \leq \epsilon_i$, and $P_i \leq P \leq 0$. The peculiar branch corresponds to $\rho_i \leq \rho \leq \rho_\Lambda$, $\epsilon_\Lambda \leq \epsilon \leq \epsilon_i$, and $P_\Lambda \leq P \leq P_i$.

The evolution of the EOS parameter $w = P/\epsilon$ with the scale factor $a$ is plotted in Fig. 14. The EOS parameter is always negative. It starts at $a = a_i$ from

$$w_i = -\frac{1}{3}. \tag{146}$$

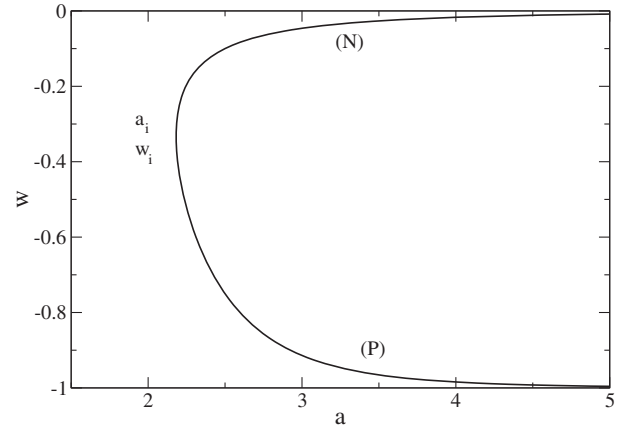


FIG. 14. EOS parameter $w$ as a function of the scale factor $a$.

For $a \to a_i$:

$$w \simeq -\frac{1}{3}\left[1 \pm 2\sqrt{2\left(\frac{a}{a_i} - 1\right)}\right]. \tag{147}$$

On the normal branch, $w$ increases as the scale factor increases and asymptotically tends to 0. For $a \to +\infty$:

$$w \sim -\frac{2\pi|a_s|\hbar^2 Q}{m^2c^2a^3}. \tag{148}$$

On the peculiar branch, $w$ decreases as the scale factor increases and asymptotically tends to

$$w_\Lambda = -1. \tag{149}$$

For $a \to +\infty$:

$$w \simeq -1 + 4\left(\frac{8\pi Q|a_s|\hbar^2}{m^2c^2a^3}\right)^2. \tag{150}$$

The total energy $E_{\rm tot}/mc^2$ starts at $a = a_i$ from

$$\frac{(E_{\rm tot})_i}{mc^2} = \frac{1}{\sqrt{3}}. \tag{151}$$

For $a \to a_i$:

$$\frac{E_{\rm tot}}{mc^2} \simeq \frac{1}{\sqrt{3}} \mp \sqrt{\frac{2}{3}\left(\frac{a}{a_i} - 1\right)}. \tag{152}$$

On the normal branch, $E_{\rm tot}/mc^2$ increases as the scale factor increases and asymptotically tends to 1. For $a \to +\infty$:

$$\frac{E_{\rm tot}}{mc^2} \simeq 1 - \frac{4\pi|a_s|\hbar^2 Q}{m^2c^2a^3}. \tag{153}$$

On the peculiar branch, $E_{\rm tot}$ decreases as the scale factor increases and asymptotically tends to 0. For $a \to +\infty$:

$$\frac{E_{\rm tot}}{mc^2} \simeq \frac{8\pi Q|a_s|\hbar^2}{m^2c^2a^3}. \tag{154}$$

### C. The temporal evolution of the parameters

In this section, we determine the temporal evolution of the parameters assuming that the Universe contains only the SF. For a quartic potential with $a_s < 0$, the differential equation (24) becomes

$$\left(\frac{d\rho}{dt}\right)^2 = 24\pi G\rho^3 \frac{(1 - \frac{6\pi|a_s|\hbar^2}{m^3c^2}\rho)(1 - \frac{8\pi|a_s|\hbar^2}{m^3c^2}\rho)^2}{(1 - \frac{12\pi|a_s|\hbar^2}{m^3c^2}\rho)^2}. \tag{155}$$

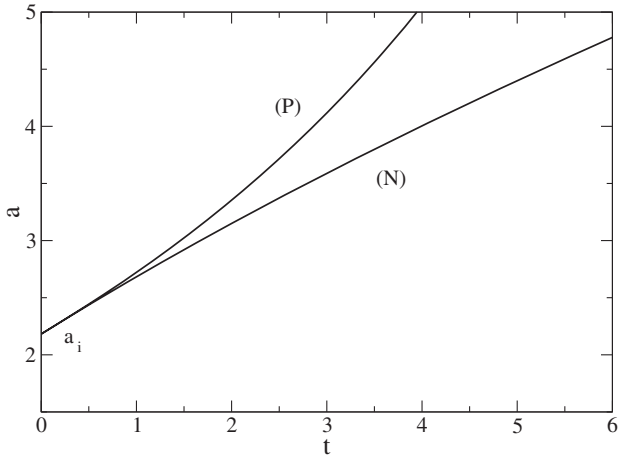


FIG. 15. Temporal evolution of the scale factor $a$.

The solution of this differential equation which takes the value $\rho_i$ at $t=0$ is

$$\int_{\frac{2\pi|a_s|\hbar^2}{m^3c^2}\rho}^{1/6}\frac{(1-6x)dx}{x^{3/2}(1-3x)^{1/2}(1-4x)}=\sqrt{\frac{12Gm^3c^2}{|a_s|\hbar^2}}t. \tag{156}$$

The integral can be computed analytically:

$$\begin{aligned}&\int\frac{(1-6x)dx}{x^{3/2}(1-3x)^{1/2}(1-4x)}\\&=-2\sqrt{\frac{1-3x}{x}}+2\ln\left(\frac{2+\sqrt{1-3x}+3\sqrt{x}}{2+\sqrt{1-3x}-3\sqrt{x}}\right)\\&\quad+2\ln\left(\frac{1-2\sqrt{x}}{1+2\sqrt{x}}\right).\end{aligned} \tag{157}$$

From these equations, we can obtain the temporal evolution of the pseudo rest-mass density $\rho(t)$. Then, using Eqs. (122)–(127), we can obtain the temporal evolution of all the parameters. The temporal evolution of the scale factor $a$ is plotted in Fig. 15. It starts from $a=a_i$ at $t=0$ and increases to $+\infty$ as $t\to+\infty$ on the two branches. We do not show the other curves because they can be easily deduced from Figs. 10, 11, 12 and 14 since $a$ is a monotonic function of time on the two branches. However, we provide below the asymptotic behaviors of all the parameters.

For $t\to 0$:

$$a\simeq a_i\left[1+\left(\frac{4\pi G\rho_i}{3}\right)^{1/2}t\pm\frac{4\sqrt{2}}{15}\left(\frac{4\pi G\rho_i}{3}\right)^{5/4}t^{5/2}\right], \tag{158}$$

$$\rho=\rho_i\left[1\pm\left(\frac{16\pi G\rho_i}{3}\right)^{1/4}\sqrt{t}\right], \tag{159}$$

$$\epsilon\simeq\epsilon_i\left[1-2\left(\frac{4\pi G\rho_i}{3}\right)^{1/2}t\right], \tag{160}$$

$$P\simeq P_i\left[1\pm 2\left(\frac{16\pi G\rho_i}{3}\right)^{1/4}\sqrt{t}\right], \tag{161}$$

$$w\simeq-\frac{1}{3}\left[1\pm 2\left(\frac{16\pi G\rho_i}{3}\right)^{1/4}\sqrt{t}\right], \tag{162}$$

$$\frac{E_{\rm tot}}{mc^2}\simeq\frac{1}{\sqrt{3}}\mp\sqrt{\frac{2}{3}\left(\frac{a}{a_i}-1\right)}. \tag{163}$$

On the normal branch, for $t\to+\infty$:

$$a\sim(6\pi GQmt^2)^{1/3}, \tag{164}$$

$$\rho\sim\frac{1}{6\pi Gt^2}, \tag{165}$$

$$\epsilon\sim\frac{c^2}{6\pi Gt^2}, \tag{166}$$

$$P\sim-\frac{|a_s|\hbar^2}{18\pi m^3G^2t^4}, \tag{167}$$

$$w\sim-\frac{|a_s|\hbar^2}{3m^3c^2Gt^2}, \tag{168}$$

$$\frac{E_{\rm tot}}{mc^2}\sim 1-\frac{2|a_s|\hbar^2}{3m^3c^2Gt^2}. \tag{169}$$

On the peculiar branch, for $t\to+\infty$:

$$a\sim\left(\frac{8\pi Q|a_s|\hbar^2}{m^2c^2}\right)^{1/3}e^{-A/12}e^{-1/6}e^{(\frac{2}{3}\pi G\rho_\Lambda)^{1/2}t}, \tag{170}$$

where

$$A=-2\sqrt{3}+2\ln\left[\frac{(2\sqrt{6}+\sqrt{3}+3)(\sqrt{6}-2)}{(2\sqrt{6}+\sqrt{3}-3)(\sqrt{6}+2)}\right]. \tag{171}$$

Numerically, $A=-6.09802\ldots$. The other parameters converge towards their asymptotic values determined in Sec. IV B exponentially rapidly.

*Remark:* If we assume that the Universe contains only a SF with an attractive self-interaction, and if we assume that the fast oscillation regime is always valid (see, however, Sec. IV E), we find that the Universe emerges from an initial state in which the scale factor is nonzero and the energy density is finite. This initial state is nonsingular for what concerns the values of $\rho_i$, $\epsilon_i$ and $a_i$. However, it is singular because the time derivative of the pseudo rest-mass density $\rho$ is infinite: $\dot{\rho}_i=\infty$. This is different from the big bang singularity in which the scale factor vanishes and the energy density is infinite. There are important claims that support the idea of a nonsingular Universe, one example being the case of bouncing Universes where the big bang is

taken as the beginning of a period of expansion that followed a period of contraction. These kinds of behaviors are often referred to as a (nonsingular) big crunch followed by a (nonsingular) big bang, or more simply, a big bounce [108–110] (see also [91] in a different context). Our solution valid for $t \geq 0$ can be extended to $t \leq 0$ by symmetry leading to a big bounce. However, this assumes that the Universe contains only the SF although this is not the case in reality.

### D. The different eras

In the fast oscillation regime, a SF with an attractive self-interaction ($a_s < 0$) undergoes two distinct eras. It emerges from an initial state where the scale factor $a_i$ is nonzero and the energy density $\epsilon_i$ is finite. The SF does not exist before $a_i$ (see, however, the limitations of our approximations in Sec. IV E). For $a \to a_i$, the EOS parameter tends to $w_i = -1/3$. This value is the same as for a gas of cosmic strings[10] described by the EOS $P = -\epsilon/3$. The EOS parameter $w = -1/3$ marks the transition between accelerating and decelerating Universes. Indeed, for the EOS $P = -\epsilon/3$, using the Friedmann equations (4) and (5), we find that $\epsilon = \epsilon_{s,0}/a^2$ so that the scale factor increases linearly with time as $a = (8\pi G\epsilon_{s,0}/3c^2)^{1/2}t$. In our model, the evolution of the scale factor is different but we note that the leading term in Eq. (158) valid for short times also scales linearly with $t$. Therefore, it is possible that the early evolution of our model shares some analogies with a gas of cosmic strings. At later times, two evolutions are possible. The normal branch is asymptotically similar to the evolution of a pressureless Universe like in the EdS model. Indeed, for $a \to +\infty$, the EOS (129) reduces to Eq. (143) and the EOS parameter tends to 0 [see Eq. (148)] so the SF behaves essentially as pressureless DM (dust) with an EOS $P = 0$.[11] In that case, the scale factor increases algebraically with time like $a \propto t^{2/3}$. On the other hand, the peculiar branch is asymptotically similar to the evolution of a de Sitter Universe. Indeed, the energy density tends to a constant given by Eq. (139) and the EOS parameter tends to $w_\Lambda = -1$ [see Eq. (149)] similar to the EOS parameter of DE with an EOS $P = -\epsilon$ [see Eq. (144)]. In that case, the scale factor increases exponentially rapidly with time like $a \propto e^{(2\pi G\rho_\Lambda/3)^{1/2}t}$. Therefore, the SF undergoes a cosmic stringlike era ($w = -1/3$) followed by a matterlike era ($w = 0$) on the normal branch or a de Sitterlike era ($w = -1$) on the peculiar branch. On the normal branch, since $w \geq -1/3$, the Universe is always decelerating. On the peculiar branch, since $w \leq -1/3$, the Universe is always accelerating. In conclusion, a SF with an attractive self-interaction behaves at early times as a gas of cosmic strings and at late times as DM (normal branch) or as DE (peculiar branch). We note that the cosmic stringlike era and the peculiar branch are due to the attractive self-interaction of the SF.

In the fast oscillation regime, the SF exists only for $a > a_i$ where $a_i$ is given by Eq. (130). Using Eq. (81) relying on the expression (E12) of the charge of the SF,[12] we can obtain $a_i = (6\sqrt{3})^{1/3}a_*$ as a function of the ratio $a_s/m^3$. In order to be consistent with the observations, we must require that $a_i \ll a_{\rm eq} = 2.95 \times 10^{-4}$. Using Eq. (E9), we obtain the constraint

$$\frac{|a_s|}{m^3} \ll \frac{c^4\Omega_{\rm r,0}^3}{12\sqrt{3}\pi\hbar^2\epsilon_0\Omega_{\rm dm,0}\Omega_{\rm m,0}^3}. \tag{172}$$

Introducing proper normalization, we get

$$\frac{|a_s|}{\rm fm}\left(\frac{\rm eV/c^2}{m}\right)^3 \ll 8.00 \times 10^6. \tag{173}$$

For a QCD axion field [see Eq. (D17)], we obtain $(|a_s|/\rm fm)((\rm eV/c^2)/m)^3 = 5.8 \times 10^{-26}$ and $a_i = 5.69 \times 10^{-15}$. For an ultralight axion [see Eq. (D19)], we obtain $(|a_s|/\rm fm)((\rm eV/c^2)/m)^3 = 1.06 \times 10^3$ and $a_i = 1.50 \times 10^{-5}$. Therefore, the constraint $a_i \ll a_{\rm eq}$ is verified.

We can estimate the transition between the cosmic stringlike era and the matterlike era (normal branch) or the de Sitter-like era (peculiar branch) of the SF as follows. First of all, using Eqs. (122) and (126), we find that the scale factor corresponding to a value $w$ of the EOS parameter is

$$a = \left(\frac{2\pi|a_s|\hbar^2Q}{m^2c^2}\right)^{1/3}\frac{(1-3w)^{1/2}}{|w|^{1/3}(1+w)^{1/6}}. \tag{174}$$

Interestingly, this equation provides an analytical expression of the function $a(w)$, the inverse of the function $w(a)$ plotted in Fig. 14. If we consider that the transition between

[10] Cosmic strings are a type of topological defects which may have formed during a symmetry breaking phase transition in the early Universe. The phase transitions leading to the production of cosmic strings are likely to have occurred during the earliest moments of the Universe's evolution, just after cosmological inflation, and are a fairly generic prediction in both quantum field theory and string theory models of the early Universe [111–113].

[11] As explained in footnote 5, the pressure of the SF is nonzero but since $P \propto -\epsilon^2 \ll \epsilon$ for $\epsilon \to 0$, everything happens at large scales as if the Universe were pressureless. However, the nonzero pressure of the SF is important at the scale of DM halos. Contrary to a repulsive self-interaction that stabilizes the halos, an attractive self-interaction has the tendency to destabilize the halos. Stable halos with $a_s < 0$ can exist only below a maximum mass [70,99,100]. For QCD axions, this mass is too small to account for the mass of DM halos. It becomes of the order of DM halos in the case of ultralight axions with a very small self-interaction (see [70,99,100] and Appendix D).

[12] In principle, this expression is only valid for the SF on the normal branch which asymptotically behaves as DM. The SF on the peculiar branch which behaves as DE is treated in Sec. IV G.

the cosmic stringlike era and the matterlike era of the SF corresponds to $w_t^{(\mathrm{N})} = -1/6$ (the arithmetic mean of $w = -1/3$ and $w = 0$), we obtain

$$\frac{a_t^{(\mathrm{N})}}{a_i} = \frac{\sqrt{3}}{2^{1/3}5^{1/6}} = 1.05129\ldots. \tag{175}$$

Similarly, if we consider that the transition between the cosmic stringlike era and the de Sitter-like era of the SF corresponds to $w_t^{(\mathrm{P})} = -2/3$ (the arithmetic mean of $w = -1/3$ and $w = -1$), we obtain

$$\frac{a_t^{(\mathrm{P})}}{a_i} = \frac{\sqrt{3}}{2^{2/3}} = 1.09112\ldots. \tag{176}$$

The transition scales $a_t^{(\mathrm{N})}$ and $a_t^{(\mathrm{P})}$ are very close to $a_i$ so that the duration of the cosmic stringlike era is extremely short. On the other hand, for QCD and ultralight axions, the transition scales $a_t^{(\mathrm{N})}$ and $a_t^{(\mathrm{P})}$ are below $a_{\mathrm{eq}} = 2.95 \times 10^{-4}$ by several orders of magnitude so that, at the equality epoch, the axionic SF already behaves as DM (normal branch) or DE (peculiar branch).

### E. Validity of the fast oscillation regime

The previous results are valid in the fast oscillation regime $\omega \gg H$. In this section, we determine the domain of validity of this regime.

In terms of dimensionless variables, the condition $\omega \gg H$ can be expressed by Eq. (83) where $\sigma$ is given by Eq. (84) in which $a_s$ is replaced by $|a_s|$. The dimensionless variables $\tilde{E}_{\mathrm{tot}}^2$ and $\tilde{\epsilon}$ are plotted as a function of $\tilde{a}$ in Fig. 16. Their ratio $\tilde{E}_{\mathrm{tot}}^2/\tilde{\epsilon}$ is plotted as a function of $\tilde{a}$ in Fig. 17. The intersection of this curve with the line $\tilde{E}_{\mathrm{tot}}^2/\tilde{\epsilon} = 1/\sigma$ determines the domain of validity of the fast oscillation regime.

We first consider the normal branch. Since $\tilde{E}_{\mathrm{tot}}^2$ (corresponding to $\omega^2$) increases with the scale factor $a$ up to 1

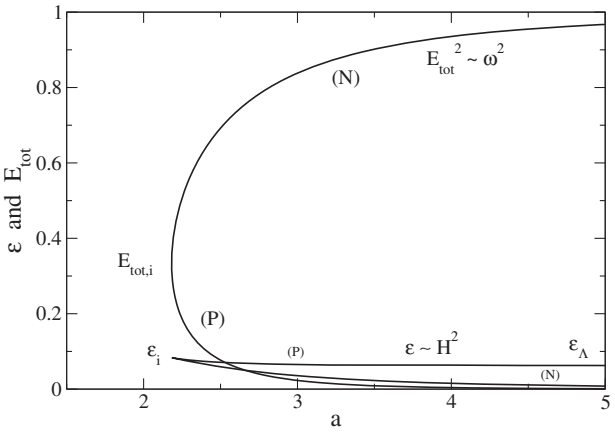


FIG. 16. Graphical construction determining the validity of the fast oscillation regime. The transition scale $a_v'$ corresponds to the intersection of the curves $\sigma\tilde{E}_{\mathrm{tot}}^2$ and $\tilde{\epsilon}$.

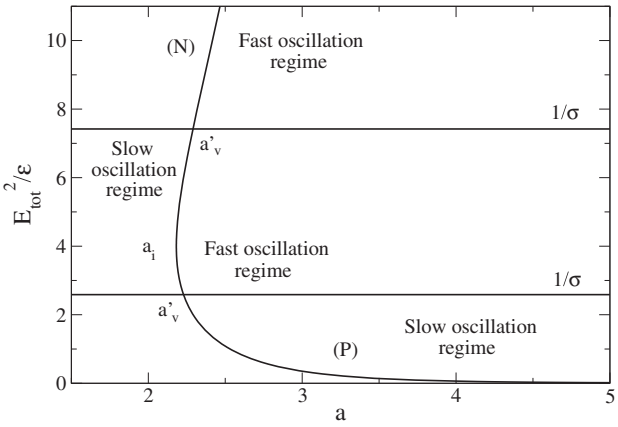


FIG. 17. Ratio $\omega/H$ as a function of the scale factor $a$.

while $\tilde{\epsilon}$ (corresponding to $H^2$) decreases to 0, the fast oscillation regime $\tilde{E}_{\mathrm{tot}}^2 \gg \tilde{\epsilon}/\sigma$ (corresponding to $\omega \gg H$) will be valid for any $a \geq a_i$ if it is valid at $a = a_i$. Since $(\tilde{E}_{\mathrm{tot}}^2)_i = 1/3$ and $\tilde{\epsilon}_i = 1/12$, we find that the fast oscillation regime is valid for any $a \geq a_i$ when

$$\sigma > \frac{1}{4}, \quad \text{i.e.,} \quad |a_s| > \frac{Gm}{3c^2} = \frac{1}{6}r_S. \tag{177}$$

When $\sigma < 1/4$, the fast oscillation regime starts to be valid for $a \gg a_v'$ with

$$a_v' = \left(\frac{2\pi|a_s|\hbar^2 Q}{m^2c^2}\right)^{1/3} g\left(\frac{3|a_s|c^2}{4Gm}\right), \tag{178}$$

where the function $g(\sigma)$ is defined by

$$g(\sigma) = \frac{1}{r^{1/3}(1-4r)^{1/6}} \tag{179}$$

with

$$r = \frac{4\sigma + 1 - \sqrt{(4\sigma+1)^2 - 12\sigma}}{6}. \tag{180}$$

For $\sigma \to 0$:

$$g(\sigma) \sim \frac{1}{\sigma^{1/3}}. \tag{181}$$

For $\sigma \to +\infty$:

$$g(\sigma) \sim 2^{4/3}\sigma^{1/6}. \tag{182}$$

The function $g(\sigma)$ takes its minimum value $g_{\min} = 2^{1/3}\sqrt{3} \simeq 2.18225\ldots$ at $\sigma = 1/4$. These asymptotic results can be written more explicitly by restoring the original variables. When $a_s = 0$, we find that $a_v'$ is given by Eq. (91) corresponding to the beginning of the fast oscillation regime in the noninteracting case. When $|a_s| = r_S/6$, we

get $a'_v = a_i$. When $|a_s| \geq r_S/6$, the fast oscillation regime is valid for any $a \geq a_i$.[13] We may wonder what happens to the SF in the early Universe, before the fast oscillation regime. Is there a stiff matter era? Does the stiff matter era exist for any value of $a_s < 0$? A stiff matter era must exist in the early Universe if $|a_s|$ is sufficiently small since it exists during a finite period of time $0 \leq a \leq a_v(0)$ when $|a_s| = 0$ and it cannot disappear suddenly when $a_s < 0$. In Sec. V we argue that the stiff matter era exists for $a_i \leq a \leq a'_v$ when $|a_s| \leq r_S/6$ and does not exist anymore when $|a_s| \geq r_S/6$. We also argue that, in the very early Universe, for $0 \leq a \leq a_i$, the SF undergoes an inflation era. However, in order to investigate these regimes, we need to solve the exact equations (10)–(12), taking quantum terms into account. This study would be particularly important to determine the duration of the inflation era (if there is really one), and its connection to the stiff matter era when $|a_s| \leq r_S/6$ or its connection to the matter era when $|a_s| \geq r_S/6$ (in particular, the inflation era is expected to stop long before $a_i$). However, this study is beyond the scope of this paper.

We now consider the peculiar branch. Since $\tilde{E}^2_{\rm tot}$ (corresponding to $\omega^2$) decreases to 0 with the scale factor $a$ while $\tilde{\epsilon}$ (corresponding to $H^2$) decreases to $\tilde{\epsilon}_\Lambda = 1/16$, the fast oscillation regime $\omega \gg H$ is not valid for large $a$. If $\sigma < 1/4$, the fast oscillation regime is never valid. If $\sigma > 1/4$, the fast oscillation regime is only valid for $a \ll a'_v$ where $a'_v$ is given by Eq. (178). The asymptotic results can be written more explicitly by restoring the original variables. When $|a_s| \leq r_S/6$, the fast oscillation regime is never valid. When $|a_s| = r_S/6$, we get $a'_v = a_i$. When $|a_s| \gg r_S$:

$$a'_v \simeq \left(\frac{768\pi^2|a_s|^3\hbar^4Q^2}{Gm^5c^2}\right)^{1/6}. \tag{183}$$

Using the expression of the charge given by Eq. (E12) (see, however, footnote 12), and introducing proper normalizations, we obtain

$$a'_v \simeq 1.55\times 10^2\left(\frac{a_s}{\rm fm}\right)^{1/2}\left(\frac{\rm eV/c^2}{m}\right)^{7/6}. \tag{184}$$

This value corresponds to the end of the fast oscillation regime in the strongly self-interacting regime. We may wonder what happens to the SF in the early ($a < a_i$) and late ($a > a'_v$) Universe when the fast oscillation regime is not valid. In that case, we have to take quantum mechanics into account and solve the exact equations (10)-(12). This is beyond the scope of the present paper but we can make the following remarks:

(i) It is shown in Sec. V C that the peculiar branch requires very particular initial conditions, so it is not clear how it can be connected to another, more primordial, era before $a_i$. Probably, the SF emerges suddenly at a nonzero scale factor $a_i$ whose exact value may be affected by quantum mechanics as discussed in footnote 13.

(ii) It is argued in Sec. V C that the de Sitter regime stops after $a'_v$ and that the SF eventually enters in a matterlike era (so that the Universe passes from acceleration to deceleration). In between, quantum mechanics must be taken into account. It is curious, but not excluded, that quantum mechanics (i.e., the quantum potential) becomes important at late times, after $a'_v$.

### F. Phase diagrams

We can represent the previous results on a phase diagram (see Figs. 18 and 19) where we plot the transition scales $a'_v$, $a_i$, $a_t^{(\rm N)}$ and $a_t^{(\rm P)}$ as a function of the scattering length $a_s$. To that purpose, it is convenient to normalize the scale factor $a$ by the reference value $a_v(0)$ given by Eq. (91) that is independent of $a_s$. The scattering length $|a_s|$ can be normalized by the effective Schwarzschild radius $r_S$ using the parameter $\sigma = 3|a_s|/2r_S$ defined by Eq. (84). With these normalizations, the scale $a_i$ marking the emergence of the SF is given by

$$\frac{a_i}{a_v(0)} = (6\sqrt{3}\sigma)^{1/3}. \tag{185}$$

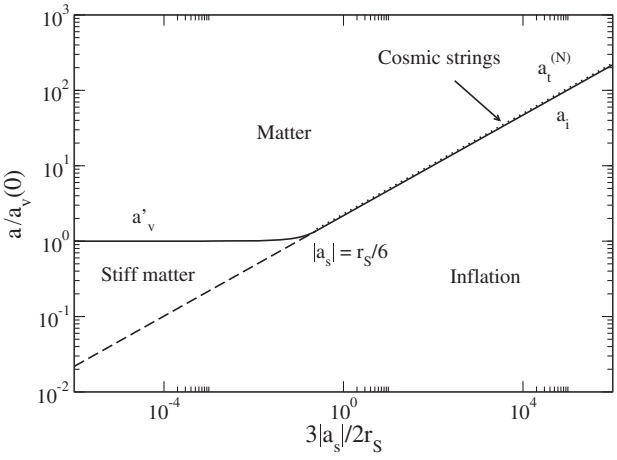


FIG. 18. Phase diagram (mainly hypothetical) showing the different eras of the SF during the evolution of the Universe as a function of the scattering length of the bosons in the case of an attractive self-interaction (normal branch).

[13] Actually, the fast oscillation condition $\omega \gg H$ is a necessary but not a sufficient condition for the validity of Eqs. (122)–(127). We must also require that $\omega \gg \dot{\rho}/\rho$ (see Appendix A). This condition is never realized by the solution of Eqs. (122)–(127) close to $a_i$ since $\dot{\rho}_i$ is infinite. This means that Eqs. (122)–(127) are never valid close to $a_i$, even when $\omega \gg H$. If we remember that Eqs. (122)–(127) are obtained from the exact equations (10)-(12) by neglecting the terms involving $\hbar$ (see Sec. II D), i.e. by neglecting the quantum potential, we come to the conclusion that quantum mechanics is important at early times and must be taken into account. In particular, it will prevent the divergence of $\dot{\rho}$ at $a_i$ and regularize the evolution of the SF in the early Universe.

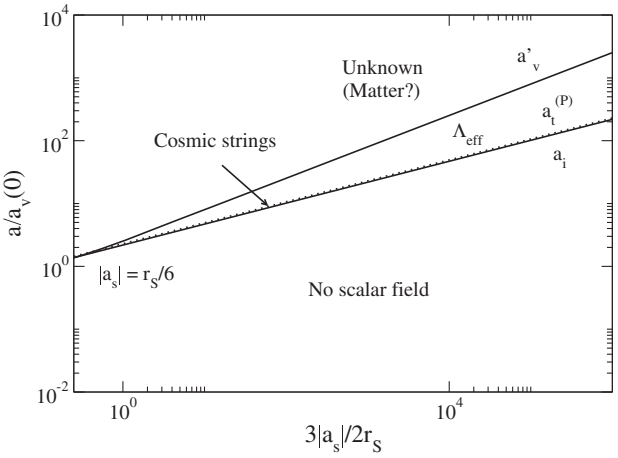


FIG. 19. Same as Fig. 18 for the peculiar branch.

It increases as $|a_s|^{1/3}$ according to Eq. (130). It starts from 0 at $a_s = 0$ and takes the value $a_i = (\sqrt{3}/2^{1/3})a_v(0)$ at $|a_s| = r_S/6$. Therefore, the SF appears later when $|a_s|$ is larger. On the other hand, the transition scale $a'_v$ determining the beginning (normal branch) or the end (peculiar branch) of the fast oscillation regime is given by

$$\frac{a'_v}{a_v(0)} = g(\sigma)\sigma^{1/3}. \tag{186}$$

For $\sigma = 0$:

$$\frac{a'_v}{a_v(0)} = 1. \tag{187}$$

For $\sigma = 1/4$:

$$\frac{a'_v}{a_v(0)} = \frac{\sqrt{3}}{2^{1/3}} \simeq 1.37. \tag{188}$$

For $\sigma \to +\infty$:

$$\frac{a'_v}{a_v(0)} \sim 2^{4/3}\sigma^{1/2}. \tag{189}$$

The transition scale $a'_v$ starts from the value $a_v(0)$ given by Eq. (91) for $a_s = 0$, increases slowly up to $a_i = (\sqrt{3}/2^{1/3})a_v(0)$ when $|a_s| = r_S/6$, and increases like $|a_s|^{1/2}$ according to Eq. (183) for $|a_s| \gg r_S$.

We can now describe the phase diagrams. We first consider the normal branch (see Fig. 18). When $|a_s| = 0$, the SF experiences a stiff matter era for $0 \le a \le a_v(0)$ (slow oscillation regime) and a matterlike era for $a \ge a_v(0)$ (fast oscillation regime). When $0 < |a_s| < r_S/6$, the SF experiences an inflation era for $0 \le a \le a_i$, a stiff matter era for $a_i \le a \le a'_v$ (slow oscillation regime) and a matterlike era for $a \ge a'_v$ (fast oscillation regime). When $|a_s| \gg r_S/6$, the SF experiences an inflation era for $0 \le a \le a_i$, a cosmic stringlike era for $a_i \le a \le a_t^{(N)}$ and a matterlike era for $a \ge a_t^{(N)}$. We now consider the peculiar branch (see Fig. 19). When $|a_s| < r_S/6$, the fast oscillation regime is never valid. When $|a_s| > r_S/6$, the SF appears suddenly at $a_i$ (presumably). It experiences a cosmic stringlike era for $a_i \le a \le a_t^{(P)}$ and a de Sitter-like era, equivalent to an effective cosmological constant $\Lambda_{\rm eff}$ (see Sec. IV G), for $a_t^{(P)} \le a \le a'_v$. For $a > a'_v$, the fast oscillation regime is not valid and the behavior of the SF is unknown. It may finally enter in a matterlike era (see Sec. V C).

Let us make a numerical application. For a QCD axion field [see Eq. (D17)], we obtain $\sigma = 3.29 \times 10^{14}$ and $a'_v = 1.73 \times 10^{-12} = 304 a_i$. For an ultralight axion [see Eq. (D19)], we obtain $\sigma = 2.87 \times 10^{7}$ and $a'_v = 3.03 \times 10^{-4} = 20.2 a_i$. Since $\sigma \gg 1/4$, the SF is strongly self-interacting and the fast oscillation regime is always valid on the normal branch (see, however, footnote 13). By contrast, the fast oscillation regime is valid on the peculiar branch only in a very small range of scale factors. Remember, however, that the expression of the charge (E12) used in the calculations is valid only for the normal branch (see footnote 12) so the numerical application may not be relevant for the peculiar branch (the peculiar branch is treated in the next section).

### G. Effective cosmological constant

A striking, and relatively mysterious, result of our study is the discovery that, under certain conditions, a complex SF with an attractive self-interaction may behave as DE. Indeed, on the peculiar branch of Fig. 11, the energy density asymptotically tends to a constant $\epsilon_\Lambda$. Furthermore, the final value of the energy density is not very different from its initial value $\epsilon_i$. According to Eqs. (136) and (139), we have $\epsilon_\Lambda = (3/4)\epsilon_i$. Therefore, a SF with a negative scattering length naturally generates a cosmological model with an approximately constant energy density $\sim\epsilon_\Lambda$. This may be a physical mechanism to produce a cosmological constant leading to a de Sitter evolution in which the scale factor increases exponentially rapidly with time.[14] This exponential

[14]Usually, one accounts for DE (or for a cosmological constant) by adding a constant term $V_0 = \epsilon_\Lambda$, called the vacuum energy, in the SF potential $V(|\varphi|^2)$. This introduces a constant term $+\epsilon_\Lambda$ in the energy density $\epsilon$ and a constant term $-\epsilon_\Lambda$ in the pressure $P$. However, particle physics predicts that the vacuum energy is of the order of the Planck energy that differs from 123 orders of magnitude from the cosmological energy. This is the cosmological constant problem [28–30]. Our model is very different in this respect since $V_0$ is equal to zero. Our effective cosmological constant comes from the properties of a complex SF with an attractive self-interaction that can maintain an almost constant energy density because of the centrifugal force resulting from its fast rotation (see Sec. V and Appendix A). This solution corresponds to a particular case of spintessence [97]. There is no such solution for a real SF, nor for a repulsive self-interaction.

growth of the scale factor may account for the early inflation or for the late acceleration of the Universe. Furthermore, the attractive self-interaction of the bosons ($a_s < 0$) could justify that the pressure is negative during these periods and that $w \simeq -1$. In this section, we try to constrain the parameters of the SF in order to make the value of the effective cosmological constant consistent with observations. This section is highly speculative so that only orders of magnitude will be considered.

The asymptotic value of the energy density of a SF with an attractive self-interaction ($a_s < 0$) on the peculiar branch is

$$\epsilon_\Lambda = \frac{m^3c^4}{32\pi|a_s|\hbar^2}. \tag{190}$$

On the other hand, the energy density produced by a cosmological constant $\Lambda$ is

$$\epsilon_\Lambda = \frac{\Lambda c^2}{8\pi G}. \tag{191}$$

Comparing Eqs. (190) and (191), we find that a SF with an attractive self-interaction is equivalent to an effective cosmological constant

$$\Lambda = \frac{Gm^3c^2}{4|a_s|\hbar^2}. \tag{192}$$

In the very early Universe, the cosmological constant may account for the phase of inflation. In that case, the energy density is of the order of the Planck energy density $\epsilon_P = \rho_P c^2$ where $\rho_P = c^5/\hbar G^2 = 5.16 \times 10^{99}\ \mathrm{g\,m^{-3}}$. Substituting this value into Eq. (190), we obtain

$$\frac{|a_s|}{m^3} = \frac{c^2}{32\pi\hbar^2\rho_P} = \frac{G^2}{32\pi\hbar c^3}. \tag{193}$$

Introducing proper normalizations, we get

$$\frac{|a_s|}{\mathrm{fm}}\left(\frac{\mathrm{eV}/c^2}{m}\right)^3 = 8.83 \times 10^{-107}. \tag{194}$$

In the late Universe, the cosmological constant may account for the phase of acceleration ($\Lambda$CDM model). In that case, the energy density is equal to the cosmological density $\epsilon_\Lambda = \Omega_{\Lambda,0}\epsilon_0 = 5.25 \times 10^{-7}\ \mathrm{g\,m^{-1}\,s^{-2}}$ where $\Omega_{\Lambda,0} = 0.687$ is the present fraction of DE and $\epsilon_0 = 3c^2H_0^2/8\pi G = 7.64 \times 10^{-7}\ \mathrm{g\,m^{-1}\,s^{-2}}$ is the present energy density of the Universe. We introduce $\rho_\Lambda = \epsilon_\Lambda/c^2 = 5.84 \times 10^{-24}\ \mathrm{g\,m^{-3}}$. Substituting this value into Eq. (190), we obtain

$$\frac{|a_s|}{m^3} = \frac{c^2}{32\pi\hbar^2\rho_\Lambda} = \frac{Gc^2}{12\hbar^2\Omega_{\Lambda,0}H_0^2}. \tag{195}$$

Introducing proper normalizations, we get

$$\frac{|a_s|}{\mathrm{fm}}\left(\frac{\mathrm{eV}/c^2}{m}\right)^3 = 7.80 \times 10^{16}. \tag{196}$$

Let us make a numerical application. For a QCD axion field [see Eq. (D17)], we obtain $|a_s|/m^3 = 5.8 \times 10^{-26}\ \mathrm{fm}/(\mathrm{eV}/c^2)^3$ and $\rho_\Lambda = 7.85 \times 10^{18}\ \mathrm{g\,m^{-3}}$. The value of $|a_s|/m^3$ is very different from the one given by Eqs. (194) and (196). We conclude that QCD axions cannot account for the value of the cosmological constant during the early inflation or the late acceleration of the Universe. The early inflation and the late acceleration of the Universe could be produced by another self-attractive complex SF with a ratio $|a_s|/m^3$ given by Eqs. (194) and (196).

Let us try to determine the parameters of this hypothetical SF. The value of the cosmological constant $\Lambda$ associated with the energy density $\epsilon_\Lambda = \rho_\Lambda c^2$ determines the ratio $|a_s|/m^3$ according to Eq. (190), i.e.,

$$\frac{|a_s|}{m^3} = \frac{c^2}{32\pi\hbar^2\rho_\Lambda}. \tag{197}$$

The beginning of the inflation era identified with $a_i$ determines the charge of the SF according to Eq. (130). Using Eq. (197), we get

$$Qm = \frac{8}{3\sqrt{3}}\rho_\Lambda a_i^3. \tag{198}$$

Finally, the end of the inflation era identified (somehow arbitrarily) with $a'_v$ determines the ratio $|a_s|/m$ from the relation

$$\frac{a'_v}{a_i} = \frac{1}{(6\sqrt{3})^{1/3}}\, g\left(\frac{3|a_s|c^2}{4Gm}\right) \tag{199}$$

obtained by combining Eqs. (130) and (178). In order to have sufficient inflation, we need $a'_v \gg a_i$. This requires $\sigma \gg 1/4$ allowing us to use the approximate expression (182) of $g(\sigma)$. In that case, Eq. (199) gives

$$\frac{|a_s|c^2}{Gm} = \frac{9}{16}\left(\frac{a'_v}{a_i}\right)^6. \tag{200}$$

From Eqs. (197) and (200), we obtain

$$m = \frac{3}{4}\left(\frac{a'_v}{a_i}\right)^3 m_\Lambda, \qquad |a_s| = \frac{27}{2048\pi}\left(\frac{a'_v}{a_i}\right)^9 r_\Lambda, \tag{201}$$

where the mass and length scales $m_\Lambda$ and $r_\Lambda$ are defined in Appendix G. Equation (201) determines the mass $m$ and the scattering length $a_s$ of the hypothetical SF producing the early inflation or the late acceleration of the Universe in our model. Their precise values depend on the ratio $a'_v/a_i$.

## V. THE TOTAL POTENTIAL

### A. Spintessence

The total potential of the SF including the rest-mass term and the self-interaction term is given by

$$V_{\rm tot}(|\varphi|^2) = \frac{m^2c^2}{2\hbar^2}|\varphi|^2 + \frac{2\pi a_s m}{\hbar^2}|\varphi|^4. \quad (202)$$

Using the relation from Eq. (7) between the modulus of the SF and the pseudo rest-mass density, we can rewrite it as

$$V_{\rm tot} = \frac{1}{2}\rho c^2 + \frac{2\pi a_s\hbar^2}{m^3}\rho^2 = \frac{1}{2}\rho c^2\left(1 + \frac{4\pi a_s\hbar^2}{m^3c^2}\rho\right). \quad (203)$$

We can study the evolution of the SF in the total potential $V_{\rm tot}(|\varphi|^2)$ by using a mechanical analogy. To that purpose, we write $\varphi = Re^{i\theta}$ where $R = |\varphi|$ (see Appendix A). The KG equation (A7) takes the form

$$\frac{1}{c^2}\frac{d^2R}{dt^2} + \frac{3H}{c^2}\frac{dR}{dt} = -\frac{dV_{\rm tot}}{dR} + R\omega^2 \quad (204)$$

with

$$\omega^2 = \frac{Q^2\hbar^2c^4}{R^4a^6}. \quad (205)$$

This is similar to the equation describing the axisymmetric motion of a damped particle in polar coordinates, where $R$ plays the role of the radial distance, $\theta$ the angle, and $\omega = \dot{\theta}$ the angular velocity. The fictive particle is submitted to a friction force $-(3H/c^2)\dot{R}$ (Hubble drag) that tends to slow it down, a radial force $-dV_{\rm tot}/dR$ that tends to decrease $R$ and a centrifugal force $R\omega^2$ that tends to increase $R$. This centrifugal force is a specificity of a complex SF called spintessence [97]. For a real SF, there is just the radial force so the SF descends the potential towards $R = 0$ and displays damped oscillations about it. Because of the presence of the centrifugal force, the evolution of a complex SF is richer. The fast oscillation regime that we have considered corresponds to a quasistatic equilibrium between the radial force and the centrifugal force:

$$\frac{dV_{\rm tot}}{dR} = R\omega^2. \quad (206)$$

A complex SF has the tendency to spin with angular velocity $\omega$ at a fixed radial distance $R$. However, according to Eq. (205) the angular velocity decreases as the scale factor increases. Therefore, the centrifugal force becomes less and less effective as time goes on. We can nevertheless maintain a quasistatic equilibrium at any time if $dV_{\rm tot}/dR$ decreases as the scale factor increases. As a result, the SF moves towards an extremum of $V_{\rm tot}$, either the minimum (when $a_s \geq 0$ or $a_s < 0$) or the maximum (when $a_s < 0$).

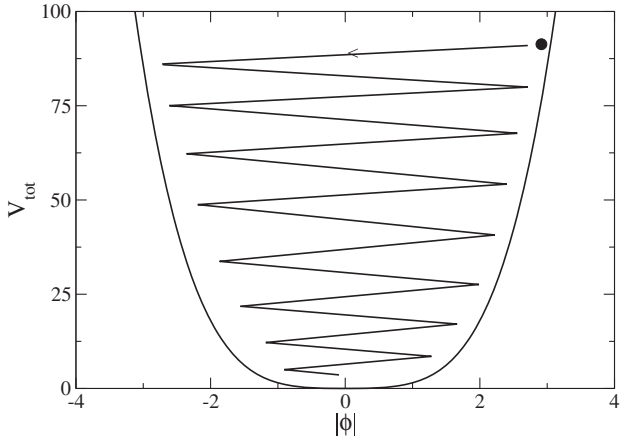


FIG. 20. Motion of the SF in the total potential $V_{\rm tot}$ when $a_s \geq 0$. The zig-zag is a rough representation of the spiralling motion of the SF in the (3D) potential.

We now describe more specifically the evolution of the SF in the total potential $V_{\rm tot}(|\varphi|^2)$ for the solutions obtained in Secs. III and IV.

### B. The case $a_s \geq 0$

When $a_s \geq 0$, the total potential (see Fig. 20) has a single minimum $V_{\rm tot} = 0$ at $|\varphi| = \rho = 0$. In the fast oscillation regime studied in Sec. III, the SF descends the potential from $+\infty$ to 0. The initial value of $|\dot{\varphi}|_i$ ("velocity") is $-\infty$ (see Appendix H).

The total potential $V_{\rm tot}$ starts at $a = 0$ from $+\infty$ and decreases to 0 as $a \to +\infty$. For $a \to 0$:

$$V_{\rm tot} \sim \frac{1}{2}(Q^4m\pi a_s\hbar^2c^4)^{1/3}\frac{1}{a^4}. \quad (207)$$

For $a \to +\infty$:

$$V_{\rm tot} \sim \frac{Qmc^2}{2a^3}. \quad (208)$$

Assuming that the Universe contains only the SF and using the results of Sec. III C, we can obtain the temporal evolution of $V_{\rm tot}$. For $t \to 0$:

$$V_{\rm tot} \sim \frac{c^2}{32\pi Gt^2}. \quad (209)$$

For $t \to +\infty$:

$$V_{\rm tot} \sim \frac{c^2}{12\pi Gt^2}. \quad (210)$$

In the stiff matter era, corresponding to the slow oscillation regime, using Eq. (87) of [77], we find that the SF behaves as

$$|\varphi| \sim \left(\frac{3c^4}{4\pi G}\right)^{1/2}(-\ln a). \tag{211}$$

The stiff matter era precedes the radiation and matter eras. The SF $|\varphi|$ starts from $+\infty$ and decreases with time. The SF descends the potential. As shown in Appendix F, the stiff matter era (slow oscillation regime) connects smoothly the radiation and matter eras (fast oscillation regime) at $a \sim a_v$ where $a_v$ is given by Eq. (86).

### C. The case $a_s < 0$

When $a_s < 0$, the total potential (see Fig. 21) has a local minimum $V = 0$ at $|\varphi| = \rho = 0$ and a maximum at

$$|\varphi_\Lambda| = \left(\frac{mc^2}{8\pi|a_s|}\right)^{1/2}, \qquad \rho_\Lambda = \frac{m^3c^2}{8\pi|a_s|\hbar^2}, \tag{212}$$

whose value is

$$(V_{\rm tot})_\Lambda = \frac{1}{4}\rho_\Lambda c^2 = \epsilon_\Lambda = \frac{m^3c^4}{32\pi|a_s|\hbar^2}. \tag{213}$$

In the fast oscillation regime studied in Sec. IV, the SF starts from

$$|\varphi_i| = \left(\frac{mc^2}{12\pi|a_s|}\right)^{1/2}, \qquad \rho_i = \frac{m^3c^2}{12\pi|a_s|\hbar^2}, \tag{214}$$

corresponding to a total potential

$$(V_{\rm tot})_i = \frac{1}{3}\rho_i c^2 = \frac{m^3c^4}{36\pi|a_s|\hbar^2}. \tag{215}$$

We note that $|\varphi_i|$ differs from the inflexion point $(d^2V_{\rm tot}/d|\varphi|^2 = 0)$ of the potential given by

$$|\varphi_{\rm I}| = \left(\frac{mc^2}{24\pi|a_s|}\right)^{1/2}, \qquad \rho_{\rm I} = \frac{m^3c^2}{24\pi|a_s|\hbar^2}, \tag{216}$$

corresponding to a total potential

$$(V_{\rm tot})_I = \frac{5}{12}\rho_I c^2 = \frac{5m^3c^4}{288\pi|a_s|\hbar^2}. \tag{217}$$

We find $\rho_i = 2\rho_{\rm I}$, $|\varphi_i| = \sqrt{2}|\varphi_{\rm I}|$, and $(V_{\rm tot})_i = (8/5)(V_{\rm tot})_I$. On the normal branch, the SF descends the potential from $|\varphi_i|$ to 0. The initial value of $|\dot\varphi|_i$ ("velocity") is $-\infty$ (see Appendix H). On the peculiar branch, the SF ascends the potential from $|\varphi_i|$ to $|\varphi_\Lambda|$. The initial value of $|\dot\varphi|_i$ ("velocity") is $+\infty$ (see Appendix H). Since $|\varphi_\Lambda|$ corresponds to the maximum $(V_{\rm tot})_\Lambda = \epsilon_\Lambda$ of the potential, we understand why the SF reaches a de Sitter regime $\epsilon \simeq \epsilon_\Lambda$ at late times.

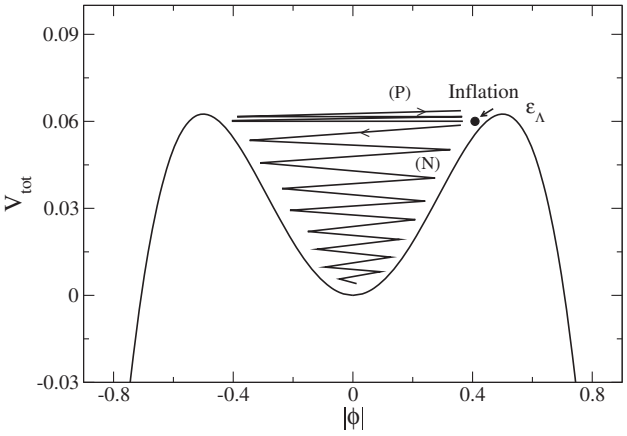


FIG. 21. Motion of the SF in the total potential $V_{\rm tot}$ when $a_s < 0$.

It is unusual, but not impossible, that the SF ascends the potential. In the present case, the SF ascends the potential, and maintains an almost constant value of $|\varphi|$, because of the centrifugal force that is specific to a complex SF. Indeed, the SF is in a quasistatic equilibrium between the "attractive" radial force and the "repulsive" centrifugal force [see Eq. (206)]. As the scale factor $a$ increases, the SF slowly moves towards the maximum of $V_{\rm tot}(|\varphi|^2)$ so as to decrease $dV_{\rm tot}/d|\varphi|$ (see Sec. V A). Therefore, the almost constant value of $|\varphi|$ giving rise to a de Sitter era and to an effective cosmological constant is a manifestation of spintessence for a complex SF with an attractive self-interaction. We now understand the origin of the two branches (N) and (P) corresponding to DM and DE. A SF with an attractive self-interaction can have two possible evolutions because the total SF potential has two extrema: a minimum at $|\varphi| = 0$ and a maximum at $|\varphi| = |\varphi_\Lambda|$. According to the discussion of Sec. V A, a SF in quasistatic equilibrium moves towards an extremum of $V_{\rm tot}$ (see Fig. 22). If the SF starts from $|\varphi_i|$ with a velocity $|\dot\varphi|_i = +\infty$ (or from $|\varphi_0| > |\varphi_i|$ with a finite positive velocity), it will ascend the potential towards the maximum in order to decrease $dV_{\rm tot}/d|\varphi|$. In that case, it will behave as DE. If the SF starts from $|\varphi_i|$ with a velocity $|\dot\varphi|_i = -\infty$ (or from $|\varphi_0| < |\varphi_i|$ with a finite negative velocity), it will descend the potential towards the minimum in order to decrease $dV_{\rm tot}/d|\varphi|$. In that case, it will behave as DM. Therefore, depending on the initial condition, the SF may behave either as DM or as DE. Note that a SF with a repulsive self-interaction can only have one possible evolution because the total SF potential has only one extremum: a minimum at $|\varphi| = 0$. It can only descend the potential towards the minimum in order to decrease $dV_{\rm tot}/d|\varphi|$.

The evolution of the total potential $V_{\rm tot}$ with the scale factor $a$ is plotted in Fig. 23. The potential starts at $a = a_i$ from $(V_{\rm tot})_i$. For $a \to a_i$:

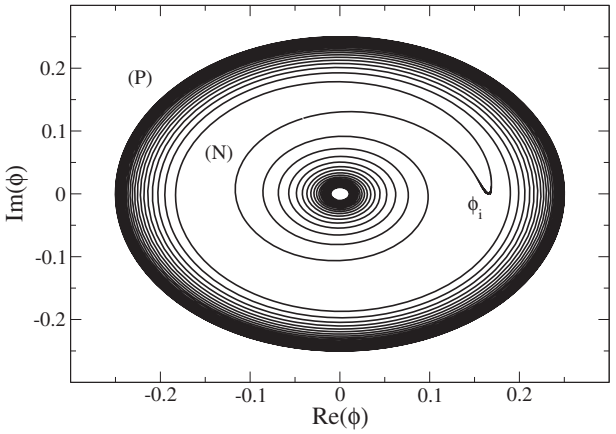


FIG. 22. Temporal evolution of the complex SF (spintessence). On the normal branch, it spirals towards the center giving rise to a matterlike era. On the peculiar branch, it reaches a limit cycle giving rise to a de Sitter era.

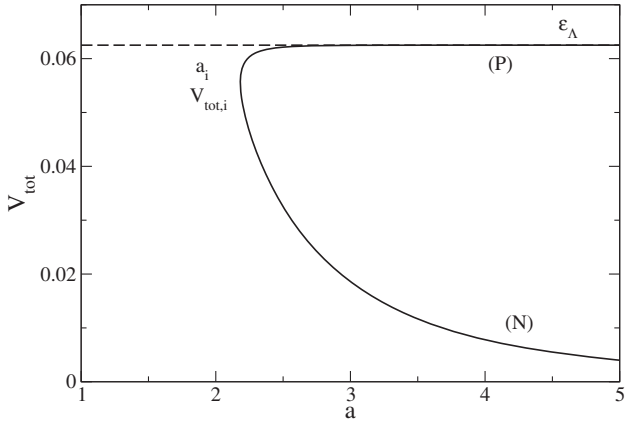


FIG. 23. Total SF potential $V_{\rm tot}$ as a function of the scale factor $a$ when $a_s < 0$.

$$V_{\rm tot} \simeq \frac{\rho_i c^2}{3}\left[1 \pm \sqrt{\frac{1}{2}\left(\frac{a}{a_i}-1\right)}\right]. \tag{218}$$

On the normal branch, the potential decreases as the scale factor increases and asymptotically tends to 0. For $a \to +\infty$:

$$V_{\rm tot} \sim \frac{Qmc^2}{2a^3}. \tag{219}$$

On the peculiar branch, the potential increases as the scale factor increases and asymptotically tends to its maximum value $(V_{\rm tot})_\Lambda = \epsilon_\Lambda$. For $a \to +\infty$:

$$V_{\rm tot} \simeq \epsilon_\Lambda\left[1 - \left(\frac{8\pi Q|a_s|\hbar^2}{m^2c^2a^3}\right)^4\right]. \tag{220}$$

Assuming that the Universe contains only the SF and using the results of Sec. IV C, we can obtain the temporal evolution of $V_{\rm tot}$. For $t \to 0$:

$$V_{\rm tot} \simeq \frac{\rho_i c^2}{3}\left[1 \pm \frac{1}{\sqrt{2}}\left(\frac{4\pi G\rho_i}{3}\right)^{1/4} t^{1/2}\right]. \tag{221}$$

On the normal branch, for $t \to +\infty$:

$$V_{\rm tot} \sim \frac{c^2}{12\pi G t^2}. \tag{222}$$

On the peculiar branch, for $t \to +\infty$, $V_{\rm tot}$ converges to its asymptotic value $\epsilon_\Lambda$ exponentially rapidly.

We now comment on the early evolution of the SF, before the fast oscillation regime. We first consider the normal branch. In the stiff matter era, corresponding to the slow oscillation regime, the evolution of the SF $|\varphi|$ is given by Eq. (211). It starts from $+\infty$ and decreases with time. When $a_s < 0$, this solution implies that the SF should climb the outer branch of the potential (see Fig. 21). This is very unlikely, if not impossible (when $a_s = 0$, there is no problem because this branch is rejected at infinity). This suggests that the stiff matter era is not valid at very early times when $a_s < 0$. On the other hand, it is shown in Appendix F that the stiff matter era can be connected smoothly to the matterlike era (at $a_v$) only when $|a_s| \lesssim r_S$ [briefly, this is because $|\tilde{\varphi}|_{\rm stiff} \sim \sigma$ according to Eq. (F2) so we need $\sigma \lesssim 1$ to have $|\tilde{\varphi}|_{\rm stiff} \lesssim |\tilde{\varphi}|_i = 1/\sqrt{6}$]. Therefore, the duration of the stiff matter era should decrease as $|a_s|$ increases up to $\sim r_S$. These results suggest that the stiff matter era exists only for $a_i \le a \le a'_v$ when $|a_s| < r_S/6$ and does not exist when $|a_s| > r_S/6$. We can now wonder what happens at very early times, before $a_i$. When $a_s < 0$, the SF could start from the top of the potential and descend the potential along the inner branch until it connects the solution described previously at $a_i$. The initial motion $0 \le a \le a_i$ is not in the fast oscillation regime, nor in the slow oscillation regime. Therefore, quantum mechanics must be taken into account, and we must solve the exact equations (10)–(12). Since the SF starts from the maximum of the potential at $(V_{\rm tot})_\Lambda = \epsilon_\Lambda$, the initial motion of the SF corresponds to a phase of inflation with a constant energy density given by Eq. (190). In our model, the inflation era is due to the negative scattering length of the SF ($a_s < 0$). This could give a physical justification of why the pressure is negative during inflation. Expanding the total potential close to the maximum, we get

$$V_{\rm tot} \simeq \epsilon_\Lambda - \frac{m^2c^2}{\hbar^2}(|\varphi| - |\varphi|_\Lambda)^2. \tag{223}$$

This corresponds to an inverted $|\varphi|^2$ potential with an effective mass $m_* = \sqrt{2}m$ interpreted as the inflaton mass (actually the mass is imaginary). In our model, the same SF

describes the inflation in the early Universe (top of the potential) and the formation of DM halos in the matterlike era (bottom of the potential). In order to account for the size of DM halos, a SF with an attractive self-interaction must have a mass given by Eq. (D3) and a very small scattering length $|a_s|$ satisfying the inequality (D21). If this same SF experiences an inflation era with a constant energy density equal to the Planck density, it must fulfill the constraint (194). Combining Eqs. (D3) and (194), we obtain

$$m = 2.92 \times 10^{-22}\ \mathrm{eV}/c^2, \qquad a_s = -2.20 \times 10^{-171}\ \mathrm{fm}, \tag{224}$$

corresponding to $\lambda/8\pi = -3.26 \times 10^{-201}$.

We now consider the peculiar branch. It is shown in Appendix F that the stiff matter era can never be connected smoothly to the peculiar branch. In addition, it is not clear what kind of phase could appear before $a_i$ because, in the most likely scenario, the SF should first descend the potential (for $a < a_i$) and suddenly reverse its motion and ascend it (for $a > a_i$). We conclude that, if the peculiar branch ever makes sense, the SF should emerge suddenly at $a_i$ from a very particular initial condition. For what concerns its evolution after $a'_v$, when the fast oscillation regime ceases to be valid, we may argue that the centrifugal force becomes inefficient to maintain an almost constant energy density and that the de Sitter regime comes to an end. The motion of the SF in the total potential is reversed. The SF descends the potential, connects the normal branch for $|\varphi| < |\varphi_i|$, and ultimately behaves as pressureless matter. In that case, there will be a transition from acceleration to deceleration in the late Universe. However, the de Sitter regime can be sufficiently long to be physically relevant (see Sec. IV G).

## VI. CONCLUSION

In this paper, we have studied the cosmological evolution of a complex SF with repulsive or attractive self-interaction using a fully general relativistic treatment. The SF may be interpreted as the wave function of a BEC. Although a SF is generally not a fluid, it can be studied through the hydrodynamic representation of the KGE equations [75–79]. For a $|\varphi|^4$ self-interaction, the parameters of the SF are the mass $m$ of the bosons and their scattering length $a_s$. We have introduced a new length scale $r_S = 2Gm/c^2$, which can be interpreted as the effective Schwarzschild radius of the bosons. The evolution of the SF depends on how the scattering length of the bosons $a_s$ compares with their effective Schwarzschild radius $r_S$. Our results can be summarized as follows.

In the case of repulsive self-interaction ($a_s \geq 0$), we have confirmed and complemented the results of Li *et al.* [94]. We have given many analytical formulas that allow us to understand the results better and play more easily with the parameters. When $a_s < (4/21)r_S$, the SF undergoes a stiff matter era ($w = 1$) followed by a matter era ($w = 0$). There is no radiationlike era, even though $a_s > 0$. For a noninteracting SF with $m = 2.92 \times 10^{-22}\ \mathrm{eV}/c^2$, the transition takes place at $a_v = 1.86 \times 10^{-8}$. When $a_s > (4/21)r_S$, the SF undergoes a stiff matter era ($w = 1$) followed by a radiationlike era ($w = 1/3$), and finally a matterlike era ($w = 0$). For a SF with $m = 3 \times 10^{-21}\ \mathrm{eV}/c^2$ and $a_s = 1.11 \times 10^{-58}$ fm, corresponding to the fiducial model of Li *et al.* [94], the transition between the stiff matter era and the radiationlike era takes place at $a_v = 5.14 \times 10^{-11}$ and the transition between the radiationlike era and the matterlike era takes place at $a_t = 1.35 \times 10^{-5}$. For a SF with $m = 1.10 \times 10^{-3}\ \mathrm{eV}/c^2$ and $a_s = 4.41 \times 10^{-6}$ fm (see Appendix D), we get $a_v = 1.45 \times 10^{-28}$ and $a_t = 1.26 \times 10^{-5}$. In both cases, the SF behaves at large scales as pressureless matter (like the CDM model) at, and after, the epoch of radiation-matter equality $a_{\mathrm{eq}} = 2.95 \times 10^{-4}$. However, its intrinsic nonzero pressure (either due to the scattering of the bosons or to the quantum potential taking into account the Heisenberg uncertainty principle) manifests itself at small scales and can balance the gravitational attraction. This leads to DM halos that present a core (BEC/soliton) instead of a cusp. These cores are surrounded by a halo with a NFW profile made of scalar radiation resulting from gravitational cooling. Therefore, a SF with $a_s \geq 0$ has a lot of nice properties and is a serious DM candidate that could solve the CDM small-scale crisis.

The case of attractive self-interaction ($a_s < 0$) has been studied in our paper for the first time. We have found that the SF can evolve along two different branches, a normal branch where it behaves as DM and a peculiar branch where it behaves as DE. We first consider the normal branch. When $|a_s| = 0$, the SF undergoes a stiff matter era ($w = 1$) followed by a matter era ($w = 0$). When $0 < |a_s| < r_S/6$, the SF undergoes an inflation era, a stiff matter era ($w = 1$), and a matter era ($w = 0$). The duration of the stiff matter era decreases as the self-interaction $|a_s|$ increases. When $|a_s| > r_S/6$, there is no stiff matter era anymore. The SF undergoes an inflation era, a very short cosmic stringlike era ($w = -1/3$), and a matterlike era ($w = 0$). For QCD axions with $m = 10^{-4}\ \mathrm{eV}/c^2$ and $a_s = -5.8 \times 10^{-53}$ m, the matterlike era starts at $a_i = 5.69 \times 10^{-15}$. For ultralight axions with $m = 2.19 \times 10^{-22}\ \mathrm{eV}/c^2$ and $a_s = -1.11 \times 10^{-62}$ fm, we get $a_i = 1.50 \times 10^{-5}$. In each case $a_i \ll a_{\mathrm{eq}} = 2.95 \times 10^{-4}$ so the axionic SF behaves at large scales as pressureless matter (like the CDM model) at, and after, the epoch of radiation-matter equality. However, its intrinsic nonzero pressure manifests itself at small scales. The quantum pressure arising from the Heisenberg uncertainty principle is always repulsive but the negative pressure due to the self-interaction is attractive and adds to the gravitational attraction. This can destabilize the halo. Stable DM halos

exist only below a maximum mass [70,99,100]. For QCD axions with $m = 10^{-4}$ eV$/c^2$ and $a_s = -5.8 \times 10^{-53}$ m this mass $M_{\rm max} = 6.5 \times 10^{-14}\ M_\odot$ is too small to account for the mass of DM halos. Therefore, QCD axions cannot form DM halos. They rather form mini axion stars that could be the constituents of DM halos in the form of mini massive compact halo objects (mini-MACHOs) [100]. However, they would essentially behave as CDM and would not solve the CDM small-scale crisis. The maximum mass of self-gravitating axions becomes of the order of the mass of DM halos $M \sim 10^8\ M_\odot$ in the case of ultralight axions with a mass $m = 2.19 \times 10^{-22}$ eV$/c^2$ and a very weak self-interaction $a_s = -1.11 \times 10^{-62}$ fm [100]. Such ultralight axions could solve the CDM small-scale crisis. We now consider the peculiar branch on which the SF behaves as DE ($w = -1$) with an almost constant energy density. This peculiar branch is valid only when $|a_s| > r_S/6$. It starts at $a_i$ and ceases to be valid at $a_v'$. On this branch, the SF is equivalent to an effective cosmological constant given by $\Lambda_{\rm eff} = Gm^3c^2/4|a_s|\hbar^2$. A complex SF with a negative scattering length could be a new mechanism to produce a cosmological constant. Cosmic acceleration could arise from the attractive self-interaction term present in the SF potential. That could justify why the pressure of DE is negative.

To our knowledge, the effective Schwarzschild radius of the bosons $r_S = 2Gm/c^2$ has not been introduced before. It arises naturally in the equations of the problem in order to separate the weakly self-interacting regime $\sigma = 3a_s/2r_S \ll 1$ from the strongly self-interacting regime $\sigma \gg 1$. Actually, for ultralight bosons with a mass $m = 2.92 \times 10^{-22}$ eV$/c^2$, even for a very small value of $a_s \sim 10^{-68}$ fm (or, equivalently, for a value of the dimensionless self-interaction constant $\lambda/8\pi$ as small as $10^{-98}$) we are in the strongly self-interacting regime, not in the weakly self-interacting regime (see Sec. III H and Appendix A. 3 of [99]). This is because $\sigma \gg 1$ while $\lambda \ll 1$. Therefore, it is important to take into account the nonzero value of the self-interaction constant in the problem even if it looks extremely small. This feature has been overlooked in previous works that often consider a noninteracting SF (see, e.g., [49,50]). In this connection, we recall that the cosmological bounds obtained by Li *et al.* [94] exclude noninteracting SFs.

Although observations tend to favor the ΛCDM model, other cosmological models cannot be rejected. The SF model is extremely rich and can have important implications concerning the nature of DM and DE in the Universe. Therefore, SFs should be considered as serious alternatives to find an answer to these paradigms. We have obtained very intriguing results that deserve to be developed in future works. For example, it is important to study what happens at very early times, before the fast oscillation regime, when $a_s < 0$. This requires to go beyond the TF approximation and take into account quantum mechanics (i.e. the quantum potential) by solving the exact equations (10)-(12). The analytical results obtained in the present paper, valid in the fast oscillation regime, may be useful to make the matching with this primordial era. An important suggestion of our work that needs to be confirmed is that a SF with an attractive self-interaction ($a_s < 0$) can produce a phase of early inflation followed by a stiff matter era and/or a matter era. It is important to determine whether this model can account for the observations because, in that case, we could describe different phases of the Universe with a single SF (see the still "hypothetical" phase diagrams of Figs. 18 and 19). Many other developments are also possible. For example, we have assumed that the SF has a $|\varphi|^4$ self-interaction potential and that this potential remains the same during the whole history of the Universe. Of course, if the SF has a different potential $V(|\varphi|^2)$, or if its potential changes during the history of the Universe (for example in the very early Universe), our conclusions must be revised. For simplicity, we have focused on a $|\varphi|^4$ interaction but we could consider more general potentials (see Appendix I). For example, when $|\varphi|$ is large (early Universe), the $|\varphi|^4$ approximation may not be valid anymore and higher order terms in the expansion of the potential should be considered. We have established the general equations to perform these studies. They will be considered in future works.

## ACKNOWLEDGMENTS

A. S. acknowledges CONACyT for the postdoctoral grant received (No. 231276). We are also grateful to the referees for their remarks.

## APPENDIX A: THE FAST OSCILLATION REGIME $\omega \gg H$ FROM THE FIELD THEORETIC APPROACH

In this Appendix, we consider the fast oscillation regime $\omega \gg H$ from the field theoretic approach based on the KG equation. We generalize the results of Li *et al.* [94] to an arbitrary potential of interaction $V(|\varphi|^2)$ and show the equivalence with the hydrodynamic approach of Sec. II.

### 1. General equations

The KG equation for a spatially homogeneous SF is given by Eq. (1). Decomposing the complex SF as

$$\varphi = |\varphi| e^{i\theta}, \tag{A1}$$

inserting this decomposition into the KG equation (1), and separating the real and imaginary parts, we obtain

$$\frac{1}{c^2}\left[\frac{d^2|\varphi|}{dt^2} - |\varphi|\left(\frac{d\theta}{dt}\right)^2\right] + \frac{3H}{c^2}\frac{d|\varphi|}{dt} + \frac{m^2c^2}{\hbar^2}|\varphi| + 2\frac{dV}{d|\varphi|^2}|\varphi| = 0, \tag{A2}$$

$$\frac{1}{c^2}\left(2\frac{d|\varphi|}{dt}\frac{d\theta}{dt}+|\varphi|\frac{d^2\theta}{dt^2}\right)+\frac{3H}{c^2}|\varphi|\frac{d\theta}{dt}=0. \quad \text{(A3)}$$

Equation (A3) can be exactly integrated once giving

$$\frac{d}{dt}\left(a^3|\varphi|^2\frac{d\theta}{dt}\right)=0. \quad \text{(A4)}$$

This can be rewritten as

$$a^3|\varphi|^2\frac{d\theta}{dt}=-Q\hbar c^2, \quad \text{(A5)}$$

where $Q$ is the charge of the SF [77,94,98,103].

In the fast oscillation regime $H=\dot{a}/a \ll d\theta/dt$, introducing the pulsation $\omega=d\theta/dt$, Eq. (A2) reduces to

$$\omega^2=\frac{m^2c^4}{\hbar^2}+2c^2\frac{dV}{d|\varphi|^2}. \quad \text{(A6)}$$

As pointed out in [94], this approximation also requires that $|\varphi|^{-1}d|\varphi|/dt \ll d\theta/dt$, a condition that is not always satisfied. For a free field ($V=0$), the pulsation $\omega$ is proportional to the mass of the SF ($|\omega|=mc^2/\hbar$) and the fast oscillation condition reduces to $mc^2/\hbar \gg H$.

*Remark:* To make the link with the hydrodynamical approach, we use $|\varphi|=(\hbar/m)\sqrt{\rho}$, $\theta=S_{\rm tot}/\hbar$ and $\omega=-E_{\rm tot}/\hbar$. Then, Eqs. (A4), (A5) and (A6) return Eqs. (14), (15) and (20), respectively.

### 2. Spintessence

From Eqs. (A2) and (A5) we obtain

$$\frac{d^2|\varphi|}{dt^2}+3H\frac{d|\varphi|}{dt}+\frac{m^2c^4}{\hbar^2}|\varphi|+2c^2\frac{dV}{d|\varphi|^2}|\varphi|-\frac{Q^2\hbar^2c^4}{a^6|\varphi|^3}=0. \quad \text{(A7)}$$

This equation differs from the KG equation of a real SF by the presence of the last term and the fact that $\varphi$ is replaced by $|\varphi|$. The last term coming from the "angular motion" of the complex SF can be interpreted as a "centrifugal force" (see Sec. V A) whose strength depends on the charge of the complex SF [103]. Equation (A7) can be rewritten as

$$\frac{d^2|\varphi|}{dt^2}+3H\frac{d|\varphi|}{dt}+\frac{m^2c^4}{\hbar^2}|\varphi|+2c^2\frac{dV_{\rm eff}}{d|\varphi|^2}|\varphi|=0, \quad \text{(A8)}$$

where

$$V_{\rm eff}(|\varphi|^2)=V(|\varphi|^2)+\frac{Q^2\hbar^2c^2}{2a^6|\varphi|^2} \quad \text{(A9)}$$

is an effective potential incorporating the centrifugal potential. The presence of the centrifugal force for a complex SF is a crucial difference with the case of a real SF (that is not charged) because the fast oscillation approximation (A6) corresponds to the equilibrium between the centrifugal potential and the total SF potential:

$$\frac{Q^2\hbar^2c^4}{a^6|\varphi|^4}=\frac{m^2c^4}{\hbar^2}+2c^2\frac{dV}{d|\varphi|^2}. \quad \text{(A10)}$$

This is what Boyle *et al.* [97] call "spintessence." Equation (A10) is equivalent to Eq. (21). Such a relation does not hold for a real SF. We note that $|\varphi|$ does not oscillate in the fast oscillation regime when the condition (A10) is fulfilled.

### 3. EOS in the fast oscillation regime

To establish the EOS in the fast oscillation regime, Li *et al.* [94] proceed as follows (see also [51,84,86,88]). Multiplying the KG equation (1) by $\varphi^*$ and averaging over a time interval that is much longer than the field oscillation period $\omega^{-1}$, but much shorter than the Hubble time $H^{-1}$, we obtain

$$\frac{1}{c^2}\left\langle\left|\frac{d\varphi}{dt}\right|^2\right\rangle=\frac{m^2c^2}{\hbar^2}\langle|\varphi|^2\rangle+2\left\langle\frac{dV}{d|\varphi|^2}|\varphi|^2\right\rangle. \quad \text{(A11)}$$

This relation constitutes a sort of virial theorem. For a spatially homogeneous SF, the energy density and the pressure are given by Eqs. (2) and (3). Taking the average value of the energy density and pressure, using Eq. (A11), and making the approximation

$$\left\langle\frac{dV}{d|\varphi|^2}|\varphi|^2\right\rangle\simeq V'(\langle|\varphi|^2\rangle)\langle|\varphi|^2\rangle, \quad \text{(A12)}$$

we obtain

$$\langle\epsilon\rangle=\frac{m^2c^2}{\hbar^2}\langle|\varphi|^2\rangle+V'(\langle|\varphi|^2\rangle)\langle|\varphi|^2\rangle+V(\langle|\varphi|^2\rangle), \quad \text{(A13)}$$

$$\langle P\rangle=V'(\langle|\varphi|^2\rangle)\langle|\varphi|^2\rangle-V(\langle|\varphi|^2\rangle). \quad \text{(A14)}$$

This returns Eqs. (27) and (28). The EOS parameter is given by

$$w=\frac{P}{\epsilon}=\frac{V'(\langle|\varphi|^2\rangle)\langle|\varphi|^2\rangle-V(\langle|\varphi|^2\rangle)}{\frac{m^2c^2}{\hbar^2}\langle|\varphi|^2\rangle+V'(\langle|\varphi|^2\rangle)\langle|\varphi|^2\rangle+V(\langle|\varphi|^2\rangle)}. \quad \text{(A15)}$$

*Remark:* Writing Eqs. (A11) and (A12) with hydrodynamic variables, and ignoring the averages, we obtain

$$\frac{\hbar^2}{8m^2c^2}\frac{1}{\rho}\left(\frac{d\rho}{dt}\right)^2+\left(\frac{E}{2mc^2}+1\right)\frac{\rho E}{m}=V'(\rho)\rho. \quad \text{(A16)}$$

If we substitute this equation into Eqs. (16) and (17), we obtain Eqs. (27) and (28) without having to neglect the term in $\hbar^2$ in Eq. (A16). However, in order to be consistent with Eq. (A6), which is equivalent to Eq. (18), the term in $\hbar^2$ can actually be neglected in Eq. (A16).

#### 4. EOS in the slow oscillation regime: Stiff matter

For a free SF with $V = 0$, Eqs. (2) and (3) reduce to

$$\epsilon = \frac{1}{2c^2}\left|\frac{d\varphi}{dt}\right|^2 + \frac{m^2c^2}{2\hbar^2}|\varphi|^2, \quad P = \frac{1}{2c^2}\left|\frac{d\varphi}{dt}\right|^2 - \frac{m^2c^2}{2\hbar^2}|\varphi|^2. \tag{A17}$$

For massless particles ($m = 0$) or for massive particles in the slow oscillation regime $\omega = mc^2/\hbar \ll H$, the kinetic term dominates the potential term (kination) and we obtain the stiff EOS:

$$P = \epsilon. \tag{A18}$$

For a self-interacting SF, we find from Eqs. (2) and (3) that the stiff EOS (A18) is valid in the slow oscillation regime $\omega \ll H$ where $\omega$ is defined by Eq. (A6). In that case, the SF cannot even complete one cycle of spin within one Hubble time so that it just rolls down the potential, without oscillating. Therefore, the comparison of $\omega$ and $H$ determines whether the SF oscillates or rolls. For the stiff EOS (A18), using the Friedmann equations (4) and (5), we easily get $\epsilon \propto a^{-6}$, $a \propto t^{1/3}$, and $\epsilon \sim c^2/24\pi G t^2$. It is also shown in [77] that $\rho \sim (3m^2c^4/4\pi G\hbar^2)(-\ln a)^2$ and $|\varphi| \sim (3c^4/4\pi G)^{1/2}(-\ln a)$. We note that quantum effects (quantum potential) give rise to a stiff matter era but do not prevent the initial big bang singularity since $\epsilon \sim c^2/24\pi G t^2$ diverges as $t \to 0$.

## APPENDIX B: SELF-INTERACTION CONSTANTS

In the main part of the paper, we have expressed all the results in terms of the scattering length of the bosons $a_s$. Instead of working with the scattering length, we can work with the dimensionless self-interaction constant [70,99]:

$$\frac{\lambda}{8\pi} = \frac{a_s}{\lambda_C} = \frac{a_s mc}{\hbar}, \tag{B1}$$

where $\lambda_C = \hbar/mc$ is the Compton wavelength of the bosons. We can also introduce a dimensional self-interaction constant

$$\lambda_s = \frac{4\pi a_s\hbar^2}{m} = \frac{\lambda\hbar^3}{2m^2c}. \tag{B2}$$

Introducing proper normalizations, we get

$$\frac{\lambda}{8\pi} = 5.07\frac{a_s}{\mathrm{fm}}\frac{m}{\mathrm{GeV/c^2}}, \tag{B3}$$

$$\frac{\lambda_s}{(mc^2)^2} = 4.89\times 10^{-22}\frac{a_s}{\mathrm{fm}}\left(\frac{\mathrm{eV/c^2}}{m}\right)^3 \mathrm{eV^{-1}\,cm^3}. \tag{B4}$$

In the TF regime (semiclassical approximation), the results depend on the single parameter

$$\frac{4\pi a_s\hbar^2}{m^3c^4} = \frac{\lambda\hbar^3}{2m^4c^5} = \frac{\lambda_s}{(mc^2)^2}. \tag{B5}$$

## APPENDIX C: DIMENSIONLESS VARIABLES

In the main part of the paper, for the sake of clarity, we have worked with dimensional variables. However, in order to simplify the calculations and make the figures, it can be convenient to introduce dimensionless variables defined by

$$\tilde{\rho} = \frac{\rho}{\rho_*}, \qquad \rho_* = \frac{m^3c^2}{2\pi|a_s|\hbar^2}, \tag{C1}$$

$$\tilde{a} = \frac{a}{a_*}, \qquad a_* = \left(\frac{2\pi|a_s|\hbar^2 Q}{m^2c^2}\right)^{1/3}, \tag{C2}$$

$$\tilde{t} = \frac{t}{t_*}, \qquad t_* = \left(\frac{2\pi|a_s|\hbar^2}{4\pi G m^3c^2}\right)^{1/2} = \frac{1}{\sqrt{4\pi G\rho_*}}, \tag{C3}$$

$$\tilde{\epsilon} = \frac{\epsilon}{\epsilon_*}, \qquad \epsilon_* = \frac{m^3c^4}{2\pi|a_s|\hbar^2} = \rho_* c^2, \tag{C4}$$

$$\tilde{P} = \frac{P}{P_*}, \qquad P_* = \frac{m^3c^4}{2\pi|a_s|\hbar^2} = \epsilon_*, \tag{C5}$$

$$\tilde{E} = \frac{E}{E_*}, \qquad E_* = mc^2, \tag{C6}$$

$$\tilde{V}_{\mathrm{tot}} = \frac{V_{\mathrm{tot}}}{\epsilon_*}, \qquad \tilde{\varphi} = \frac{\varphi}{\varphi_*}, \qquad \varphi_* = \left(\frac{mc^2}{2\pi|a_s|}\right)^{1/2}. \tag{C7}$$

Working with the dimensionless variables $\tilde{\rho}$, $\tilde{a}$, $\tilde{t}$, $\tilde{\epsilon}$, $\tilde{P}$ and $\tilde{E}$ is equivalent to taking

$$4\pi G = c = m = Q = 2\pi|a_s|\hbar^2 = 1 \tag{C8}$$

in the original equations.

## APPENDIX D: THE PARAMETERS ($m$,$a_s$) OF THE SF

In order to make numerical applications, we need to specify the values of the mass $m$ and scattering length $a_s$ of the SF. They can be obtained by the argument developed in Appendix D of [114]. If DM is a self-gravitating BEC, there

must be a minimum halo radius $R$ and a minimum halo mass $M$ in the Universe corresponding to the ground state of the self-gravitating BEC at $T=0$. This result is in agreement with the observations. Indeed, there is no DM halo with a radius less than $R\sim 1$ kpc and a mass less than $M\sim 10^8\ M_\odot$, the typical values of the radius and mass of dwarf spheroidal galaxies (dSph). Larger halos have a core-halo structure with a solitonic core corresponding to a pure BEC at $T=0$ and an "atmosphere" made of scalar radiation that has an approximate Navarro-Frenk-White (NFW) profile. It is the atmosphere, resulting from gravitational cooling, that fixes their size. We shall consider a dwarf halo of radius $R=1$ kpc and mass $M=10^8\ M_\odot$ (Fornax). Assuming that this halo represents the ground state of a self-gravitating BEC, we can obtain constraints on the parameters $(m,a_s)$ of the SF. In our previous works [77,114], we took $M=0.39\times 10^6\ M_\odot$ and $R=33$ pc corresponding to Willman 1 [115]. However, these values may not be relevant because Willman 1 is usually not considered as a DM halo [116].

### 1. Noninteracting SF

A self-gravitating BEC without self-interaction has the mass-radius relation [53,99,117][15]:

$$MR=9.95\frac{\hbar^2}{Gm^2}. \tag{D1}$$

This gives

$$\frac{m}{\mathrm{eV}/c^2}=9.22\times 10^{-17}\left(\frac{\mathrm{pc}}{R}\right)^{1/2}\left(\frac{M_\odot}{M}\right)^{1/2}. \tag{D2}$$

Using the values of $M$ and $R$ corresponding to Fornax, we obtain a boson mass

$$m=2.92\times 10^{-22}\ \mathrm{eV}/c^2. \tag{D3}$$

We note that, inversely, the specification of $m$ does not determine the mass and the radius of the halo but only their product $MR$.

*Remark:* The maximum mass of the bosonic core (soliton) of a noninteracting SFDM halo fixed by general relativity is $M_{\max}=0.633\hbar c/Gm$ and its minimum radius is $R_{\min}=9.53GM_{\max}/c^2$ [52]. Introducing scaled variables, we get

$$\frac{M_{\max}}{M_\odot}=8.48\times 10^{-11}\frac{\mathrm{eV}/c^2}{m},\qquad \frac{R_{\min}}{\mathrm{km}}=14.1\frac{M_{\max}}{M_\odot}. \tag{D4}$$

For $m=2.92\times 10^{-22}$ eV$/c^2$, we obtain $M_{\max}=2.90\times 10^{11}\ M_\odot$ and $R_{\min}=0.133$ pc. We note that the bosonic core of DM halos is generally nonrelativistic ($M_c\ll M_{\max}$).

### 2. Repulsive self-interaction

A self-gravitating BEC with a repulsive self-interaction in the TF approximation has a unique radius [69,70,118,119]:

$$R=\pi\left(\frac{a_s\hbar^2}{Gm^3}\right)^{1/2} \tag{D5}$$

that is independent of its mass. This gives

$$\frac{a_s}{\mathrm{fm}}\left(\frac{\mathrm{eV}/c^2}{m}\right)^3=3.28\times 10^{-3}\left(\frac{R}{\mathrm{pc}}\right)^2. \tag{D6}$$

Using the value of $R$ corresponding to Fornax, we obtain

$$\frac{a_s}{\mathrm{fm}}\left(\frac{\mathrm{eV}/c^2}{m}\right)^3=3.28\times 10^{3}. \tag{D7}$$

This fixes the ratio $a_s/m^3$. In order to determine the mass of the bosons, we need another relation. This relation is provided by the constraint $\sigma/m<1.25\ \mathrm{cm}^2/\mathrm{g}$ set by the Bullet Cluster [120], where $\sigma=4\pi a_s^2$ is the self-interaction cross section. Assuming that this bound is reached, we get $(a_s/\mathrm{fm})^2(\mathrm{eV}/mc^2)=1.77\times 10^{-8}$. From this relation and Eq. (D7), we obtain

$$m=1.10\times 10^{-3}\ \mathrm{eV}/c^2,\qquad a_s=4.41\times 10^{-6}\ \mathrm{fm}, \tag{D8}$$

corresponding to $\lambda/8\pi=2.46\times 10^{-17}$. This boson mass is in agreement with the limit $m<1.87\ \mathrm{eV}/c^2$ obtained from cosmological considerations [121].

The TF approximation is valid when the radius given by Eq. (D5) is much larger than the radius given by Eq. (D1). This corresponds to $a_s\gg\hbar^2/GM^2m$ or $\lambda/8\pi\gg\hbar c/GM^2$ (see Sec. II. G. of [70] and Appendix A. 3 of [99]). Using the value of $M$ corresponding to Fornax, we get

$$\frac{a_s}{\mathrm{fm}}\frac{m}{\mathrm{eV}/c^2}\gg 2.36\times 10^{-84}, \tag{D9}$$

or, equivalently, $\lambda/8\pi\gg 1.20\times 10^{-92}$ (note the smallness of this quantity already emphasized in Appendix A. 3 of [99]). This condition is clearly satisfied by the parameters of Eq. (D8). Inversely, when $a_s\ll\hbar^2/GM^2m$, we can ignore the self-interaction of the bosons. We then find

[15]This relation can be understood qualitatively by identifying the halo radius $R$ with the de Broglie wavelength $\lambda_{dB}=\hbar/mv$ of a boson with a velocity $v\sim(GM/R)^{1/2}$ equal to the virial velocity of the halo.

that the boson mass is given by Eqs. (D2) and (D3). An estimate of the critical scattering length separating the TF regime from the noninteracting regime can be obtained by substituting Eq. (D2) into Eq. (D6). This gives $a_c = 31.4(R\hbar^2/GM^3)^{1/2}$, i.e.

$$\frac{a_c}{\mathrm{fm}} = 2.57\times 10^{-51}\left(\frac{R}{\mathrm{pc}}\right)^{1/2}\left(\frac{M_\odot}{M}\right)^{3/2}. \quad \text{(D10)}$$

Using the values of $M$ and $R$ corresponding to Fornax, we obtain

$$m = 2.92\times 10^{-22}\ \mathrm{eV}/c^2, \qquad a_c = 8.13\times 10^{-62}\ \mathrm{fm}. \quad \text{(D11)}$$

The mass $m = 2.92\times 10^{-22}\ \mathrm{eV}/c^2$ obtained for bosons without self-interaction gives a lower bound on the mass of the bosonic dark matter particle. Inversely, the mass $m = 1.10\times 10^{-3}\ \mathrm{eV}/c^2$ obtained for self-interacting bosons in the TF approximation gives an upper bound on the mass of the bosonic dark matter particle. Therefore, we predict that the mass of the bosonic particle is in the range $2.92\times 10^{-22}\ \mathrm{eV}/c^2 \leq m \leq 1.10\times 10^{-3}\ \mathrm{eV}/c^2$. The TF limit is valid for sufficiently large scattering lengths, i.e., above $a_c$. For $a_s < a_c$, the mass of the bosonic particle is $m = 2.92\times 10^{-22}\ \mathrm{eV}/c^2$ and for $a_c < a_s < 4.41\times 10^{-6}\,\mathrm{fm}$ the mass of the bosonic particle is $2.92\times 10^{-22} < m/(\mathrm{eV}/c^2) = 6.73\times 10^{-2}(a_s/\mathrm{fm})^{1/3} < 1.10\times 10^{-3}$. We note that, inversely, the specification of $m$ and $a_s$ does not determine the mass of the halo but only its radius $R$.

*Remark:* The maximum mass of the bosonic core (soliton) of a self-interacting SFDM halo fixed by general relativity is $M_{\max} = 0.307\hbar c^2\sqrt{a_s}/(Gm)^{3/2}$ and its minimum radius is $R_{\min} = 6.25GM_{\max}/c^2$ [56]. Introducing scaled variables, we get

$$\frac{M_{\max}}{M_\odot} = 1.12\left(\frac{a_s}{\mathrm{fm}}\right)^{1/2}\left(\frac{\mathrm{GeV}/c^2}{m}\right)^{3/2}, \quad \text{(D12)}$$

$$\frac{R_{\min}}{\mathrm{km}} = 9.27\frac{M_{\max}}{M_\odot}. \quad \text{(D13)}$$

We note that these results do not depend on the specific mass $m$ and scattering length $a_s$ of the bosons, but only on the ratio $m^3/a_s$. For $(a_s/\mathrm{fm})(\mathrm{eV}/mc^2)^3 = 3.28\times 10^3$, we obtain $M_{\max} = 2.03\times 10^{15}\ M_\odot$ and $R_{\min} = 609$ pc. We note that the bosonic core of DM halos is generally nonrelativistic ($M_c \ll M_{\max}$).

### 3. Attractive self-interaction

A self-gravitating BEC with an attractive self-interaction ($a_s < 0$) is stable only below a maximum mass $M_{\max}$ and above a radius $R_*$ given by [70,99]

$$M_{\max} = 1.012\frac{\hbar}{\sqrt{Gm|a_s|}}, \qquad R_* = 5.5\left(\frac{|a_s|\hbar^2}{Gm^3}\right)^{1/2}. \quad \text{(D14)}$$

This gives

$$\frac{M_{\max}}{M_\odot} = 1.56\times 10^{-34}\left(\frac{\mathrm{eV}/c^2}{m}\right)^{1/2}\left(\frac{\mathrm{fm}}{|a_s|}\right)^{1/2}, \quad \text{(D15)}$$

$$\frac{R_*}{R_\odot} = 1.36\times 10^{9}\left(\frac{|a_s|}{\mathrm{fm}}\right)^{1/2}\left(\frac{\mathrm{eV}/c^2}{m}\right)^{3/2}. \quad \text{(D16)}$$

Considering standard (QCD) axions [122] with

$$m = 10^{-4}\ \mathrm{eV}/c^2, \qquad a_s = -5.8\times 10^{-53}\ \mathrm{m}, \quad \text{(D17)}$$

$$\frac{|a_s|}{\mathrm{fm}}\left(\frac{\mathrm{eV}/c^2}{m}\right)^3 = 5.8\times 10^{-26}, \quad \text{(D18)}$$

corresponding to $\lambda = -7.4\times 10^{-49}$, we obtain $M_{\max} = 6.5\times 10^{-14}\ M_\odot$ and $R_* = 3.3\times 10^{-4}R_\odot$. Obviously, QCD axions cannot form DM halos of relevant mass and size; they rather form mini axion stars [100]. DM halos could be made of numerous mini axion stars (mini-MACHOs) that would behave as CDM. On the other hand, ultralight axions can form DM halos. Assuming that Fornax corresponds to a self-gravitating BEC with attractive self-interaction at the limit of stability, we can use Eqs. (D15) and (D16) to obtain the values of $m$ and $a_s$. We get [100]

$$m = 2.19\times 10^{-22}\ \mathrm{eV}/c^2, \qquad a_s = -1.11\times 10^{-62}\ \mathrm{fm}, \quad \text{(D19)}$$

$$\frac{|a_s|}{\mathrm{fm}}\left(\frac{\mathrm{eV}/c^2}{m}\right)^3 = 1.06\times 10^3, \quad \text{(D20)}$$

corresponding to $\lambda/8\pi = -1.23\times 10^{-92}$. Actually, the halo does not need to be at the limit of stability. On the contrary, we need to impose that $M \ll M_{\max}$ for the halo to be robustly stable. This corresponds to $|a_s| \ll \hbar^2/GM^2m$ or $|\lambda|/8\pi \ll \hbar c/GM^2$ leading to the reverse of Eq. (D9) with $a_s$ replaced by $|a_s|$. In that case, we can ignore the self-interaction of the bosons. We then find that the boson mass is given by Eq. (D3). This is valid as long as its scattering length satisfies

$$|a_s| \ll 1.11\times 10^{-62}\ \mathrm{fm} \quad \text{(D21)}$$

or, equivalently, $|\lambda|/8\pi \ll 1.23\times 10^{-92}$ because above this value the halo mass becomes larger than the maximum mass and the halo undergoes gravitational collapse [100]. We note that this value is of the same order as the value (D11) marking the transition between the noninteracting

limit and the TF limit in the case $a_s > 0$. This is expected in view of the similar scalings. In conclusion, bosons with attractive self-interaction must have an ultralight mass and an extraordinarily small scattering length to form stable DM halos of relevant size.

*Remark:* In the high resolution numerical simulations of self-gravitating BECs performed by [50], the self-interaction of the bosons is not taken into account ($\lambda = 0$). Our results show that even an apparently tiny attractive ($\lambda < 0$) self-interaction with $|\lambda| \gtrsim 10^{-90}$ can considerably change the physics of the problem. For example, the solitonic core ($M \sim 10^8\ M_\odot$) of the dark matter halos considered in [50] is stable for $\lambda = a_s = 0$ but becomes unstable in the case of an attractive self-interaction with $|\lambda|/8\pi = |a_s|mc/\hbar > 1.02\hbar c/GM^2 = 1.02(M_P/M)^2 = 1.23 \times 10^{-92}$, or $|a_s| > 1.11 \times 10^{-62}$ fm for $m = 2.19 \times 10^{-22}$ eV/c$^2$, because in that case $M > M_{\rm max}$ [70,100]. Therefore $\lambda/8\pi = -1.23 \times 10^{-92}$ is very different from $\lambda = 0$ (!). It would be therefore extremely interesting to perform numerical simulations of the GPP and KGE equations for self-interacting bosons.

### 4. Cosmological constraints

Li *et al.* [94] have obtained stringent bounds on the values of $m$ and $a_s$ (assuming $a_s \geq 0$) by using cosmological constraints coming from the CMB and from the abundances of the light elements produced by the BBN. First of all, their bounds exclude the possibility that the bosons are noninteracting ($a_s \neq 0$). On the other hand, by combining all their constraints they obtain a fiducial model:

$$m = 3 \times 10^{-21}\ \text{eV}/c^2, \qquad a_s = 1.11 \times 10^{-58}\ \text{fm}, \quad \text{(D22)}$$

$$\frac{a_s}{\text{fm}}\left(\frac{\text{eV}/c^2}{m}\right)^3 = 4.10 \times 10^3, \quad \text{(D23)}$$

corresponding to $\lambda/8\pi = 1.69 \times 10^{-87}$. We note that the ratio (D23) obtained by Li *et al.* [94] from cosmological (large scales) arguments is of the same order as the ratio (D7) obtained from astrophysical (small scales) arguments (it corresponds to a minimum halo radius $R = 1.12$ kpc). This agreement is very satisfactory. On the other hand, the value of the boson mass (D22) obtained by Li *et al.* [94] is relatively close to the mass (D3) of a noninteracting boson. This is because their fiducial model is relatively close to the transition between the noninteracting limit and the TF limit [compare Eq. (D22) with Eq. (D11)]. However, the fact that their mass (D22) is substantially larger (by one order of magnitude) than the mass (D3) reflects the fact that the bosons are self-interacting (their fiducial model is at the beginning of the TF regime). Actually the mass (D3) of a noninteracting SF is excluded by their bound $m \geq 2.4 \times 10^{-21}$ eV/$c^2$ [94]. Note that their fiducial model uses a mass close to the minimum allowed mass. However, the mass of the SF could be much larger than this bound like the mass of Eq. (D8) which is deeper in the TF regime.

*Remark:* In a very recent paper, Hui *et al.* [123] have given further support to the BECDM/SFDM model. They focused on the noninteracting case ($a_s = 0$), considering an ultralight axion of mass $m \sim 1$–$10 \times 10^{-22}$ eV/$c^2$ [consistent with Eq. (D3)]. While mentioning several virtues of this model, they noted that this mass is in tension with observations of the Lyman-$\alpha$ forest, which favor masses 10–$20 \times 10^{-22}$ eV/$c^2$ or higher. A similar conclusion was reached by Menci *et al.* [124] based on the measured abundance of ultrafaint lensed galaxies at redshift $z \simeq 6$ in the Hubble Frontier Fields (HFF). We note that such larger masses are in agreement with Eq. (D22). Therefore, large-scale observations could reflect the fact that axions are self-interacting. In that case, all the known observational constraints seem to be satisfied.

### 5. Fermions

In this paper, we have assumed that DM halos are made of bosons. If they are made of fermions, their mass-radius relation is $MR^3 = 1.49 \times 10^{-3}h^6/(G^3m^8)$ [125]. This gives

$$\frac{m}{\text{eV}/c^2} = 2.27 \times 10^4\left(\frac{\text{pc}}{R}\right)^{3/8}\left(\frac{M_\odot}{M}\right)^{1/8}. \quad \text{(D24)}$$

Using the values of $M$ and $R$ corresponding to Fornax, we find a fermion mass $m = 170$ eV/$c^2$. We note that, inversely, the specification of $m$ does not determine the mass and the radius of the halo but only the product $MR^3$.

*Remark:* The maximum mass of the fermionic core (fermion ball) of a DM halo fixed by general relativity is $M_{\rm max} = 0.376(\hbar c/G)^{3/2}/m^2$ and its minimum radius is $R_{\rm min} = 9.36GM_{\rm max}/c^2$ [126]. Introducing scaled variables, we get

$$\frac{M_{\rm max}}{M_\odot} = 6.13 \times 10^{17}\left(\frac{\text{eV}/c^2}{m}\right)^2, \qquad \frac{R_{\rm min}}{\text{km}} = 13.8\,\frac{M_{\rm max}}{M_\odot}. \quad \text{(D25)}$$

For $m = 170$ eV/$c^2$, we obtain $M_{\rm max} = 2.12 \times 10^{13}\ M_\odot$ and $R_{\rm min} = 9.49$ pc. We note that the fermionic core of DM halos is generally nonrelativistic ($M_c \ll M_{\rm max}$).

## APPENDIX E: COMPARISON BETWEEN THE STANDARD MODEL AND THE SF MODEL

In this Appendix, we compare the standard model and the SF model with $a_s \geq 0$. In the first two subsections, for the clarity of the presentation, we do not take the baryonic matter and the DE (or cosmological constant) into account. The complete model is discussed in the third subsection. For the numerical applications, we adopt the values of the

cosmological parameters given by Li *et al.* [94]. They are listed in the fourth subsection.

### 1. The standard model

In the standard model, DM (which corresponds to WIMPs) and radiation (which accounts for the photons and neutrinos of the CMB) are two different species described by the EOSs $P_{\rm dm}=0$ and $P_{\rm r}=\epsilon_{\rm r}/3$ respectively. Solving the continuity equation (4) for each species, we obtain

$$\frac{\epsilon_{\rm dm}}{\epsilon_0}=\frac{\Omega_{\rm dm,0}}{a^3},\qquad \frac{\epsilon_{\rm r}}{\epsilon_0}=\frac{\Omega_{\rm r,0}}{a^4}, \tag{E1}$$

where $\Omega_{\rm dm,0}$ is the present fraction of dark matter and $\Omega_{\rm r,0}$ is the present fraction of radiation. We have taken $a_0=1$. The total energy density of these two species is

$$\frac{\epsilon}{\epsilon_0}=\frac{\Omega_{\rm r,0}}{a^4}+\frac{\Omega_{\rm dm,0}}{a^3}. \tag{E2}$$

From the Friedmann equation (5) we obtain the differential equation

$$\left(\frac{\dot a}{a}\right)^2=\frac{8\pi G\epsilon_0}{3c^2}\left(\frac{\Omega_{\rm r,0}}{a^4}+\frac{\Omega_{\rm dm,0}}{a^3}\right) \tag{E3}$$

that determines the evolution of the scale factor $a$. This equation can be integrated exactly, giving [91]

$$H_0t=-\frac{2}{3}\frac{1}{\Omega_{\rm dm,0}^{1/2}}\left(\frac{2\Omega_{\rm r,0}}{\Omega_{\rm dm,0}}-a\right)\sqrt{\frac{\Omega_{\rm r,0}}{\Omega_{\rm dm,0}}+a}+\frac{4\Omega_{\rm r,0}^{3/2}}{3\Omega_{\rm dm,0}^2}. \tag{E4}$$

Equation (E4) can also be written as

$$a^3-3\frac{\Omega_{\rm r,0}}{\Omega_{\rm dm,0}}a^2=\frac{9}{4}\Omega_{\rm dm,0}H_0^2t^2-6\frac{\Omega_{\rm r,0}^{3/2}}{\Omega_{\rm dm,0}}H_0t. \tag{E5}$$

This is a cubic equation for $a$ of the form $a^3+Aa^2+Ba+C=0$ which can be solved by standard methods. Using Cardano's formula, the real root is given by

$$a=-\frac{A}{3}+\left(-\frac{q}{2}+\sqrt{R}\right)^{1/3}+\left(-\frac{q}{2}-\sqrt{R}\right)^{1/3} \tag{E6}$$

with $R=(p/3)^3+(q/2)^2$, $p=B-A^2/3$, and $q=C-AB/3+2A^3/27$ (in our case $R>0$). However, to obtain $a(t)$, it is easier to use Eq. (E4) that gives $t(a)$, and plot the inverse function. For $a\to 0$ (radiation era):

$$\frac{\epsilon}{\epsilon_0}\sim\frac{\Omega_{\rm r,0}}{a^4},\qquad a\sim\left(\frac{32\pi G\epsilon_0\Omega_{\rm r,0}}{3c^2}\right)^{1/4}t^{1/2}. \tag{E7}$$

For $a\to+\infty$ (matter era, EdS solution):

$$\frac{\epsilon}{\epsilon_0}\sim\frac{\Omega_{\rm dm,0}}{a^3},\qquad a\sim\left(\frac{6\pi G\epsilon_0\Omega_{\rm dm,0}}{c^2}\right)^{1/3}t^{2/3}. \tag{E8}$$

The epoch of matter-radiation equality ($\epsilon_{\rm m}=\epsilon_{\rm r}$) corresponds to[16]

$$a_{\rm eq}=\frac{\Omega_{\rm r,0}}{\Omega_{\rm m,0}}=\frac{\Omega_{\rm r,0}}{\Omega_{\rm dm,0}+\Omega_{\rm b,0}}. \tag{E9}$$

Numerically, $a_{\rm eq}=2.95\times10^{-4}$. For $a<a_{\rm eq}$, we are in the radiation-dominated regime and for $a>a_{\rm eq}$, we are in the matter-dominated regime.

The energy density of radiation can be written as

$$\epsilon_{\rm r}=\kappa\sigma T^4=\frac{\kappa\pi^2}{15c^3\hbar^3}(k_BT)^4, \tag{E10}$$

where $T$ is the temperature, $\sigma$ is the Stefan-Boltzmann constant, and $\kappa=\kappa_\gamma+\kappa_\nu=1+3.046(7/8)(4/11)^{4/3}\simeq 1.692$ is a constant that accounts for the fact that radiation comes from photons and neutrinos in thermal equilibrium [11]. According to Eqs. (E1) and (E10), the relation between the temperature and the scale factor is given by

$$k_BT=\left(\frac{15c^3\hbar^3\Omega_{\rm r,0}\epsilon_0}{\kappa\pi^2}\right)^{1/4}\frac{1}{a}=\frac{k_BT_0}{a}, \tag{E11}$$

where $T_0$ is the present temperature of radiation. Numerically, $T_0=2.7255$ K.

### 2. The SF model

In the standard model, the Universe undergoes a radiation era followed by a pressureless DM era. Similarly, a SF with $a_s>0$ undergoes a radiationlike era followed by a pressureless dark matter era (see Sec. III D). However, the two models are physically different. In the standard model, radiation and dark matter correspond to different species that exist in permanence. For $a<a_{\rm eq}$ radiation dominates over matter and for $a>a_{\rm eq}$ matter dominates over radiation. In the SF model, there is just one species. The radiation and the matter are two manifestations of the same entity. For $a<a_t$, the SF behaves as radiation and for $a>a_t$ it behaves as pressureless matter. The relation between the energy density and the scale factor is different in the two models [see Eq. (E2) for the standard model and Eqs. (45) and (47) for the SF model]. However, their asymptotic behaviors for $a\to 0$ and $a\to+\infty$ are similar.

For $a\to+\infty$, the SF behaves as pressureless matter. Since the SF is expected to describe DM, we can identify

[16]Here, we take the contribution of baryonic matter into account noting that baryonic matter behaves as dark matter, i.e., it is described by an EOS $P_{\rm b}=0$.

the matterlike era of the SF with the DM era of the standard model. Comparing Eqs. (56) and (E8) valid for $a \to +\infty$, we find that the charge of the SF is given by

$$Q = \frac{\Omega_{\rm dm,0}\epsilon_0}{mc^2}. \tag{E12}$$

This relation is also valid for the SF model with $a_s < 0$ on the normal branch since it also behaves as pressureless matter for $a \to +\infty$.

For $a \to 0$, the SF behaves as radiation which adds to the standard radiation (photons, neutrinos, etc.). We define the initial ratio between the radiation of the SF and the standard radiation by

$$\mu = \lim_{a\to 0} \frac{\epsilon_{\rm SF}}{\epsilon_{\rm r}}, \tag{E13}$$

where $\epsilon_{\rm SF}$ is the energy density of the SF and $\epsilon_{\rm r}$ is the energy density of the standard radiation. Using Eqs. (55) and (E7) valid for $a \to 0$, we obtain

$$\mu = \left(\frac{27\pi Q^4 m a_s \hbar^2 c^4}{8\Omega_{\rm r,0}^3 \epsilon_0^3}\right)^{1/3}. \tag{E14}$$

Substituting the expression of the charge from Eq. (E12) into Eq. (E14), we get

$$\mu = \left(\frac{27\pi a_s \hbar^2 \Omega_{\rm dm,0}^4 \epsilon_0}{8\Omega_{\rm r,0}^3 m^3 c^4}\right)^{1/3}. \tag{E15}$$

We see that $\mu$ is determined by the ratio $a_s/m^3$. Inversely, if we know the value of $\mu$, Eq. (E15) determines the ratio $a_s/m^3$ through the relation

$$\frac{a_s}{m^3} = \frac{8\mu^3 \Omega_{\rm r,0}^3 c^4}{27\pi \Omega_{\rm dm,0}^4 \epsilon_0 \hbar^2}. \tag{E16}$$

Introducing proper normalizations, we get

$$\frac{a_s}{\rm fm}\left(\frac{{\rm eV}/c^2}{m}\right)^3 = 8.18 \times 10^7\ \mu^3. \tag{E17}$$

On the other hand, in the radiationlike era of the SF valid for $a \to 0$, we can write

$$\epsilon_{\rm SF} = \kappa\sigma T_{\rm eff}^4 = \frac{\kappa\pi^2}{15c^3\hbar^3}(k_B T_{\rm eff})^4, \tag{E18}$$

where $T_{\rm eff}$ is an effective temperature of SF radiation. Using Eq. (55), we obtain

$$k_B T_{\rm eff} = \left(\frac{91125 c^{13}\hbar^{11} Q^4 m a_s}{8\pi^5\kappa^3}\right)^{1/12}\frac{1}{a}. \tag{E19}$$

Although the SF is at $T = 0$, we can define an effective temperature of radiation for the SF that depends on its charge $Q$ and on the self-interaction strength $a_s$. Using Eq. (E12) to evaluate $Q$, we get

$$k_B T_{\rm eff} = \left(\frac{91125 c^5\hbar^{11} a_s \Omega_{\rm dm,0}^4 \epsilon_0^4}{8\pi^5 m^3\kappa^3}\right)^{1/12}\frac{1}{a}. \tag{E20}$$

Using Eq. (E16) to evaluate $a_s/m^3$, we obtain

$$k_B T_{\rm eff} = \left(\frac{15\mu c^3\hbar^3\epsilon_0\Omega_{r,0}}{\pi^2\kappa}\right)^{1/4}\frac{1}{a}. \tag{E21}$$

Comparing Eqs. (E11) and (E21), we find that

$$\frac{T_{\rm eff}}{T} = \mu^{1/4} \tag{E22}$$

in the radiative regime of the SF.

*Remark:* In the standard model we can calculate the present temperature of radiation $T_0$. We cannot define $(T_{\rm eff})_0$ for the SF because $T_{\rm eff}$ is only defined in the radiationlike regime so this effective temperature has no meaning in the present Universe.

### 3. The complete model

Since the SF is expected to represent DM (replacing the WIMP hypothesis), the complete model incorporating standard radiation and SFDM is obtained by replacing the second term in Eq. (E2) by the energy density of the SF. To be even more complete, we must also include baryonic matter and DE (cosmological constant). Therefore, the total energy reads

$$\frac{\epsilon}{\epsilon_0} = \frac{\Omega_{\rm r,0}}{a^4} + \frac{\epsilon_{\rm SF}(a)}{\epsilon_0} + \frac{\Omega_{\rm b,0}}{a^3} + \Omega_{\Lambda,0}. \tag{E23}$$

This complete model has been studied by Li *et al.* [94]. In the fast oscillation regime, introducing the dimensionless variables of Appendix C, the energy density of the SF is given by

$$\frac{\epsilon_{\rm SF}}{\epsilon_0} = \frac{27}{16}\frac{\Omega_{\rm dm,0}^4}{\Omega_{\rm r,0}^3}\frac{1}{\mu^3}\tilde{\epsilon}_{\rm SF}(\tilde{a}) \tag{E24}$$

with

$$a = \left(\frac{16}{27}\right)^{1/3}\frac{\Omega_{\rm r,0}}{\Omega_{\rm dm,0}}\mu\tilde{a}, \tag{E25}$$

where the function $\tilde{\epsilon}_{\rm SF}(\tilde{a})$ is given in parametric form by Eqs. (45) and (47). This fast oscillation regime has been investigated in detail in Sec. III.

#### 4. Values of the cosmological parameters

For the values of the cosmological parameters, following Li *et al.* [94], we take $\Omega_{r,0} = 9.23765 \times 10^{-5}$, $\Omega_{dm,0} = 0.2645$, $\Omega_{b,0} = 0.0487273$, $\Omega_{m,0} = 0.313228$, $\Omega_{\Lambda,0} = 0.687$, $H_0 = 2.18 \times 10^{-18}\ \mathrm{s}^{-1}$, and $\epsilon_0 = 7.64 \times 10^{-7}\ \mathrm{g\,m^{-1}\,s^{-2}}$

## APPENDIX F: MATCH ASYMPTOTICS

In the stiff matter era, corresponding to the slow oscillation regime, the pseudo rest-mass density and the energy density evolve with the scale factor as [77]

$$\rho_{\rm stiff} \sim \frac{3m^2c^4}{4\pi G\hbar^2}(-\ln a)^2, \qquad \epsilon_{\rm stiff} \sim \frac{K}{a^6}, \tag{F1}$$

where $K$ is a constant. We note that the pseudo rest-mass density changes very slowly with the scale factor as compared to the energy density. We want to see when it is possible to connect the slow oscillation regime $\rho_{\rm stiff}(a)$ to the fast oscillation regime $\rho(a)$. Using the dimensionless variables introduced in Appendix C, the condition $\rho(a) \sim \rho_{\rm stiff}(a)$ corresponds to

$$\tilde{\rho}(\tilde{a}) \sim \tilde{\rho}_{\rm stiff}(\tilde{a}) = 2\sigma(-\ln a)^2, \tag{F2}$$

where $\sigma$ is defined by Eq. (84). Therefore, the matching point corresponds to the intersection of the curve $\tilde{\rho}(\tilde{a})$ drawn in Figs. 1 and 10 with the curve $\rho_{\rm stiff}(\tilde{a}) = 2\sigma(-\ln a)^2$ that is almost a straight line due to the slow variation of the logarithmic term.

We first consider a SF with $a_s \geq 0$. Matching the pseudo rest-mass density of the slow oscillation regime [see Eq. (F1)] with the pseudo rest-mass density of the fast oscillation regime [see Eq. (45)], we obtain

$$a_v^* = \left(\frac{2\pi a_s\hbar^2 Q}{m^2c^2}\right)^{1/3} f_*\left(\frac{3a_sc^2}{4Gm}\right), \tag{F3}$$

where the function $f_*(\sigma)$ is defined by

$$f_*(\sigma) = \frac{1}{r^{1/3}(1+4r)^{1/6}} \tag{F4}$$

with

$$r = 2\sigma(-\ln a_v^*)^2. \tag{F5}$$

It is easy to see that, up to logarithmic corrections, $a_v^*$ is of the same order of magnitude as the scale $a_v$ marking the transition between the slow and fast oscillation regimes given by Eq. (86). Mathematically, this is because the function $r$ defined by Eq. (88) behaves as $r \sim 4\sigma/3$ for $\sigma \to +\infty$ and as $r \sim \sigma$ for $\sigma \to 0$ which is the same scaling as the function $r \propto \sigma$ defined by Eq. (F5). This is most easily seen by considering the asymptotic limits. Matching the pseudo rest-mass density of the stiff matter era [see Eq. (F1)] with the pseudo rest-mass density of the radiationlike era [see Eq. (53)], we obtain a transition scale of the same order as Eq. (93). Matching the pseudo rest-mass density of the stiff matter era [see Eq. (F1)] with the pseudo rest-mass density of the matterlike era [see Eq. (54)], we obtain a transition scale of the same order as Eq. (91). Of course, these qualitative agreements are to be expected. They just provide a consistency check of our approximations.

We can also use match asymptotics to estimate the constant $K$ in Eq. (F1). Matching the energy density of the slow oscillation regime [see Eq. (F1)] with the energy density of the fast oscillation regime [see Eq. (47)] at the transition scale $a_v$ determined by Eq. (86), we obtain

$$K = \frac{2\pi a_s\hbar^2Q^2}{m} h\left(\frac{3a_sc^2}{4Gm}\right), \tag{F6}$$

where the function $h(\sigma)$ is defined by

$$h(\sigma) = \frac{1+3r}{(1+4r)r} \tag{F7}$$

with

$$r = \frac{4\sigma - 1 + \sqrt{(4\sigma-1)^2+12\sigma}}{6}. \tag{F8}$$

For $\sigma \to +\infty$, we obtain

$$K = \frac{3\pi G\hbar^2Q^2}{2c^2} \tag{F9}$$

which can also be obtained by matching the energy density of the stiff matter era [see Eq. (F1)] with the energy density of the radiationlike era [see Eq. (55)] at the transition scale (93). For $\sigma \to 0$, we obtain

$$K = \frac{8\pi G\hbar^2Q^2}{3c^2} \tag{F10}$$

which can also be obtained by matching the energy density of the stiff matter era [see Eq. (F1)] with the energy density of the matterlike era [see Eq. (56)] at the transition scale (91). We note that the value of $K$ does not sensibly depend on $a_s$. Now that the constant $K$ is known, the Friedmann equation (5) can be integrated with the stiff energy density given by Eq. (F1) yielding

$$a = \left(\frac{24\pi GK}{c^2}\right)^{1/6} t^{1/3}. \tag{F11}$$

Using the foregoing results, we can determine the transition between the stiff matter era of the SF and the standard radiation era. Equating Eqs. (E1) and (F1), and using Eq. (F9) valid for $\sigma \gg 1$ (the most relevant case), we obtain

$$a_{\rm sr}=\left(\frac{3\pi G\hbar^2\Omega_{\rm dm,0}^2\epsilon_0}{2m^2c^6\Omega_{r,0}}\right)^{1/2}. \tag{F12}$$

For a SF with $m=3\times10^{-21}\,{\rm eV}/c^2$ and $a_s=1.11\times10^{-58}\,{\rm fm}$, corresponding to the fiducial model of Li *et al.* [94], we obtain $a_{\rm sr}=9.87\times10^{-12}$. This analytical result is in qualitative agreement with their numerical result (see their Fig. 3).

We now consider a SF with $a_s<0$. We first consider the normal branch. If $\sigma\gg1$, it is not possible to match the pseudo rest-mass density of the slow oscillation regime [see Eq. (F1)] with the pseudo rest-mass density of the fast oscillation regime [see Eq. (122)]. This suggests that there is no stiff matter era when $\sigma\gg1$, or that it cannot be smoothly connected to the matterlike era. When $\sigma\ll1$, we obtain

$$(a_v')^*=\left(\frac{2\pi|a_s|\hbar^2Q}{m^2c^2}\right)^{1/3}g_*\left(\frac{3|a_s|c^2}{4Gm}\right), \tag{F13}$$

where the function $g_*(\sigma)$ is defined by

$$g_*(\sigma)=\frac{1}{r^{1/3}(1-4r)^{1/6}} \tag{F14}$$

with

$$r=2\sigma(-\ln a_v^*)^2. \tag{F15}$$

It is easy to see that, up to logarithmic corrections, $(a_v')^*$ is of the same order of magnitude as the scale $a_v'$ marking the transition between the slow and fast oscillation regimes given by Eq. (178). Mathematically, this is because the function $r$ defined by Eq. (180) behaves as $r\sim\sigma$ for $\sigma\to0$ which is the same scaling as the function $r\propto\sigma$ defined by Eq. (F15). This is most easily seen by considering asymptotic limits. Matching the pseudo rest-mass density of the stiff matter era [see Eq. (F1)] with the pseudo rest-mass density of the matterlike era [see Eq. (133)], we obtain a transition scale of the same order as Eq. (91).

We now consider the peculiar branch. In that case, we find that it is not possible to match the pseudo rest-mass density of the slow oscillation regime with the pseudo rest-mass density of the fast oscillation regime, except when $\sigma\sim1$. This suggests that the peculiar branch cannot be connected to a stiff matter era when $\sigma\neq1$. On the other hand, when $\sigma\sim1$ the domain of validity of the fast oscillation regime is very small so this case is not very relevant.

## APPENDIX G: MASS AND LENGTH SCALES

In Sec. IV G we have obtained a relation between the effective cosmological constant $\Lambda$ associated with the energy $\epsilon_\Lambda$ and the mass $m$ and the scattering length $a_s<0$ of the SF [see Eqs. (190) and (192)]. The energy scale $\epsilon_\Lambda$ corresponds to the maximum of the total potential $V_{\rm tot}$ [see Eq. (213)]. If we assume that $|a_s|\sim r_S=2Gm/c^2$ (effective Schwarzschild radius), and substitute this relation into Eqs. (190) and (192), we obtain a mass scale

$$m_\Lambda=\frac{\hbar}{c^2}\sqrt{\frac{\Lambda}{8\pi}}=\frac{\hbar}{c^2}\sqrt{G\rho_\Lambda} \tag{G1}$$

and a length scale

$$r_\Lambda=\frac{G\hbar}{c^4}\sqrt{\frac{\Lambda}{8\pi}}=\frac{G\hbar}{c^4}\sqrt{G\rho_\Lambda}. \tag{G2}$$

Of course, $|a_s|$ can be different from $r_S$ but the scales (G1) and (G2) can be introduced on a dimensional basis, just like the Planck scales. Actually, they can be written as

$$m_\Lambda=\left(\frac{\rho_\Lambda}{\rho_P}\right)^{1/2}M_P,\qquad r_\Lambda=\left(\frac{\rho_\Lambda}{\rho_P}\right)^{1/2}l_P, \tag{G3}$$

so they reduce to the Planck mass $M_P=(\hbar c/G)^{1/2}=1.22\times10^{19}\ {\rm GeV}/c^2$ and Planck length $l_P=(\hbar G/c^3)^{1/2}=1.62\times10^{-35}$ m if we identify $\rho_\Lambda$ to the Planck density $\rho_P=c^5/\hbar G^2=5.16\times10^{99}\ {\rm g\,m^{-3}}$. However, we shall consider here that $\rho_\Lambda$ represents the cosmological density. Writing $\rho_\Lambda=\Omega_{\Lambda,0}\epsilon_0/c^2$ and using the Friedmann equation (5), we get

$$m_\Lambda=\sqrt{\frac{3\Omega_{\Lambda,0}}{8\pi}}\frac{H_0\hbar}{c^2},\qquad r_\Lambda=\sqrt{\frac{3\Omega_{\Lambda,0}}{8\pi}}\frac{GH_0\hbar}{c^4}. \tag{G4}$$

Numerically (see Appendix E 4),

$$m_\Lambda=4.11\times10^{-34}\ {\rm eV}/c^2,\qquad r_\Lambda=5.44\times10^{-82}\ {\rm fm}. \tag{G5}$$

Other mass and length scales can be introduced similarly. If we assume that $|a_s|\sim\lambda_C=\hbar/mc$ (Compton wavelength), and substitute this relation into Eq. (190), we obtain a mass scale and a length scale

$$m_\Lambda^*=\left(\frac{\rho_\Lambda\hbar^3}{c^3}\right)^{1/4},\qquad r_\Lambda^*=\left(\frac{\hbar}{\rho_\Lambda c}\right)^{1/4}. \tag{G6}$$

Numerically (see Appendix E 4),

$$m_\Lambda^*=2.24\times10^{-3}\ {\rm eV}/c^2,\qquad r_\Lambda^*=8.81\times10^{10}\ {\rm fm}. \tag{G7}$$

The Compton wavelength of a particle of mass $M_P$ is the Planck length $l_P$. It is also equal to the effective semi-Schwarzschild radius $r_S/2$. The Compton wavelength of a particle of mass $m_\Lambda$ is the cosmological length $l_\Lambda=c(8\pi/\Lambda)^{1/2}=4.80\times10^{26}$ m, i.e., the typical size

of the visible Universe (since $\Lambda \sim G\rho_\Lambda \sim H_0^2$ implies $l_\Lambda \sim c/\sqrt{\Lambda} \sim c/H_0$).

## APPENDIX H: THE INITIAL CONDITION FOR THE SF

The KG equation is a second order differential equation in time. To solve this equation, we need to specify the values of $\varphi$ and $\dot{\varphi}$ at $t = 0$. In this appendix, we show how they are related to the hydrodynamic variables used in Secs. III C and IV C.

If we restrict ourselves to a spatially homogeneous SF, we have

$$\varphi(t) = \frac{\hbar}{m}\sqrt{\rho(t)}e^{iS_{\rm tot}(t)/\hbar}. \tag{H1}$$

Taking the time derivative of Eq. (H1), we get

$$\dot{\varphi} = \frac{\hbar}{2m\sqrt{\rho}}\left(\dot{\rho} - i\frac{2\rho}{\hbar}E_{\rm tot}\right)e^{iS_{\rm tot}/\hbar}. \tag{H2}$$

Substituting the results of Secs. III C and IV C into Eq. (H2), we obtain the asymptotic behaviors of $\varphi$ and $\dot{\varphi}$ for $t \to 0$. Considering the modulus of the SF, we find

$$|\varphi(t)| = \frac{\hbar}{m}\sqrt{\rho(t)}, \qquad |\dot{\varphi}| = \frac{\hbar}{2m\sqrt{\rho}}\dot{\rho}. \tag{H3}$$

For a SF with $a_s > 0$, using the results of Sec. III C, we get for $t \to 0$:

$$|\varphi| \propto t^{-1/2}, \qquad |\dot{\varphi}| \propto -t^{-3/2}. \tag{H4}$$

Therefore, $|\varphi| \to +\infty$ and $|\dot{\varphi}| \to -\infty$ for $t \to 0$. For a SF with $a_s < 0$, using the results of Sec. IV C, we get for $t \to 0$:

$$|\varphi| \to |\varphi_i|, \qquad |\dot{\varphi}| \propto \pm t^{-1/2}. \tag{H5}$$

In that case, the initial value of $|\varphi|$ is finite while $|\dot{\varphi}| \to -\infty$ on the normal branch and $|\dot{\varphi}| \to +\infty$ on the peculiar branch. This is a very singular initial condition. The choice of the branch is selected by the initial condition, i.e., by the sign of $|\dot{\varphi}|$.

## APPENDIX I: THE CASE OF POWER-LAW SF POTENTIALS

In this appendix, we briefly discuss the evolution of a homogeneous SF with a general power-law potential. For a power-law SF potential of the form (see Appendix C. 5. 2 of [127])

$$V(|\varphi|^2) = \frac{K}{\gamma - 1}\left(\frac{m}{\hbar}\right)^{2\gamma}|\varphi|^{2\gamma}, \tag{I1}$$

we obtain

$$V(\rho) = \frac{K}{\gamma - 1}\rho^\gamma, \qquad h(\rho) = V'(\rho) = \frac{K\gamma}{\gamma - 1}\rho^{\gamma-1}, \tag{I2}$$

$$P(\rho) = K\rho^\gamma, \qquad c_s^2 = K\gamma\rho^{\gamma-1}. \tag{I3}$$

The pressure law $P(\rho)$ is that of a polytrope of index $\gamma$ ($h$ is the enthalpy). For a quartic potential, we recover the polytropic EOS (44) with the exponent $\gamma = 2$. For a $|\varphi|^6$ potential, which is the next order term in an expansion of the SF potential $V(|\varphi|^2)$ in powers of $|\varphi|^2$, we get a polytropic EOS $P = K\rho^3$ with the exponent $\gamma = 3$.

The equations of the problem are

$$\rho\sqrt{1 + \frac{2}{c^2}\frac{K\gamma}{\gamma - 1}\rho^{\gamma-1}} = \frac{Qm}{a^3}, \tag{I4}$$

$$\frac{3H^2}{8\pi G} = \rho + \frac{\gamma + 1}{\gamma - 1}\frac{K}{c^2}\rho^\gamma, \tag{I5}$$

$$\epsilon = \rho c^2 + \frac{\gamma + 1}{\gamma - 1}K\rho^\gamma, \tag{I6}$$

$$P = K\rho^\gamma, \tag{I7}$$

$$w = \frac{\frac{K}{c^2}\rho^{\gamma-1}}{1 + \frac{\gamma+1}{\gamma-1}\frac{K}{c^2}\rho^{\gamma-1}}, \tag{I8}$$

$$E_{\rm tot} = mc^2\sqrt{1 + \frac{2}{c^2}\frac{K\gamma}{\gamma - 1}\rho^{\gamma-1}}. \tag{I9}$$

From Eqs. (I6) and (I7), we obtain

$$\epsilon = \left(\frac{P}{K}\right)^{1/\gamma}c^2 + \frac{\gamma + 1}{\gamma - 1}P, \tag{I10}$$

which determines the EOS $P(\epsilon)$ of the SF under the inverse form $\epsilon(P)$. The differential equation governing the temporal evolution of the pseudo rest-mass density is

$$\frac{c^2}{24\pi G}\left(\frac{\dot{\rho}}{\rho}\right)^2 = \frac{\rho c^2 + \frac{K(\gamma+1)}{\gamma-1}\rho^\gamma}{[1 + \frac{K\gamma\rho^{\gamma-1}}{c^2 + \frac{2K\gamma}{\gamma-1}\rho^{\gamma-1}}]^2}. \tag{I11}$$

These equations can be used to determine the cosmological evolution of a homogeneous SF for any value of $K$ and $\gamma$. This general study will be considered in a future work.

To be more specific, we now assume $\gamma > 1$ and $K > 0$. For $a \to +\infty$, the SF experiences a pressureless matterlike era. For $a \to 0$, we get

$$\rho \sim \left[\frac{(\gamma-1)Q^2m^2c^2}{2K\gamma}\right]^{1/(\gamma+1)}\frac{1}{a^{6/(\gamma+1)}}, \tag{I12}$$

$$\epsilon \sim \frac{\gamma+1}{\gamma-1}K\rho^{\gamma} \propto \frac{1}{a^{6\gamma/(\gamma+1)}}, \tag{I13}$$

$$P \sim \frac{\gamma-1}{\gamma+1}\epsilon \propto \frac{1}{a^{6\gamma/(\gamma+1)}}, \tag{I14}$$

$$w_i = \frac{\gamma-1}{\gamma+1}, \tag{I15}$$

$$\frac{E_{\rm tot}}{mc^2} \sim \left(\frac{\gamma}{\gamma-1}\frac{2K}{c^2}\right)^{1/2}\rho^{(\gamma-1)/2} \propto \frac{1}{a^{3(\gamma-1)/(\gamma+1)}}. \tag{I16}$$

In that limit, the SF behaves as a fluid with a linear EOS $P=\alpha\epsilon$ where $\alpha=(\gamma-1)/(\gamma+1)$. For a quartic potential ($\gamma=2$), we recover the EOS of radiation $P=\epsilon/3$. For a $|\varphi|^6$ potential ($\gamma=3$), we get $\alpha=1/2$. More generally, for $\gamma\geq 1$, the exponent $\alpha$ goes from 0 to 1. These results coincide with those obtained in Refs. [51,86] for a real SF.

The case $\gamma<1$ and $K<0$ is interesting because it leads to a model of Universe that behaves as pressureless DM for $a\to 0$ and as DE for $a\to+\infty$. Therefore, it provides a unification of DM and DE. For $\gamma=0$ we recover the ΛCDM model and for $\gamma=-1$ we recover the Chaplygin gas model [128]. It is interesting that these two famous models are selected by our approach among the infinite family of polytropic models described by an EOS of the form $P=K\epsilon^{\gamma}$ [92,93]. For $\gamma<1$ and $K>0$ we obtain models of Universe that oscillate (phoenix Universes). For $\gamma=0$ we recover the anti-ΛCDM model and for $\gamma=-1$ we recover the anti-Chaplygin gas model (see, e.g., [92,93] for more details).

*Remark:* Some of these results were previously obtained by Bilic *et al.* [104] by considering the inverse problem. Assuming an EOS of the form $P=-A/\epsilon$ (Chaplygin gas) and using Eq. (31), we easily obtain $\epsilon=\rho c^2$ and

$$V_{\rm tot}(\rho) = \frac{1}{2}\left(\rho c^2+\frac{A}{\rho c^2}\right). \tag{I17}$$

This corresponds to Eq. (13) of [104] if we recall Eq. (7). This is also a particular case of Eq. (I2) corresponding to $\gamma=-1$ and $K=-A/c^2$. If we consider a constant EOS of the form $P=-\rho_\Lambda c^2$ (ΛCDM model [93]), we obtain $\epsilon=\rho c^2+\rho_\Lambda c^2$ and

$$V_{\rm tot}(\rho) = \frac{1}{2}\rho c^2+\rho_\Lambda c^2. \tag{I18}$$

This is a particular case of Eq. (I2) corresponding to $\gamma=0$ and $K=-\rho_\Lambda c^2$.


[1] F. Zwicky, Helv. Phys. Acta **6**, 110 (1933).
[2] V. C. Rubin and W. K. Ford, Astrophys. J. **159**, 379 (1970).
[3] R. Massey, T. Kitching, and J. Richard, Rep. Prog. Phys. **73**, 086901 (2010).
[4] A. Vikhlinin *et al.*, Astrophys. J. **640**, 691 (2006).
[5] A. G. Riess *et al.*, Astron. J. **116**, 1009 (1998).
[6] S. Perlmutter *et al.*, Astrophys. J. **517**, 565 (1999).
[7] A. G. Riess *et al.*, Astron. J. **117**, 707 (1999).
[8] H.-J. Seo and D. J. Eisenstein, Astrophys. J. **598**, 720 (2003).
[9] G. F. Smoot *et al.*, Astrophys. J. **396**, L1 (1992).
[10] N. Jarosik *et al.*, Astrophys. J. Suppl. Ser. **192**, 14 (2011).
[11] P. A. R. Ade *et al.* (Planck Collaboration), Astron. Astrophys. **571**, A16 (2014).
[12] A. Drukier, K. Freese, and D. Spergel, Phys. Rev. D **33**, 3495 (1986).
[13] K. Freese, J. Friedman, and A. Gould, Phys. Rev. D **37**, 3388 (1988).
[14] C. E. Aalseth *et al.* (CoGeNT Collaboration), Phys. Rev. Lett. **106**, 131301 (2011).
[15] G. Jungman, M. Kamionkowski, and K. Griest, Phys. Rep. **267**, 195 (1996).
[16] A. Einstein, Sitzungsber. Preuss. Akad. Wiss. Phys. Math. Kl. **1**, 142 (1917).
[17] P. J. E. Peebles and B. Ratra, Rev. Mod. Phys. **75**, 559 (2003).
[18] A. Liddle, *An Introduction to Modern Cosmology* (Wiley, London, 2003).
[19] S. Dodelson, *Modern Cosmology* (Academic Press, San Diego, CA, 2003).
[20] C. Frenk and S. White, Ann. Phys. (Amsterdam) **524**, 507 (2012).
[21] P. Kroupa *et al.*, Astron. Astrophys. **523**, A32 (2010).
[22] W. J. G. de Block, Adv. Astron. **2010**, 789293 (2010).
[23] M. D. Lehnert *et al.*, Nature (London) **467**, 940 (2010).
[24] M. S. Bovill and M. Ricotti, Astrophys. J. **741**, 18 (2011).
[25] J. F. Navarro, C. S. Frenk, and S. D. M. White, Astrophys. J. **462**, 563 (1996).
[26] A. Burkert, Astrophys. J. **447**, L25 (1995).
[27] G. Kauffmann, S. D. M. White, and B. Guiderdoni, Mon. Not. R. Astron. Soc. **264**, 201 (1993); A. Klypin, A. V. Kravtsov, and O. Valenzuela, Astrophys. J. **522**, 82 (1999); M. Kamionkowski and A. R. Liddle, Phys. Rev. Lett. **84**, 4525 (2000).
[28] S. Weinberg, Rev. Mod. Phys. **61**, 1 (1989).
[29] S. Weinberg, arXiv:astro-ph/0005265v1.
[30] J. Martin, C.R. Phys. **13**, 566 (2012).

[31] E. W Kolb and M. S. Turner, *The Early Universe* (Addison-Wesley Publishing Company, New York, 1989).
[32] A. Zee, *Quantum Field Theory in a Nutshell* (Princeton University Press, Princeton, NJ, 2003).
[33] P. S. Wesson, *Space-Time-Matter, Modern Kaluza-Klein Theory* (World Scientific, Singapore, 1999).
[34] A. Linde, *Particle Physics and Inflationary Cosmology* (Harwood, Chur, Switzerland, 1990).
[35] S. M. Carroll, Living Rev. Relativ. **4**, 1 (2001).
[36] R. Rakhi and K. Indulekha, arXiv:0910.5406
[37] R. R. Caldwell, R. Dave, and P. J. Steinhardt, Phys. Rev. Lett. **80**, 1582 (1998).
[38] S. Tsujikawa, Classical Quantum Gravity **30**, 214003 (2013).
[39] R. R. Caldwell, Phys. Lett. B **545**, 23 (2002).
[40] R. R. Caldwell, M. Kamionkowski, and N. Weinberg, Phys. Rev. Lett. **91**, 071301 (2003).
[41] M. P. Dabrowski, C. Kiefer, and B. Sandhoefer, Phys. Rev. D **74**, 044022 (2006).
[42] S. Capozziello, S. Nojiri, and S. D. Odintsov, Phys. Lett. B **632**, 597 (2006).
[43] A. Sen, J. High Energy Phys. 04 (2002) 048; 07 (2002) 065.
[44] S. M. Carroll, Phys. Rev. Lett. **81**, 3067 (1998).
[45] L. Amendola and S. Tsujikawa, *Dark Energy* (Cambridge University Press, Cambridge, England, 2010).
[46] A. Suárez, V. H. Robles, and T. Matos, Astrophys. Space Sci. Proc. **38**, 107 (2014).
[47] T. Rindler-Daller and P. R. Shapiro, Astrophys. Space Sci. Proc. **38**, 163 (2014).
[48] P. H. Chavanis, in *Quantum Aspects of Black Holes*, edited by X. Calmet (Springer, New York, 2015).
[49] D. Marsh, Phys. Rep. **643**, 1 (2016).
[50] H. Y. Schive, T. Chiueh, and T. Broadhurst, Nat. Phys. **10**, 496 (2014).
[51] L. H. Ford, Phys. Rev. D **35**, 2955 (1987).
[52] D. J. Kaup, Phys. Rev. **172**, 1331 (1968).
[53] R. Ruffini and S. Bonazzola, Phys. Rev. **187**, 1767 (1969).
[54] M. Colpi, S. L. Shapiro, and I. Wasserman, Phys. Rev. Lett. **57**, 2485 (1986).
[55] D. Page *et al.*, Phys. Rev. Lett. **106**, 081101 (2011).
[56] P. H. Chavanis and T. Harko, Phys. Rev. D **86**, 064011 (2012).
[57] W. Hu, R. Barkana, and A. Gruzinov, Phys. Rev. Lett. **85**, 1158 (2000).
[58] J. W. Lee and I. Koh, Phys. Rev. D **53**, 2236 (1996).
[59] J. Preskill, M. Wise, and F. Wilczek, Phys. Lett. **120B**, 127 (1983).
[60] L. Abbott and P. Sikivie, Phys. Lett. **120B**, 133 (1983).
[61] M. Dine and W. Fischler, Phys. Lett. **120B**, 137 (1983).
[62] M. S. Turner, Phys. Rep. **197**, 67 (1990).
[63] D. Hooper and L.-T. Wang, Phys. Rev. D **70**, 063506 (2004).
[64] R. L. Davis, Phys. Lett. B **180**, 225 (1986).
[65] R. L. Davis and E. P. S. Shellard, Nucl. Phys. **B324**, 167 (1989).
[66] C. Hagmann and P. Sikivie, Nucl. Phys. **B363**, 247 (1991).
[67] R. A. Battye and E. P. S. Shellard, Phys. Rev. D **53**, 1811 (1996).
[68] E. Madelung, Z. Phys. **40**, 322 (1927).
[69] C. G. Böhmer and T. Harko, J. Cosmol. Astropart. Phys. 06 (2007) 025.
[70] P. H. Chavanis, Phys. Rev. D **84**, 043531 (2011).
[71] T. Rindler-Daller and P. R. Shapiro, Mon. Not. R. Astron. Soc. **422**, 135 (2012).
[72] L. de Broglie, J. Physique **8**, 225 (1927).
[73] L. de Broglie, Comp. Rend. Acad. Sci. Paris **185**, 380 (1927).
[74] L. de Broglie, Comp. Rend. Acad. Sci. Paris **185**, 1118 (1927).
[75] A. Suárez and T. Matos, Mon. Not. R. Astron. Soc. **416**, 87 (2011).
[76] A. Suárez and T. Matos, Classical Quantum Gravity **31**, 045015 (2014).
[77] A. Suárez and P. H. Chavanis, Phys. Rev. D **92**, 023510 (2015).
[78] A. Suárez and P. H. Chavanis, J. Phys. Conf. Ser. **654**, 012008 (2015).
[79] P. H. Chavanis and T. Matos, Eur. Phys. J. Plus **132**, 30 (2017).
[80] J. H. Jeans, *Astronomy and Cosmogony* (Cambridge University Press, Cambridge, England, 1929).
[81] P. H. Chavanis, Eur. Phys. J. B **85**, 229 (2012).
[82] M. Y. Khlopov, B. A. Malomed, and Y. B. Zeldovich, Mon. Not. R. Astron. Soc. **215**, 575 (1985).
[83] P. H. Chavanis, Astron. Astrophys. **537**, A127 (2012).
[84] T. Matos and L. A. Ureña-López, Phys. Rev. D **63**, 063506 (2001).
[85] J. Magaña, T. Matos, A. Suárez, and F. J. Sánchez-Salcedo, J. Cosmol. Astropart. Phys. 10 (2012) 003.
[86] M. S. Turner, Phys. Rev. D **28**, 1243 (1983).
[87] P. B. Greene, L. Kofman, A. Linde, and A. A. Starobinsky, Phys. Rev. D **56**, 6175 (1997).
[88] P. J. E. Peebles and A. Vilenkin, Phys. Rev. D **60**, 103506 (1999).
[89] T. Matos, A. Vázquez-González, and J. Magaña, Mon. Not. R. Astron. Soc. **393**, 1359 (2009).
[90] T. Harko, Mon. Not. R. Astron. Soc. **413**, 3095 (2011).
[91] P. H. Chavanis, Phys. Rev. D **92**, 103004 (2015).
[92] P. H. Chavanis, Eur. Phys. J. Plus **129**, 38 (2014).
[93] P. H. Chavanis, Eur. Phys. J. Plus **129**, 222 (2014).
[94] B. Li, T. Rindler-Daller, and P. R. Shapiro, Phys. Rev. D **89**, 083536 (2014).
[95] D. Scialom and P. Jetzer, Phys. Rev. D **51**, 5698 (1995).
[96] P. Jetzer and D. Scialom, Phys. Rev. D **55**, 7440 (1997).
[97] L. A. Boyle, R. R. Caldwell, and M. Kamionkowski, Phys. Lett. B **545**, 17 (2002).
[98] A. Arbey, J. Lesgourgues, and P. Salati, Phys. Rev. D **65**, 083514 (2002).
[99] P. H. Chavanis and L. Delfini, Phys. Rev. D **84**, 043532 (2011).
[100] P. H. Chavanis, Phys. Rev. D **94**, 083007 (2016).
[101] E. Seidel and W. M. Suen, Phys. Rev. Lett. **66**, 1659 (1991).
[102] S. Weinberg, *Gravitation and Cosmology* (John Wiley, New York, 2002).
[103] J.-A. Gu and W.-Y. P. Hwang, Phys. Lett. B **517**, 1 (2001).
[104] N. Bilic, G. B. Tupper, and R. D. Viollier, Phys. Lett. B **535**, 17 (2002).

[105] V. A. Belinsky, L. P. Grishchuk, I. M. Khalatnikov, and Ya. B. Zeldovich, Phys. Lett. **155B**, 232 (1985).
[106] T. Piran and R. M. Williams, Phys. Lett. **163B**, 331 (1985).
[107] V. H. Robles, A. Suárez, and P. H. Chavanis (work in progress).
[108] A. Ashtekar and P. Singh, Classical Quantum Gravity **28**, 213001 (2011).
[109] N. Poplawski, Phys. Rev. D **85**, 107502 (2012).
[110] Y.-F. Cai, D. A. Easson, and R. Brandenberger, J. Cosmol. Astropart. Phys. 08 (2012) 020.
[111] R. Schild *et al.*, Astron. Astrophys. **422**, 477 (2004).
[112] A. Fraisse *et al.*, Phys. Rev. D **78**, 043535 (2008).
[113] P. A. R. Ade *et al.* (Planck Collaboration), Astron. Astrophys. **571**, A25 (2014).
[114] P. H. Chavanis, M. Lemou, and F. Méhats, Phys. Rev. D **92**, 123527 (2015).
[115] C. Destri, H. J. de Vega, and N. G. Sanchez, New Astron. **22**, 39 (2013).
[116] F. Combes (private communication).
[117] M. Membrado, A. F. Pacheco, and J. Sanudo, Phys. Rev. A **39**, 4207 (1989).
[118] J. Goodman, New Astron. **5**, 103 (2000).
[119] A. Arbey, J. Lesgourgues, and P. Salati, Phys. Rev. D **68**, 023511 (2003).
[120] S. W. Randall, M. Markevitch, D. Clowe, A. H. Gonzalez, and M. Bradac, Astrophys. J. **679**, 1173 (2008).
[121] T. Fukuyama, M. Morikawa, and T. Tatekawa, J. Cosmol. Astropart. Phys. 06 (2008) 033.
[122] J. E. Kim and G. Carosi, Rev. Mod. Phys. **82**, 557 (2010).
[123] L. Hui, J. Ostriker, S. Tremaine, and E. Witten, arXiv: 1610.08297 [Phys. Rev. D (to be published)].
[124] N. Menci *et al.*, arXiv:1701.01339
[125] S. Chandrasekhar, *An Introduction to the Theory of Stellar Structure* (Dover, New York, 1942).
[126] J. R. Oppenheimer and G. M. Volkoff, Phys. Rev. **55**, 374 (1939).
[127] P. H. Chavanis, Eur. Phys. J. Plus **130**, 130 (2015).
[128] A. Kamenshchik, U. Moschella, and V. Pasquier, Phys. Lett. B **511**, 265 (2001).